2012-03-13

A Methodology for Strategically Designing Physical Products that are Naturally Resistant to Reverse Engineering

Stephen P. Harston
Brigham Young University - Provo

A Methodology for Strategically Designing Physical Products that are Naturally Resistant to Reverse Engineering

Stephen P. Harston

A dissertation submitted to the faculty of
Brigham Young University
in partial fulfillment of the requirements for the degree of

Doctor of Philosophy

Christopher A. Mattson, Chair
Brent L. Adams
Brian D. Jensen
Spencer P. Magleby
Alan R. Parkinson

Department of Mechanical Engineering

Brigham Young University

April 2012

ABSTRACT

A Methodology for Strategically Designing Physical Products that are Naturally Resistant to Reverse Engineering

Stephen P. Harston
Department of Mechanical Engineering, BYU
Doctor of Philosophy

Reverse engineering - defined as extracting information about a product from the product itself - is a design tactic commonly used in industry from competitive benchmarking to product imitation. While reverse engineering is a legitimate practice - as long as the product was legally obtained - innovative products are often reverse engineered at the expense of the pioneering company. However, by designing products with built-in barriers to reverse engineering, competitors are no longer able to effectively extract critical information from the product of interest. Enabling the quantification of barriers to reverse engineering, this dissertation presents a set of metrics and parameters that can be used to calculate the barrier to reverse engineer any product as well as the time required to do so. To the original designer, these numerical representations of the barrier and time can be used to strategically identify and improve product characteristics so as to increase the difficulty and time to reverse engineer them. On the other hand, these quantitative measures enable competitors who reverse engineer original designs to focus their efforts on products that will result in the greatest return on investment.

In addition to metrics that estimate the reverse engineering barrier and time, this dissertation also presents a methodology to strategically plan for, select, design, and implement reverse engineering barriers. The methodology presented herein considers barrier development cost, barrier effectiveness in various product components, impact on performance, and return on investment. This process includes sensitivity analysis, modeling of the return on investment, and exploration of multiobjective design spaces. The effectiveness of the presented methodology is demonstrated by making a solar-powered unmanned aerial vehicle difficult to reverse engineer. In the example, the propeller is selected to be the critical component where a series of voids are introduced to decrease the propeller weight and increase the flutter speed (a desirable attribute in propellers). Our tenet is that the use of such a framework contributes greatly to the sustainability of technological, economical, and security advantages enjoyed by those who developed the technology. Designers benefit because (i) products do not readily disclose trade secrets, (ii) competitive advantages can be maintained by impeding competitors from reverse engineering and imitating innovative products, and (iii) the return on investment can be increased.

Keywords: reverse engineering, barriers to reverse engineering, product imitation, hardware imitation, counterfeit prevention, return on investment, microstructure sensitive design

ACKNOWLEDGMENTS

I would like to acknowledge and express appreciation for all those who have helped and inspired me throughout this research.

I especially would like to thank my advisor, mentor, and friend, Dr. Christopher A. Mattson. His innate ability to inspire and motivate one to perform above and beyond their natural capabilities is evident in the level of success we have had in the research. Because of his guidance, this research experience has been excellent as he has molded me into being a better person in all aspects of my life.

I am also grateful for the members of my Doctoral Committee, Dr. Brent L. Adams, Dr. Brian D. Jensen, Dr. Spencer P. Magleby, and Dr. Alan R. Parkinson for their support, advice, and willingness to serve on the committee.

I would also like to acknowledge the National Science Foundation and the funding that was received from them under grant CMMI-0800904 for Christopher A. Mattson and Brent L. Adams.

Importantly, I want to express my undying gratitude to my amazing wife and family who were so willing and supportive during the many long days and nights that were devoted to research. Above all, I acknowledge and am grateful for the Divine guidance that has been a constant blessing throughout all aspects of the research and my life.

TABLE OF CONTENTS

LIST OF TABLES

LIST OF FIGURES

α	Bass Diffusion Model coefficient of early adoption
$\alpha_{ij}^{(s)}$	Combination of slip directions and slip plane normals for the s-th slip system
B	Barrier to extract information about a product from the product itself
β	Bass Diffusion Model coefficient of late adoption
C	Costs related to a product
C_{11}	Material property constant obtained from literature for selected material class
C_{12}	Material property constant obtained from literature for selected material class
C_{44}	Material property constant obtained from literature for selected material class
$\overline{C}_{wxyz}$	Sample stiffness (average crystal stiffness)
D^*	Critical strain rate
$\overline{D}$	Macroscopic strain rate
D_k^N	Normal direction of the k-th lamina, also an axis for the lamina reference frame
D_k^R	Rolling direction of the k-th lamina, also an axis for the lamina reference frame
D_k^T	Transverse direction of the k-th lamina, also an axis for the lamina reference frame
δ	Prescribed displacement
F	Estimated rate at which information is extracted from a product
F_m	Fourier coefficients representing volume fraction of crystals in the m-th bin of the Fundamental Zone
g	Euler angles from Sample to Crystal reference frames
g_{wx}	Orientation matrix of Euler angles from Sample to Crystal reference frames
$\dot{\gamma}_0$	Reference shear rate
γ	The lowest unextracted information level of interest
J	Aggregate optimization objective statement
K	Estimated or actual information contained by a product
M	Material class, (e.g., nickel, copper)
M_0	Selected alloy from material class
m	Estimated market size in number of units
μ	Design objective
N	Number of laminae to be used in layer-by-layer creation of material
n	Bass Diffusion Model sales probability density function
n_c	Number of columns in the binned Fundamental Zone
n_h	Number of layers in the binned Fundamental Zone
n_K	Total number of unextracted information levels

n_r	Number of rows in the binned Fundamental Zone
n_s	Total number of reverse engineering samples
n_T	Total number of information types
ν	Constraint violation
P	Estimated power exerted to extract information contained by a product
$\phi_{1,n}$	Lamination orientation for the n-th layer
Ψ	The sales volume of a product
Q	Force
R	Return on investment ratio
r	Product revenue
ρ	Product retail price
S	A measure of a product's ability to contain information
s	Slip systems. Comprised of slip plane normals, $\{111\}$, and slip directions $< 110 >$
σ_i	6x1 stress vector for the i-th node
σ'_{kl}	Deviatoric stress
T	Estimated time to extract information K
t	Reference time frame for reverse engineering a product
τ	Reference time frame when all parameters are known
$\tau^{*(s)}$	Critical resolved shear stress for the s-th slip system
X	The dollar sales of a product
Z	Learning factor, a measure of a person's resistance to change in information flow rate

Subscripts, superscripts, and other indicators

$\hat{[\,]}$	indicates [ ] pertains to a single reverse engineering sample
$[\,]_0$	indicates [ ] is evaluated at time t or τ equal to zero
$[\,]_c$	indicates crystal reference frame
$[\,]_d$	Indicates [ ] pertains to product development
$[\,]_g$	Indicates [ ] pertains to goods sold
$[\,]_I$	Indicates [ ] pertains to a competitor or product imitation

reverse engineering sample j

$[\,]^k$	indicates [ ] is evaluated for information type k
$[\,]_l$	indicates lamina reference frame
$[\,]_M$	Indicates [ ] pertains to market entry
$[\,]_m$	Indicates [ ] pertains to manufacturing
$[\,]_p$	indicates part reference frame
$[\,]_R$	Indicates [ ] pertains to reverse engineering
$[\,]^*$	indicates total measure or effective property of [ ] unless otherwise noted
$[\,](t)$	indicates [ ] is a function of time, in the t domain
$[\,](\tau)$	indicates [ ] is a function of time, in the τ domain
$[\,]_t$	indicates target value
$[\,]_u$	Indicates [ ] occurs at the upper limit of sales

CHAPTER 1. INTRODUCTION

The introduction of innovative products into the marketplace is often accompanied by an interesting engineering and design dichotomy; on the one hand, the original designer is intent on maintaining his/her competitive advantage, gained through innovation, by offering the product to the masses without easily disclosing its enabling technology [4]. On the other hand, however, the competitor is determined to reverse engineer the innovative product so as to uncover the enabling technology and potentially earn a portion of the market by capitalizing on it [5–11]. Although seen from different perspectives, the notion of *barriers to reverse engineering* is critical in both cases. Ideally, to the original designer, all efforts are made to increase the barrier and time required to reverse engineer his/her design, thus protecting trade secrets and proprietary information. To those reverse engineering the original designs, minimal time and barrier is desired so as to enter the market before it is saturated. In either case, these designers could benefit from general metrics, parameters, definitions, and methodologies for quantifying the time and barrier to reverse engineer a product [12, 13]. For clarity of scope, we provide three important definitions in the context of this dissertation:

Reverse Engineering is the process of extracting information about a product from the product itself. A similar, but distinctly different concept, is that of product imitation – the process of discovering how to physically manufacture and reproduce the performance of the reverse engineered product.

Time to Reverse Engineer is the total required man-time to reverse engineer a product without consideration to parallel activities.

Barrier to Reverse Engineering is anything that impedes reverse engineering.

Barriers to reverse engineering include, for example, critical complex surfaces that are difficult to quantify, localized heat treating that creates difficult-to-discover heterogeneous material charac-

teristics, and hidden *in situ* sensors that monitor performance. Importantly we note that there are distinct differences between time and barrier and that a large time to reverse engineer a product does not necessarily imply that there is also a large barrier to reverse engineering. For example, the barrier to extract geometric information from keys on a keyboard is relatively small as it only requires simple measurements that are easy to obtain. However, the time to reverse engineer the keys on a keyboard may not be small due to the quantity of keys requiring analysis.

Historically there have been few, and often ineffective, options to impede competitors from acquiring valuable information from innovative products through reverse engineering [14]. One such example is that of the Chevy Spark (a compact car sold in Asia). Soon after the release of the Chevy Spark it was being reproduced nearly identically as the Chery QQ by the Chinese automotive company Chery. Notably, in 2005, the Chery QQ was outselling the Chevy Spark nearly five to one [15]. Other times, market share lost due to a reverse engineered product is negligible in significance when compared to the national security lost when Armed Forces' equipment is captured and reverse engineered. The B-29 Superfortress is an American bomber that was captured by the Soviet Union during World War II. Only two years after the capture of the B-29, the Soviet Union was performing their own bombing raids with the first of 847 Soviet Tu-4's, a nearly identical copy of the American B-29. The Tu-4 was engineered so precisely that it even had the same problems as the B-29, such as notoriously unreliable engines [16].

Unfortunately, there is little incentive for original designers to develop innovative products if competitors can imitate the products at a significantly reduced development cost with a larger return on investment [13, 17]. Therefore, barriers to reverse engineering are desirable, as they (i) impede competitors from gaining valuable insight from the innovative product, and (ii) minimize loss of market share due to imitations of the innovative product [14]. With the possible exception of some military products, barriers to reverse engineering do not need to make a product impossible to reverse engineer. Instead, they must make the cost of reverse engineering more than the cost to design the same product from scratch [18, 19]. In general, any improvement that can be economically taken to reduce the risk of the product being successfully reverse engineered is worth taking [20].

While others have previously presented the idea of barriers to reverse engineering [21–23], the developments presented in this dissertation focus on an articulated, yet unmet need in the

literature – namely the need for design metrics, parameters, and methodologies enabling products to be developed that are inherently difficult to reverse engineer. As such, the principle objective of this dissertation is to:

Dissertation Objective Develop an effective design framework that results in products that can be handled, used, dissected, or similarly analyzed by a competitor without disclosing the phenomena by which the product functions.

The successful development of such a framework contributes greatly to the sustainability of technological, economical, and security advantages enjoyed by those who developed the technology. As shown is subsequent chapters, the dissertation objective is accomplished by completing the six research sub-objectives listed below. The six sub-objectives are:

Sub-Objective 1 Develop metrics that quantitatively approximate (i) the time to reverse engineer any product, and (ii) the barrier to reverse engineering that must be overcome to successfully reverse engineer any product. As a note, the quantitative approximations of the reverse engineering barrier and time are termed *reverse engineering metrics*.

Sub-Objective 2 Quantify the error of the reverse engineering metrics and what it means to the designer.

Sub-Objective 3 Explore how microstructure sensitive design results in effective and efficient barriers to reverse engineering.

Sub-Objective 4 Explore the tradeoffs between reverse engineering barriers, cost, and return on investment.

Sub-Objective 5 Determine what products – or product components within a system – most benefit from implementing barriers to reverse engineering.

Sub-Objective 6 Use numerical optimization to search for designs that (i) meet or exceed performance requirements, (ii) maximize return on investment, and (iii) are difficult to reverse engineer.

The remainder of the dissertation is presented as follows. Providing a deeper motivation for this work, Chapter 2 discusses the relevant completed work and unmet needs as expressed by the literature. In Chapter 3, we present an anecdotal understanding of barriers to reverse engineering, followed by the presentation of the reverse engineering metrics in Chapter 4. Building on the reverse engineering metrics, additional metrics are presented in Chapter 5 that may be used to estimate the reverse engineering barrier and time when multiple samples of the same product are being reverse engineered. This is followed by the return on investment analysis for reverse engineering barriers in Chapter 6. The culminating chapter is Chapter 7 where the methodology used to plan for, select, and implement barriers to reverse engineering is presented and explained in the context of an example of a solar-powered unmanned aerial vehicle. This is followed by Chapter 8, which explores in detail the effectiveness of material microstructures as barriers to reverse engineering. The final chapter, Chapter 9, presents concluding remarks and future work.

CHAPTER 2. LITERATURE SURVEY

2.1 Chapter Overview

The purpose of this chapter is to present technical preliminaries and unmet needs expressed by the literature as they relate to reverse engineering and reverse engineering barriers. To facilitate the discussion, this chapter has been divided into sections – Section 2.2 discusses the need to characterize and quantify barriers to reverse engineering, Section 2.3 discusses existing techniques for selecting the critical components of a product, and Section 2.4 discusses methods and models that may be used to strategically manipulate material microstructures to create barriers to reverse engineering.

2.2 The Need to Characterize and Quantify Barriers to Reverse Engineering

Innovative products have changed the world. Reverse engineering and imitation of such products has been to the detriment of pioneering companies. One such example is the company EMI. In 1975, EMI created the first CAT scanner and used it to distinguish between healthy and diseased brain tissue [24,25]. Since its creation, doctors have been using CAT scans to improve the lives of hundreds of millions. In fact, in 2007 alone, an estimated 72 million scans were performed in the United States [26]. However, within six years of the CAT scanner's release to market, EMI had lost market leadership and within eight years EMI had discontinued competing in the market it originally created [27]. The culprit was competing companies that reverse engineered, imitated, and improved upon the original design. If competitors were not able to successfully reverse engineer and understand EMI's product, it is likely that EMI would have been able to maintain their competitive advantage and continue to be the market leader for a number of years. This is just one of many examples where product imitations have captured market share from an innovative product and reduced the return on investment for the innovator [10, 15, 28–32].

Before we further explore the reverse engineering of physical products, let us first explore the variety of similar, yet unique, ways various disciplines have approached the topic in the literature. Among the disciplines that have addressed the topic of reverse engineering, the following three areas are predominant; (i) reverse engineering of software [33–37] (ii) reverse engineering of hardware [5, 6, 12, 21, 38], and (iii) reverse engineering of biological systems [39–42]. The reverse engineering of software is pervasive in the literature and is of particular interest as it relates to reverse engineering because software is being delivered to end-users with more mobile code in architecture-independent formats – thereby facilitating the reproduction of original code with less effort. Strategies to prevent reverse engineering of software include tamper proofing, obfuscation, and watermarking [43].

The reverse engineering of hardware is generally addressed in the literature from within three areas of research; (i) performance benchmarking [5, 6, 38], which is the evaluation of competitive products in order to specify performance criteria and generate concepts for new products, (ii) geometric surface and shape recovery [44, 45], which is the automated extraction of geometry from an existing product and the construction of 3D CAD models from the data, and (iii) empirical parameter estimation and surrogate model building by statistical sampling of hardware [46, 47], which is simply the estimation of performance measures through testing an existing product and fitting a mathematical model to the test data, thereby developing an approximate parametric model of the product's performance.

Of particular interest to this dissertation, Ingle provides a basic four-stage methodology for the reverse engineering of hardware [5]. Stage 1 is the evaluation and verification of a product or system. Stage 2 is the documentation of the findings, usually in the form of technical data. Stage 3 is prototype verification, and Stage 4 is project implementation.

Finally, research in the reverse engineering of biological systems has gained more and more momentum as scientists and engineers seek to discover the building blocks of nature [40, 41] and successful ways in which natural systems accomplish complex tasks [42]. While many insights of reverse engineering may be gained from analyzing software or biological systems, the developments presented in this dissertation focus on reverse engineering of physical hardware.

Although they may not use the same terminology, many researchers state the need for (i) estimations of the time and barrier to reverse engineer a product, and (ii) methodologies for incor-

porating barriers to reverse engineering. These ideas are presented from various perspectives in the literature which range from those of the original designer [12, 21, 38], to those who reverse engineer, [5,6,13], to market analysts [12,48,49]. Despite the fact that these perspectives are insightful and suggest the need for quantitative measures and barrier implementation methodologies, none of them provide them.

While there are not any *quantitative* metrics presented in the literature, Weingart presents a *qualitative* measure that is termed *attack difficulty* [1] and is summarized in Tab. 2.1. This classification system ranges from 1 to 6, based on the tools and skills required to reverse engineer a product. Similar qualitative classifications have been presented by Christiansen [50] and Abraham et al. [51]. An advantage of these measures is that they are intuitive, and can be easily evaluated in the early stages of the product development process. However, these metrics are not quantitative in nature and cannot be used in conjunction with numerical optimization to maximize the reverse engineering time and barrier.

In addition to the need for quantitative metrics, many authors discuss the importance of understanding and designing for reverse engineering barriers. Macmillan et al. [12] state that it is critical to estimate competitors' response lag (or time to reverse engineer and imitate a product) in order to understand the potential financial risks and profits. Pahl et al. [38] state that effective product planning includes understanding the life cycle of the proposed product as well as understanding competitors' products. Therefore, effective product planning and definition of product life cycle is likely to (i) consider the time required for competitors to conduct reverse engineering activities *and* (ii) require a full understanding of competitive products through reverse engineering activities.

Shapiro [52] and Nelson and Winter [53] emphasize that the harder a product is to reverse engineer – dependent upon the competitor and their resources and skills available – the less incentive a competitor has to imitate the technology. On the other hand, there is little incentive for original designers to develop innovative products if competitors can imitate the products at a significantly reduced development cost with a larger return on investment [13]. Many companies have adopted a strategy of entering into a well-developed market so as to take advantage of the marketing, innovation, and the development of the customer base by the pioneering company [27] in spite of the benefits associated with being the first to enter a market [54]. In fact, imitators are

Table 2.1: Qualitative attack difficulty classifications [1]

Level	Name	Description
1	None	The attack can succeed "by accident," without the attacker necessarily being aware that a defense was intended to exist. No tools or skills are needed.
2	Intent	The attacker must have a clear intent in order to succeed. Universally available tools (e.g., screwdriver, hobby knife) and minimal skills may be used.
3	Common Tools	Commonly available tools and skills may be used (e.g., those tools available from retail department or computer stores, such as a soldering iron or security driver bit set).
4	Unusual Tools	Uncommon tools and skills may be used, but they must be available to a substantial population (e.g., multimeter, oscilloscope, logic analyzer, hardware debugging skills, electronic design and construction skills.) Typical engineers will have access to these tools and skills.
5	Special tools	Highly specialized tools and expertise may be used, as might be found in the laboratories of universities, private companies, or governmental facilities. The attack requires a significant expenditure of time and effort.
6	In Laboratory	A successful attack would require a major expenditure of time and effort on the part of a number of highly qualified experts, and the resources available only in a few facilities in the world.

often able to surpass the innovators to become the market leader [27,54]. However, if imitators are impeded – requiring potential imitators to develop their own competing product – the innovators can maintain their competitive advantage [21,54]. Preventing competitors from extracting critical information from a product is especially significant when trade secrets may be kept secret even when the product is readily available to the masses [22].

Interestingly, there are few laws to prevent the reverse engineering of hardware [55]. Current laws state that reverse engineering is an acceptable method of obtaining trade secrets as long

as the product acquisition was done legitimately [55]. These laws are rationalized, by many, since the time and effort required to reverse engineer a product is often viewed as substantial enough to allow the original designer to maintain a large market share [55]. If the justification of the current laws was true, then reverse engineering would not be a common issue.

One common approach to secure intellectual property is through patents. However, patents disclose the enabling technology of a product and aid imitators in avoiding patent infringement while maintaining comparable performance [9]. Another common approach from the literature is to develop business strategies that minimize market loss due to product imitations. These strategies range from analysis of the marketing mix and corporate strategy [56], to providing measures that help a company structure its business model to maintain a competitive advantage [57]. Furthermore, Reed and DeFillippi [21] argue that barriers to reverse engineering are created through tacitness, complexity, and specificity in a firm's skills and resources. While each of these insights are useful, each of these approaches focus on business strategies alone. Building off these strategies, this doctoral work adds a design/engineering element to minimize market loss due to reverse engineering. Specifically, a design methodology is presented which enables the design of products that are inherently difficult to dissect, reverse engineer, and imitate – thus further increasing the return on investment.

2.3 Selection of Critical Components of a Product

It may not be practical to incorporate reverse engineering barriers into all products. One must weigh the consequences of the product being reverse engineered, determine the additional cost to develop the barriers, and calculate the expected return on investment of a product that does, or does not, implement a reverse engineering prevention strategy. However, designing reverse engineering barriers into a product can be costly – both in time and resources. This can result in a delayed market entry and a reduced return on investment. On the other hand, innovative products have lost a significant portion of the market share due to reverse engineering and product imitations – some companies have even discontinued competing in the markets which they originally created due to competitors reverse engineering and imitating their innovative product [27]. While barriers to reverse engineering may be costly to implement, entire products can be made difficult to reverse engineer by strategically selecting and designing barriers to reverse engineering into one, or a few,

critical components [32]. Therefore, it is important that the critical components of a system be identified, and that strategies be selected for making them more difficult to reverse engineer.

Identifying, characterizing, and understanding the critical components of a system is not a novel idea. The basis of risk management [17, 58], security [59] and defense in depth [60, 61] is to identify the critical components and improve their designs to decrease risk or increase security of the system. In product design, designers seek to understand what features of a product are critical to user satisfaction [62], understand the impact of critical components on a system when they are redesigned and replaced [63], and perform analyses to systematically identify possible failures and estimated risks [38]. Grand [19] suggests that before any security/barrier features are designed into a product, risk assessment in the following three areas should be performed to help identify critical components: (i) what needs to be protected (ii) why does it need to be protected, and (iii) who are you protecting against. Pooley and Graves [64] recommend locating the most valuable information in a product, and focusing resources and efforts on that component recognizing that a larger barrier may be required to discourage qualified engineers from reverse engineering a product than for non-technical workers.

While Grand, [19] and Pooley and Graves [64] offer great insight on critical component selection of hardware, this dissertation takes the critical component selection process further by developing a systematic approach that can be automated, and used in conjunction with numerical optimization, to help designers select the critical components of a physical system. Similar methods are used in the software industry where graph theory concepts are used to improve information security evaluations for electronic communication devices. Rae and Fidge [65] present an approach that significantly reduces analysis time by forgoing analysis on components that do not affect information security and focusing on the critical components that are most likely to cause failures. Furthermore, Ebert [66] presents a number of classification techniques to help software designers detect source code defects early in the development process and to focus defect detection on the error-prone areas.

A number of these approaches (i) may be automated, and (ii) provide useful insight on how to select critical components; however they cannot be directly adopted for discovering critical components of physical hardware. As such, a method for selecting the critical components of physical

hardware – which builds upon the discussed methods and ideas – is developed and presented in this doctoral work.

2.4 Microstructure Manipulation to Create Barriers to Reverse Engineering

Throughout the doctoral work, many barriers to reverse engineering have been explored. Of the barriers explored, the strategic manipulation of material microstructures has been found to be a very effective barrier reverse engineering barrier. As such, we explore the literature for existing models and techniques that may be used to strategically design and manipulate material microstructures with the purpose of creating reverse engineering barriers.

The optimization of macroscopic geometry, known in the literature as size [67], shape [68, 69], and topology [69, 70] optimization, is a powerful approach to identify hardware with desirable performance characteristics [71]. A different, yet equally powerful, approach is to manipulate microscopic metallurgical material characteristics to enhance material properties and achieve desirable hardware performance [72]. Individually, these two approaches have improved products and allowed for more advanced designs over those of the past [71, 72]. Through an integrated approach, however, macroscopic *and* microscopic features can be manipulated in a complementary way to identify hardware designs with desirable *and* unexpected mechanical performance, thus resulting in a large barrier to reverse engineering.

It is known that one or more microstructures can be used as a starting point to obtain any combination of properties in the *property closure*, which is the set of all theoretically possible material properties [73]. Unfortunately, it is not known how to consistently manufacture all microstructures required to obtain every combination of properties in the property closure. Therefore, only a small, discrete, set of material properties contained within the full property closure are commonly used in practice. This is one of the main reasons why material properties are rarely considered continuous variables in the material selection activities of product design.

However, with the strategic combination of laminations, microstructures that were previously difficult to obtain become simple combinations of optimally-layered, well-known microstructures [74]. This process is similar to a carbon-fiber composite material design where many thin layers are ideally aligned to obtain desired material properties in specific directions [75, 76]. For years, carbon-fiber composite researchers have studied the effect of material microstructures

on product performance [75]. Specifically, fiber composites have been analyzed and tested to determine fiber composition, epoxy composition, fiber/epoxy mixtures, and layer orientation resulting in desired product performance [75–78]. Some have even studied the effects of alternating layers of fiber/epoxy and thin metal sheets [79].

Significant contributions have also been made by others who have recognized performance improvements that can be achieved by microstructure design with metals [80–84]. While the origins of the modern theories used for analyzing metallic microstructures may be traced back to the mid 1900's, it is only in recent years that microstructure theories have matured to the point that enables the design of metals at the micro level resulting in a desired macro level performance [80]. Notably, McDowell [80, 81] discusses the challenges when designing for microstructure plasticity characteristics and also presents a methodology that effectively overcomes microstructure design challenges [82]. Olson [83] and Kuehmann and Olson [84] discuss the computational design of materials to meet specific engineering needs. Specifically they address the handling of conflicting design objectives and expensive computations to obtain desired material properties and desired product performance.

By building upon the work of others in the areas of microstructure analysis and design, this doctoral work takes an unique approach by strategically manipulating material microstructures with the purpose of making products difficult to reverse engineer. Specifically, this doctoral work presents a new design framework, in conjunction with numerical optimization, that couples microstructure manipulation and modeling with existing manufacturing processes to create products that are resistant to reverse engineering attempts. The microstructure sensitive design approach, as presented in Chapter 8, enables a product to perform (e.g., deflection, yield characteristics, shear characteristics) in a way that cannot be obtained without manipulating the material. Furthermore, the source of performance improvement is difficult to determine and recreate from a reverse engineering perspective, thus impeding competitors from successfully reverse engineering the product.

CHAPTER 3. AN ANECDOTAL UNDERSTANDING OF BARRIERS TO REVERSE ENGINEERING

3.1 Chapter Overview

Reverse engineering is a common design strategy in industry. It is a term that has come to encompass a large array of engineering and design activities in the literature; however, in its basic form, reverse engineering is simply the process of extracting information about a product from the product itself. Depending on its use, it may or may not be advantageous to utilize a reverse engineering strategy. As with any rational decision, reverse engineering is only favorable when the benefits from its use outweigh the investment. Therefore, a general understanding of the principles that increase the difficulty or investment required to reverse engineer mechanical products would be helpful for everyone affected by reverse engineering activities. In this chapter, we articulate and explore these fundamental principles after reviewing examples from the literature and from our own experience.

3.2 Introduction

Reverse engineering carries various connotations in different industry settings. At one end of the spectrum, reverse engineering is associated with design theft and piracy with the intent to plagiarize and capitalize on the work of others [43, 85]. On the other hand, reverse engineering can be as conventional as competitive benchmarking [86] or as benign as the dissection of a popular product by a curious consumer [87]. Notice that the definition of reverse engineering used here is different from *imitation*, which we define as the process of replicating the performance of an existing product in one or more of its performance areas [88]. Reverse engineering often leads to imitation; however, the definition of reverse engineering as defined here limits the discussion to simply the information extraction process.

There are many reasons to employ reverse engineering as a viable engineering design tactic. A few common reasons are listed below:

- To compare products through competitive benchmarking [89, 90]
- In preparation for imitating a product [91]
- To obtain technical data that does not exist [92–94]
- To obtain technical data that the original supplier is no longer willing or able to provide [90, 95]
- To shorten market entry times [90]
- To enhance existing data [5]
- To perform product verification [5]
- To aid in product design [96]
- To investigate patent law infringement [97]
- To assist in academia or other learning environments [97, 98]

While this list is not exhaustive, it illustrates how reverse engineering is used in a variety of settings. As such, it is important to know what factors affect reverse engineering difficulty. This knowledge is beneficial – both for original designers and those reverse engineering. It can potentially help original designers to design products that are more difficult to reverse engineer, thereby maintaining a market advantage over their competitors. On the other hand, those reverse engineering can use this knowledge to select projects that will be *successful*, meaning that the payoff is sufficiently greater than the reverse engineering cost.

This chapter is devoted to investigating *barriers* in the reverse engineering process. Some examples of barriers to reverse engineering include the complexity of turbine blade surfaces, inaccessibility of hidden or microscopic features of an embedded circuit, inadequate measurement equipment, or even an inexperienced engineer. Barriers for mechanical systems can be classified into *internal* and *external* barriers. Internal barriers are physical features of the product itself, or

lack thereof, that hinder reverse engineering, while external barriers are extrinsic to the product. The *total* barrier is affected by all barriers whether internal, external, or a combination of the two.

Not all products benefit from incorporating barriers to reverse engineering. Some products may be so simple, or sold at low margins, so that incorporating barriers to reverse engineering is not practical. Deciding which products are suitable for barrier implementation is a critical question that is answered by the methodology presented in Chapter 7.

In this chapter, we characterize the fundamental types of barriers to reverse engineer mechanical components. We provide examples and theories from related fields to illustrate how these barriers can potentially stymie reverse engineering efforts. In so doing, we provide valuable insight into how one can either increase or decrease the magnitude of a barrier to reverse engineering. Our tenet is that the difficulty to reverse engineer a product can (i) be controlled and (ii) designed in a strategic manner. Further, the methods presented in this dissertation facilitate the implementation of our tenet.

3.3 Barriers in the Reverse Engineering Process

The general procedure of reverse engineering has been defined and examined in detail by both Ingle [5] and Otto and Wood [6]. Additional techniques for digitizing physical objects for CAD applications have been presented by Varady [99], Sarkar and Menq [100], and Raja [90]. Though there exist multiple descriptions of the reverse engineering process, they can all be distilled to three simple steps as seen in Fig. 3.1. The three basic reverse engineering steps are: (i) planning, (ii) data collection, and (iii) data processing. As Fig. 3.1 suggests, the process can be iterative in nature. During data processing, for example, the reverse engineering team must validate extracted information, so as to know when the process is complete. If errors are discovered, due to missing or low quality data, the reverse engineering team must extract more information from the product. When barriers to reverse engineering are strategically implemented, the process would ideally have to be repeated several times.

Before presenting the methodology that impedes competitors from gaining valuable information from a product we classify barriers into the following three categories, which will facilitate the presentation of the said methodology:

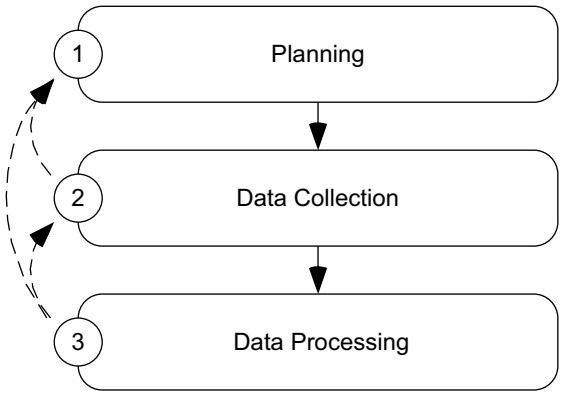

Figure 3.1: Steps of the reverse engineering process

- Technical complexity of the product or feature
- Availability of the necessary resources [101]
- Skill of the reverse engineering team [101]

Barriers associated with the technical complexity of the product or feature are internal barriers to reverse engineering, while the remaining types of barriers are external. The skill of the reverse engineering team could be considered a necessary resource, i.e., a human resource; however, as skill is an intangible asset with unique characteristics, we consider it separately in the discussion of the barrier types presented in this section. While the original designer has direct control over internal barriers, it will be shown that he or she can also indirectly affect the external barriers as well.

When a simple product is evaluated by someone with the necessary resources and adequate skill, then the total barrier to reverse engineer that product is small. The opposite is also true – the total barrier is high if the product is technically complex and the reverse engineering team lacks necessary resources and skills. It follows that the magnitude of the total barrier is directly proportional to the technical complexity of the product, while inversely proportional to both the availability of the necessary resources and the skill of the person or team reverse engineering the product.

We note here that while legal barriers can and do exist to prevent the commercialization of copied products, there are few laws to prevent the reverse engineering of hardware [55]. Current

laws state that reverse engineering is an acceptable method of obtaining trade secrets as long as the product acquisition was done legitimately [55,87]. These laws are justified by many, since the time and effort required to reverse engineer a product is often viewed as substantial enough to allow the original designer to maintain a large market share [55]. Interestingly, patents facilitate reverse engineering as they disclose critical product information and key technologies. In some cases, laws are outright violated and products are continually built directly from patent information even though the patent owners have claimed patent infringement and seek compensation [102]. Thus, it may not be wise for an original designer to rely solely on legal barriers to mitigate reverse engineering attempts of their product.

The remainder of this section investigates in greater detail how these three barrier categories interact to create information-extraction difficulties during the reverse engineering process.

3.3.1 Technical Complexity of the Product

Perhaps the most apparent barrier to reverse engineering is the technical complexity of the product. We decompose technical complexity into the quantity of information, the information type (e.g. geometric dimensions, material composition), and the extent to which different information types interact. If a product is more technically complex, it will be more difficult to reverse engineer. As this is an internal barrier, the original designer can literally build physical features into the product to increase the difficulty to reverse engineer the product. Therefore, the original designer has a direct influence on this type of barrier.

A product can contain many disparate types of information, such as geometric, material, chemical, electrical, or even aesthetic information. Certain types of information are inherently more difficult to extract than others [14]. Von Hippel articulates this in [103] by defining the "stickiness" of a unit of information as the *incremental expenditure required to transfer that unit of information to a specified locus in a form useable by a given information seeker*. In other words, stickiness is a measure of the rate at which usable information may be extracted from a product while reverse engineering. When systems containing sticky information interact with other systems in a product, the result is a powerful barrier to reverse engineering. For example, when material properties that are difficult to reverse engineer are heterogeneously placed at critical

geometric locations, the barrier to reverse engineer is larger than when the same microstructure is homogeneously distributed.

Information stickiness varies for different information types, even within the geometric domain. Free form surfaces are not easily measured with traditional measurement devices such as micrometers or calipers [104]; therefore, their complexity could be potentially difficult to capture during the data collection step, as they require more expensive, and user intensive, measurement equipment. This is exemplified by Soo et al. in [105] where the difficulties of digitally capturing the complicated and arbitrary curves of a Chinese bamboo-net handicraft are discussed in detail. Additionally, the physical size of the measurement can have a large impact on the information stickiness. For instance, as computer chips have decreased in size, they have become increasingly more difficult to reverse engineer [106].

Products can contain a large amount of information. One challenge for the reverse engineering team lies in distinguishing between information that is *superfluous* and information that is *pertinent* to product performance [14]. This distinction can be difficult to make, especially when products contain a plethora of nonessential information or when essential information is disguised to appear trivial [87]. Extracting superfluous information will decrease the return on reverse engineering investment, as resources are wasted on information that does not provide significant benefits. Therefore, it is important for the reverse engineering team to make this distinction, if possible in the planning step (see Fig. 3.1), before collecting data from the product.

Additionally, one must ensure that all pertinent information is extracted from the product. This is typically done during the data processing step. McEvily [32] presents a case study of reverse engineering failure, where a defective butterfly valve in an aircraft engine caused the plane to crash. He states that the *original alloy and part dimensions [of the butterfly valve] were accurately duplicated*; however, the firm reverse engineering the valve failed to extract the heat treating process required to properly reconstruct the valve. As a result, the valve was inadequately manufactured and failed in use.

Another aspect of product complexity is the accessibility of pertinent information. Products can be difficult to dissect; essential components of the product can be enclosed in the product in such a way that nondestructive disassembly is nearly impossible [64]. This is the case with many computer chips, where the coating on the chip is designed so that when the coating is removed, one

or more layers of the chip are also destroyed, thereby making the rest of the chip difficult, if not impossible, to reverse engineer [18]. Another way to limit accessibility of pertinent information is to add locks to a product. For mechanical products, this may be in the form of custom made fasteners [19,104]. In general, the harder it is to access the information, the stickier the information becomes.

The fundamental principles to understand about the technical complexity of barriers to reverse engineering can be summarized with the following:

- The technical complexity of a product or feature is an internal barrier to reverse engineering – the original designer has a direct influence over the magnitude of this barrier.
- When sticky information interacts with other sticky information in a product, the result is a powerful barrier to reverse engineering.
- The stickiness of pertinent information can be increased by reducing its accessibility or including more superfluous information in the product to disguise pertinent features.

We note that in Section 3.4 a list of specific actions to increase product complexity is provided.

3.3.2 Availability of the Necessary Resources

We now turn our attention to external barriers to reverse engineering, specifically, the barriers associated with the availability of necessary resources. By necessary resources we mean required tools (including tools for disassembly, performance analysis, data synthesis, measurement etc.), samples of the product, and any other object or software that is required to successfully extract information from the product itself. Unlike internal barriers, the original designer can only indirectly influence the magnitude of external barriers as they may not be able to control the resources extrinsic to the product. However, by strategically designing the product, original designers can require those engaged in reverse engineering to use resources that are expensive or not readily available in order to be successful at reverse engineering. While there may be more than one approach to extract information from a product, some information can only be acquired with the correct tools such as the material microstructure of a custom made material that is critical for

proper performance of the product. On the other hand, a reverse engineering team can overcome many barriers by acquiring essential resources.

First and foremost, the product or system being analyzed needs to be accessible. Even if a product is readily available on the market, it may be expensive or may only be available in limited quantities, thereby discouraging others from attempting to reverse engineer the product as the required investment increases. Often times it is of interest to those reverse engineering to know how the original product fails, possibly to prevent or improve the conditions of failure. Clearly, when only a few sample parts are available, extracting this type of information can be difficult [5].

Second, equipment used during the data collection step (see step two of Fig. 3.1) needs to be available. Often, a high level of precision and accuracy is needed when collecting information from a product. This is much easier to accomplish with appropriate equipment, which for geometric information could include micrometers, gages, coordinate measuring machines, and optical scanning equipment [95] or for material microstructure information could include a scanning electron microscope [73]. At the same time, a significant amount of skill and experience, see Sec. 3.3.3, may be needed to operate these measuring tools, as well as to understand their limitations and shortcomings [45, 107–109].

Third, converting collected data into a usable form during the data processing step (see step three of Fig. 3.1) can also be challenging. For geometric information, this form is often digital, meaning in the form of a CAD model or drawing. This, of course, requires CAD or CAE software. Much care is needed during this process to ensure that minimal error is introduced when processing the data [93, 107]. For material microstructure information, the data collected through scanning electron microscopy needs to be analyzed with orientation image microscopy (OIM) software [73]. Clearly, if this equipment is unavailable, the magnitude of the barrier to reverse engineering will be large.

Finally, proper testing and validation of extracted data is vital to the success of a reverse engineering project. Assumptions made in the planning step in Fig. 3.1, such as decisions regarding information relevance, need to be verified as the data collected may or may not actually be pertinent. Additionally, some information may still be needed to adequately reverse engineer the product. Verification can take on many different forms, each requiring specific resources. CAD systems can help verify that all the needed geometric dimensions have been extracted. CAE sys-

tems can further aid in this process by analyzing motion, stress, heat transfer, and failure modes. If the necessary equipment is available, prototypes can be built and subsequently tested for the purpose of verification.

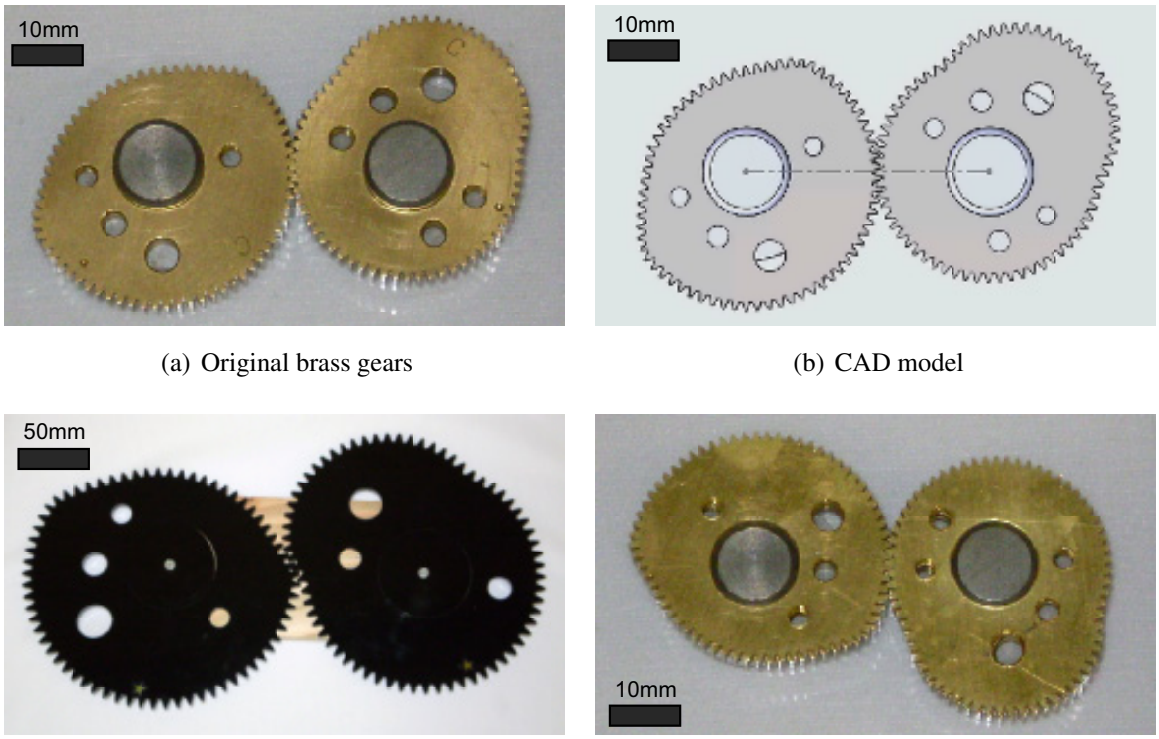

(a) Original brass gears

(b) CAD model

(c) Acrylic prototypes

(d) Reconstructed brass gears

Figure 3.2: Reverse engineering example of non-circular gears

For example, the non-circular brass gears in Fig. 3.2(a) were originally part of a photocopy machine. As part of this study, we reverse engineered the gears to illustrate the verification process. The gears were measured using an optical comparator, and the data was manually entered into a CAD system. The resulting CAD model appears in Fig. 3.2(b). A motion analysis was done using CAE software to verify that the gears properly meshed. Acrylic prototypes were then manufactured using a laser cutter, and are shown in Fig. 3.2(c). The acrylic prototype was made five times larger, to accommodate for the resolution of the laser cutter. Finally, brass gears were cut in true scale using wire electric discharge machining (EDM), as shown in Fig. 3.2(d). Multiple tools were needed to verify that we extracted the correct information about the non-circular gears. In fact, the prototypes revealed some flaws in our extracted data, as the reconstructed brass gears did not

perform as well as the original gears. If the necessary resources were not readily available (optical comparator, CAD and CAE software, laser cutter, wire EDM), then this process would have taken a different path characterized by its own difficulty. Therefore, we can see that the resources available to the reverse engineering team influence the difficulty to reverse engineer the product.

The fundamental principles to understand about the resource-availability category of barriers can be summarized with the following:

- The availability of the necessary resources is an external barrier to reverse engineering – the original designer typically has an indirect influence on this barrier.
- When few or no samples of the product are available, the magnitude of this barrier increases dramatically.
- Proper equipment is often required for efficient product dissection, information extraction, and data processing. The absence of this equipment could severely reduce the quality of collected data. The barrier can be made larger by embedding information that requires specialized and/or unavailable tools to extract.

Section 3.4 provides specific actions that can be taken to increase the magnitude of this type of barriers.

3.3.3 Skill of the Reverse Engineering Team

The third and last category of barriers to reverse engineering is the skill of the reverse engineering team. Clearly when required skills are absent, the barrier to reverse engineering is larger. Skill can be considered from two perspectives. First, a familiarity or basic understanding of the science governing the system being analyzed is often essential for effective reverse engineering. For instance, a working knowledge of chemistry is necessary to extract chemical information from a battery. Second, expertise and experience with the reverse engineering process and its associated tools is also extremely important. More than likely, a successful reverse engineering project will require the synergy and collaboration of a group of professionals with different skill sets – economists, market analysts, accountants, engineers, managers, etc. Thus, skills in multidisciplinary design and project management are valuable.

The reverse engineering team must begin by considering the purpose for reverse engineering in the planning step of Fig. 3.1. This will determine whether or not there is a need to capture *as-built* information from the product or *design intent* information [110]. In its extreme form, the as-built approach aims to copy every bit of information from a product to the best ability of the team. Even though the as-built approach focuses on copying all information, it is likely that some assumptions will be made, i.e. assuming that bolts in a system are consistent sizes therefore not requiring a detailed analysis of each bolt of a similar shape and size. Some deviation from the original product may also occur due to manufacturing tolerances and errors made during the reverse engineering process. On the other hand, design intent attempts to determine the nominal performance and understand the desired relationship between components. For simple features, recovering design intent may be straight forward; however, with more complex features such as a turbine blade [111], distinguishing between manufacturing variations and design intent becomes significantly more difficult, or in other words, the likelihood of making an invalid assumption increases. Although methodologies do exist for extracting design intent when reverse engineering [112], recovering design intent is likely to require more resources and time [110] when compared to the as-built approach. Therefore, experience with reverse engineering would help in selecting an appropriate extraction strategy.

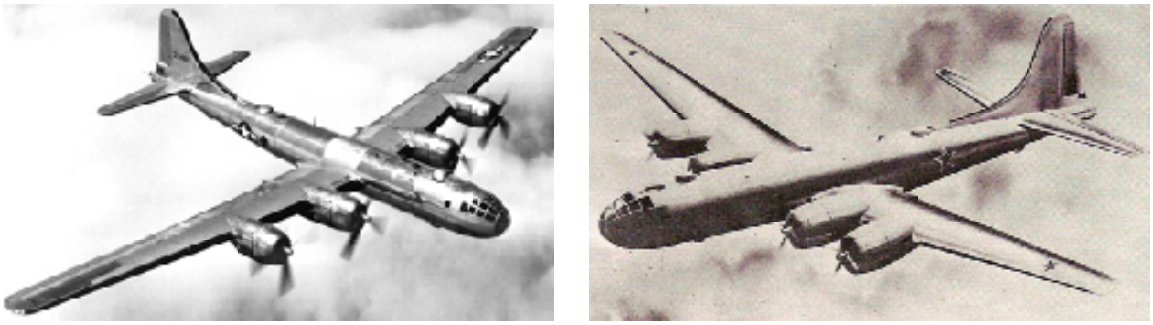

(a) United States Air Force B-29 bomber [30, 113] (b) Soviet Union Tupolev Tu-4 bomber [114]

Figure 3.3: Example of reverse engineering from WWII; The Tu-4 is a reverse engineered copy of the B-29

A well-known historical example that illustrates this type of barrier to reverse engineering occurred during World War II. After a forced landing in the former Soviet Union, an American

B-29 bomber, pictured in Fig. 3.3(a), was reverse engineered by the Soviets to yield the Tupolev Tu-4 bomber, shown in Fig. 3.3(b). Josef Stalin ordered that the downed B-29 (eventually, a total of four such aircraft came under Soviet control) be copied *exactly* [30, 31], so as to ensure that all the separate components would assemble correctly. It has even been rumored that existing damage on the B-29 fuselage [115] and manufacturing defects such as a small, misplaced rivet hole on the B-29 left wing [31] were incorporated into the original Tu-4 design. This would indicate that the Soviets took more of an as-built approach to reverse engineering the B-29. As a result, the Tu-4 is nearly an exact replica of the B-29, with the exception of some subsystems such as the cannons [30].

Additionally, the Soviet's thought it beneficial to extract information in the native units of the design (English units). Therefore, the Soviets needed to buy measuring equipment in Canada, England, and the United States and retrain thousands of engineers and technicians to work with the new measurement system [31]. Although the magnitude of the total barrier to reverse engineer the B-29 was large, the Soviets were able to utilize nearly unlimited resources in conjunction with enough skill to successfully reverse engineer the B-29.

The fundamental principles to understand about the barriers associated with the skill of the reverse engineering team can be summarized with the following:

- A reverse engineering team is more likely to succeed if they have a basic understanding of the science being analyzed *and* a familiarity with the process and tools of reverse engineering.
- Knowing which approach is needed – as-built, design intent, or a combination of both – will help maximize the return on reverse engineering investment.

Similar to technical complexity and availability of resources previously discussed, in Section 3.4 we provide a list of ways to make a product more difficult to reverse engineer.

3.4 Barriers to Reverse Engineering Tips and Guidelines

Often the market advantage achieved when a firm successfully develops an innovative product acts as the driving force for technological progress. However, if a competing firm can successfully reverse engineer the innovative product, then the market advantage of the original firm is

Table 3.1: Guidelines for implementing effective barriers to reverse engineering.

Guideline
The barrier to reverse engineering may be increased by increasing the technical complexity, increasing the resources needed, and/or increasing the skills required to reverse engineer a product or feature.
The barrier produces a benefit greater than the cost of its development, implementation, and manufacture.
The barrier requires competitors to use more resources or time to reverse engineer a product/feature than to independently develop their own.
The barrier protects a product/feature that is at risk of being reverse engineered.
The barrier's effectiveness increases when it protects a product/feature with few alternative feasible designs.
The barrier does not degrade product performance past a tolerable point determined by the designer.

quickly lost [12]. When this occurs, the incentive for innovation is reduced [52]. Therefore, it is in the best interest of original designers to design products that are difficult to reverse engineer. A product can be made difficult to reverse engineer simply by making one critical component difficult to reverse engineer. For example, consider how the performance of an entire aircraft system was influenced by a single critical component, namely the butterfly valve described in Sec. 3.3.1. As a note, components that are heavily constrained are often the best candidates for implementing barriers. The more a component is constrained by specifications or interactions with other components, the less likely competitors will be able to design around the barriers, thus requiring competitors to overcome the barriers. Other guidelines have been presented in Table 3.1 to facilitate implementation of barriers into products.

Different barriers are more effective in different scenarios. If the goal is to impede consumers from discovering what components are used in an electrical circuit, some have found an effective barrier to be encoding labels for resistors and capacitors in the electronics [87]. If the goal is to protect proprietary information, creating a product that cannot be opened without destruction of critical components may be a sufficient barrier. If the goal is to reduce skills and resources available to competitors, one may use material microstructures that are anisotropic and heteroge-

neous which are difficult to detect and reproduce. By understanding what information needs to be protected, the design team can determine if multiple small barriers will be more effective or a single large barrier. Multiple small barriers are beneficial as they require competitors to solve several problems that may be completely independent. A careful review of the metrics presented in Chapter 4 shows that the difficulty of overcoming multiple independent barriers is more than the sum of those same barriers. If only a single barrier is implemented, and competitors are able to efficiently overcome the barrier, the information may not be adequately protected. However, a single large barrier, if sufficiently difficult to overcome, may be the best protection. Some questions to be answered while exploring potential barriers and their effectiveness might include:

- What information is the barrier trying to protect?
- Are the resources available to implement the barrier? If not, are we willing to acquire the resources?
- What resources are available to competitors?
- A cost-efficient barrier may be to implement a barrier in an area that we are experienced in and competitors are not. Does such an area exist?
- When is the barrier going to be implemented into the product? Now? 2 years?
- Does there exist barriers from other products that can be directly implemented?

These types of questions help define the nature of the required barriers. Discovering this information is a critical step to strategic barrier creation.

In addition to understanding the nature of the problem, it is also important that various barrier concepts are generated in an effort to find optimal barriers to reverse engineering. While barriers vary from industry to industry, and generating effective candidate barriers will come with experience, here we list a few generic barriers that might serve as a catalyst for concept generation in specific applications:

- Design components that are difficult to access [19]
- Require unique tools to extract information [19, 104]

- Require unique skills to extract information [21]
- Avoid explicitly disclosing information such as labels on electrical components [19, 43, 87]
- Obfuscate information [87]
- Avoid standard sizes [31]
- Increase or decrease geometric scale [91, 106]
- Couple component functions [103]
- Design components that self destruct when tampered with [18, 19, 64]
- Remove evidence of manufacturing processes [4]
- Create anti-robust designs – components only work at within a small tolerance [87]
- Design components that require multiple disciplines that are typically not coupled [21]
- Design a component to appear, or have the performance, of another component [116]
- Design a critical component to look like an insignificant component [116] or vice versa [87]
- Design components that look different but have the same function [4] or vice versa [43]
- Design and implement multiple functionally-equivalent configurations of the same product [117]

While not all of these candidate barriers may always be practical to implement, the goal is to make the competitors spend time and resources on gathering information that is either not needed or require them to extract information that is expensive (either in time and/or resources). Ideally, any barrier introduced would require multiple iterations through the reverse engineering process. It is important to note that a barrier does not need to be impossible to overcome. Some believe that a barrier is sufficient when competitors spend as much time and resources as was spent in developing the original product, [18, 19] while others believe that a barrier is sufficient if it can keep competitors out of the market until market saturation [88].

3.5 Chapter Summary

In this chapter, we have explored the fundamentals of barriers that can stymie reverse engineering efforts during any step of the reverse engineering process. We have demonstrated that by increasing the complexity of a product – such as making information inaccessible and introducing complicated information interactions – we can increase the reverse engineering barrier. An example of a reverse-engineered butterfly valve that failed demonstrated the difficulty of extracting information that interacts with other information, and to extract information that is difficult to access. We next demonstrated how reverse engineering can be made more difficult when competitors lack necessary resources. Although original designers may not have direct control over the resources available to competitors, when a product design requires special tools or materials that the competitors are likely not to have, the barrier to reverse engineering is increased. An example of non-circular gears was given which shows that resources available influence the reverse engineering difficulty. Finally, we demonstrated how the skills of the reverse engineering team also affect the reverse engineering barrier. Similar to resources available, the original designers can only indirectly affect what skills are required, since they cannot control what skills the reverse engineering team will have. The example of the Soviet replicate of an American B-29 bomber demonstrates that even technically complex products can be adequately reverse engineered when the team has the proper skill set. With an anecdotal understanding of what affects barriers to reverse engineering, in the next chapter we present metrics that have been developed to systematically characterize the reverse engineering barrier. This systematic barrier characterization enables designers to quantify what barriers are most effective and efficient in specific design applications. This can even be done in conjunction with numerical optimization which is the topic of Chapter 7 .

CHAPTER 4. EVALUATING THE BARRIER AND TIME TO REVERSE ENGINEER A PRODUCT

4.1 Chapter Overview

This chapter presents a set of metrics and parameters that can be used to calculate the barrier to reverse engineer any product as well as the time required to do so. To the original designer, these numerical representations of the barrier and time can be used to strategically identify and improve product characteristics so as to increase the difficulty and time to reverse engineer them. As the metrics and parameters developed in this chapter are quantitative in nature, they can also be used in conjunction with numerical optimization techniques, thereby enabling products to be developed with a maximum reverse engineering barrier and time – at a minimum development cost. On the other hand, these quantitative measures enable competitors who reverse engineer original designs to focus their efforts on products that will result in the greatest return on investment.

4.2 A Foundation in Ohm's Law

The metrics that are developed in this chapter have a foundation in Ohm's law. Ohm's law serves as an appropriate foundation because of an interesting phenomenon which will be described later in this section. The observed phenomenon was sufficient to motivate the investigation into the application of Ohm's law to reverse engineering. The results documented herein, indicate that the developed relationships are appropriate for nearly all products and are accurate to the degree of an average error of 12.2%.

The history of Ohm's law is rich; Ohm first presented Ohm's law in an 1827 publication [118]. Since then, it has been adapted and used to meaningfully characterize the behavior of many systems including fluid systems [119], mechanical systems [120], thermal systems [121], and electrical systems [122, 123].

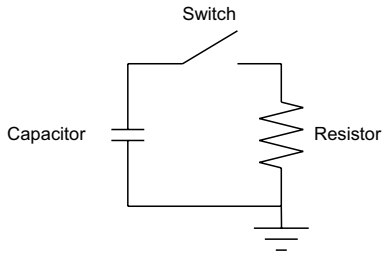

Figure 4.1: Simple resistor-capacitor circuit. The capacitor is initially fully charged and begins to discharge the instant the switch is closed at $t = 0$.

To facilitate the ensuing developments, we consider the analysis of the simple resistor-capacitor circuit shown in Fig. 4.1, and outline mathematical relationships that enable the evaluation of a circuit's resistance, R, capacitance, C, and the time, T, to drain an initially charged capacitor. We present the following fundamental principles of Ohm's Law because it is the foundation for the reverse engineering metrics and parameters presented in Sec. 4.3. Ohm's law characterizes the relationship between resistance, current, and voltage in a circuit as

$$R = \frac{V(t)}{I(t)} \tag{4.1}$$

while the capacitance, C, can be expressed as [122]

$$C = \frac{Q(t)}{V(t)} \tag{4.2}$$

where $V(t)$ represents the voltage difference across the resistor at current $I(t)$, and $Q(t)$ represents the charge stored in the capacitor. Notice that while V, I, and Q are time dependent, R and C are not. This important principle is used later in the chapter to assist the designer in specifying reverse engineering parameters.

The resistance and capacitance of the circuit can be expressed in a way that is convenient to our discussion of reverse engineering. The convenience of this form is made evident in the next section. When Q, I, and P are known and the following well-accepted [123] relationships are considered

$$V(t) = \frac{W(t)}{Q(t)} \tag{4.3}$$

$$I(t) = \frac{Q(t)}{t} \tag{4.4}$$

and

$$W(t) = P(t)t \tag{4.5}$$

it follows that

$$R = \frac{P(t)}{I(t)^2} \tag{4.6}$$

and

$$C = \frac{Q(t)I(t)}{P(t)} \tag{4.7}$$

We reiterate that this form of the resistance and capacitance relationships is particularly useful in the context of information extraction during reverse engineering.

When R and C are known for a given system, the time to discharge a capacitor can be quantified as a function of the charge remaining in the capacitor by

$$T = -RC \ln\left(\frac{Q}{Q_0}\right) \tag{4.8}$$

where it is assumed that the capacitor begins to discharge at $t = 0$, and T represents the time when the specified charge, Q, is remaining in the capacitor. An interesting characteristic of a discharging capacitor is that the discharge rate is dependent upon the voltage difference across the resistor shown in the resistor-capacitor circuit of Fig. 4.1. When the difference is large, the capacitor discharges quickly. When the difference is small, the capacitor discharges slowly. This behavior is exponential in nature.

This phenomenon is also observable in the reverse engineering of products. That is, the rate at which information can be extracted from a product is dependent upon the difference between the unextracted information that exists in a product and how much of that information is known by the individual reverse engineering the product – we hereafter refer to this difference as *information difference*. For this reason, Ohm's law is the foundation for the metrics developed in this chapter.

Table 4.1: Comparison of electrical circuit parameters and reverse engineering parameters

Electrical Circuit Parameters	Reverse Engineering Parameters
Resistance (R)	Barrier (B)
Capacitance(C)	Storage Ability (S)
Charge (Q)	Unit of Information (K)
Current (I)	Information Flow Rate (F)
Voltage (V)	Work per Information Extracted (U)
Power (P)	Power (P)

As Eq. 4.8 is an exponential relationship, the time to fully discharge the capacitor is infinite. For this reason, Q is often selected to be a positive non-zero value with the bounds

$$0 < Q \leq Q_0 \tag{4.9}$$

which results in a finite quantity of time.

Therefore, by these relationships, any resistor-capacitor circuit can be analyzed and, importantly, a prediction of time to discharge the circuit's capacitor can be made. Additionally, by using Ohm's law as a basic building block, circuits of any complexity can be analyzed using well structured, well-known, approaches such as Kirchhoff's current and voltage laws [123]. As presented in the next section, we use this same basic relationship to estimate the time required to discharge information about a product, from the product itself.

4.3 Development of Metrics and Parameters for Reverse Engineering

In this section, we present metrics and parameters for characterizing the barrier and time to reverse engineer any product. The presentation of the metrics and parameters is divided into three main parts in this section. Section 4.3.1 presents the general relationship for barrier and time to reverse engineer any product, with a brief description of the supporting parameters and metrics. Section 4.3.2 provides practical insight into specifying the needed parameters, and quantifying barriers and time for small subsets of a larger problem. Section 4.3.3 shows how the solutions to these small subsets can be reintegrated to solve the large problem.

4.3.1 General Metrics for Reverse Engineering

The barrier, B, to reverse engineer a product can be expressed as

$$B = \frac{P}{F^2} \tag{4.10}$$

where P is the power – the work per time to extract information – and F is the rate at which information can be extracted from a product. The time, T, to reverse engineer a product is

$$T = -BS\ln\left(\frac{K}{K_0}\right) \tag{4.11}$$

where K is the information contained by a product at a specific moment in time and K_0 is the information initially contained by a product. For simplicity, K is often defined as a fraction of K_0 (i.e., $K = 0.05K_0$). Specifically, the quantity K is constrained to

$$0 < K \leq K_0 \tag{4.12}$$

which ensures that Eq. 4.11 yields a finite quantity of time. The quantity S in Eq. 4.11 is evaluated as

$$S = \frac{KF}{P} \tag{4.13}$$

where S is termed *information storage ability* of a product, which is analogous to electrical capacitance. As a note, while the general form of the equations presented in this section are true for K, F, and P at any time, it is worth noting that K_0, F_0, and P_0 are typically the simplest to specify.

Similar to the electrical relationships, the reverse engineering metrics can be rearranged to solve for any variable that is known or easily determined. In this chapter, the metrics have been presented in a form that utilizes the variables K, F, and P as they are more readily determined than S, B, or T.

4.3.2 Decomposition of a Product for Barrier and Time Analysis

This section discusses how to determine the values of K, F, and P for the computation of the metrics as presented in this chapter. In a realistic setting, it can be difficult to accurately determine

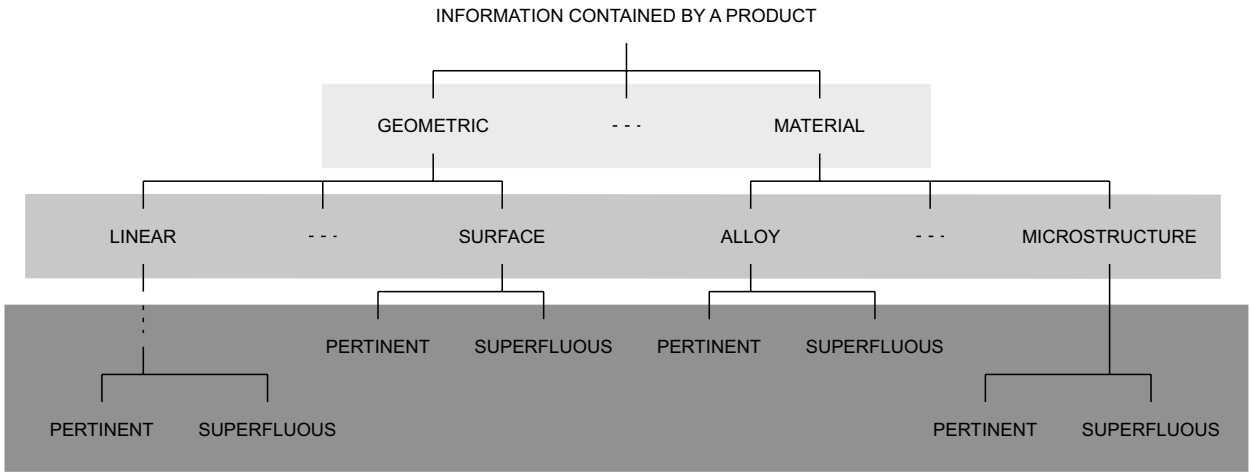

Figure 4.2: A basic taxonomy of information contained by a product.

the values of K, F, and P for the product as a whole. However, a product can be decomposed into disparate information components allowing for a more simple quantification of K, F, and P for each component. In this section, we present an approach for decomposing a product based on information components, and analyzing each component to determine B and T. In Sec. 4.3.3, we discuss how the quantities B and T for each component can be systematically combined to determine the total barrier, B^*, and the total time, T^*, to reverse the product as a whole.

We start by discussing the parameter K, and the categorization of it. Recall that K is the estimated or actual information contained by a product, and that the purpose of reverse engineering is to extract information contained by a product from the product itself. Some examples of information contained by a product include material, geometry, electrical conductivity, and color. While there are many different ways a product can be decomposed, we present a process by which products are decomposed according to categories of information contained by the product. For the purposes of the present chapter, information contained by a product, K, is categorized according to the taxonomy chart in Fig. 4.2.

As seen in the taxonomy chart, the general information contained by a product can be separated into three basic levels. At the highest level, information is categorized into information types such as geometric information, material information, and function information. The second level of categorization separates each information type into information classes. For geometry, information classes include linear dimensions and radial dimensions, among others. When appli-

cable, another categorization of geometric information class can include micro dimensions, meso dimensions, and macro dimensions. The final level of categorization on the taxonomy chart is the information sub-class which only has two categories – information that is pertinent to product performance and information that is superfluous. Generally speaking, the product should be decomposed into the minimum number of levels needed to easily specify the parameters K, F, and P for all the information contained by the product. As values for K, F, P, S, B, and T are specified or calculated for each information type, a subscript $[\,]_i$ is used to distinguish information types or information classes – depending on the level for which K, F, and P are being analyzed – while the superscript $[\,]^*$ represents the values of $[\,]$ that pertain to the product as a whole.

With the different information types defined, K is more fully defined as the *estimated*, *unextracted*, *pertinent* information contained by a product *at a specific time*. The quantity of information contained by a product is therefore a function of information type, i, and time, t. The quantity of pertinent information contained by a product is determined as the number of relevant units of information that is critical to the performance of the product.

For convenience in specifying the parameters K, F, and P, we define two reference time frames. Time in the t domain is the traditional representation of time, which captures any moment during the reverse engineering process. As it may be difficult to determine the quantity of pertinent information contained by a product, and the rate at which it is extracted, at any time t when the product contains both pertinent and superfluous information, a second reference time frame is used. This second reference time frame, in the domain τ, is a theoretical time frame when all the values of K, F, and P are known, and all information is deemed pertinent. In the τ time frame, the time-independent quantities of B and S are more easily calculated. Since these quantities are time independent, they can also be used directly in the t time frame where there exists many unknown factors.

We pause now to make a clear distinction between $K(\tau)$ and $K(t)$. The parameter $K(t)$ represents only the pertinent information contained by a product, while the parameter $K(\tau)$ represents the *total* information contained by a product, be it pertinent or superfluous. In general, the most conservative value of $K(\tau)$ is when $K(\tau)$ is set equal to $K(t)$ implying that competitors know exactly what information is pertinent and what is superfluous. The quantity $K(\tau)$ is principally used for calculating S. A similar process of using two different reference frames is often used to

determine the capacitance and resistance of electrical elements. If a resistor value is unknown, one can apply a known voltage and measure the current and determine the resistance of the system using Ohm's law. The resistance of a resistor is not dependent upon electrical current, voltage or time. Therefore the resistance may be known for all times, t, once it is known for a single time τ where a known voltage and current has been applied.

When a product is reverse engineered, no amount of superfluous information will benefit those extracting the information. For this reason we are only interested in the rate, F, at which *pertinent* information can be extracted. For a product that contains both pertinent and superfluous information, it may be difficult to determine the flow rate of pertinent information when both pertinent and superfluous information is being extracted. For this reason, the flow rate of information is determined in the τ reference frame where all information is assumed pertinent. The quantity $F(\tau)$ is principally used for calculating S and B for individual information types.

Typically when extracting information contained by a product, the information that is quickly and easily extracted is extracted at a high flow rate. At times in the information extraction process, information becomes more difficult to extract resulting in a lower flow rate. It is also apparent that the flow rate of one information type such as geometric linear dimensions may not be the same flow rate as another information type such as material grain orientations. The flow rate of information in the τ reference frame can be determined experimentally by measuring the time to extract information of particular information classes, such as geometric linear dimensions.

The measure of work per time to extract information contained by a product is characterized as power, P. It is important to note that while an individual may put forth a consistent effort, the quantity of work achieved per unit of time does not remain constant during the reverse engineering process since some information requires little work to extract while other information require significantly more work. Not only was this obvious from the empirical validations, but also the equations that define P – both in the electrical engineering perspective and in the metrics presented in this chapter – show that P decays exponentially as a function of time. The quantity P is also determined in the τ reference frame and is used in calculating both S and B. The value of P is constrained by

$$0 < P \leq 1 \tag{4.14}$$

where zero represents no work being accomplished and one represents that maximum work is accomplished per unit of time while reverse engineering a product. The value of power should be selected to accurately represent the competitor's actual performance. Often it is simplest to specify P when $t = 0$, therefore, we have specified P_0 to be a value of one for this study – which is the most conservative value of P_0. With the values of K, F, and P defined, B and S can be calculated according to Eqs. 4.10 and 4.13 for each information type i or for the product as a whole if it can be evaluated as a whole. When the product cannot be evaluated as a whole, the developments of the next section become important.

4.3.3 Integration of Analyses for Overall Product Evaluation

In this section, the total time to reverse engineer, and the total barrier to reverse engineering, are calculated by strategically combining the barrier and time to reverse engineer each information component as discussed previously. In the previous section, we discussed how a product can be decomposed into various information types to facilitate the selection of K, F, and P resulting in a B and T for each information type. Importantly, when multiple barriers exist for the same information type, those barriers may be added together in the same way electrical resistors in parallel and in series may be added together.

A different approach is required for calculating the total barrier and time to reverse engineer a product when it contains *multiple types* of information. Under this approach, each information type, including the respective barrier and storage ability, may be considered as an independent resistor-capacitor circuit. Calculating the total time to reverse engineer a product is analogous to quantifying the total time required to discharge multiple independent resistor-capacitor circuits where the number of circuits is equivalent to the number of information types contained by the product. Knowing the length of time required to discharge the independent circuits, the combined quantity of charge initially stored by the circuits, and the capacitance of the capacitors enables us to create a pseudo resistor-capacitor circuit that will result in the same quantity of time to discharge as the summed time of the independent circuits – when the pseudo circuit has the same capacitance and charge as the sum of the individual circuits. With the capacitance, charge, and time to discharge known for the pseudo circuit, the resistance of the pseudo circuit can be calculated.

To estimate the total barrier and time to reverse engineer the product as a whole, we perform a similar analysis on a pseudo product that has the same performance as one that has the considered information types combined enabling an estimation of B and T for the entire product.

The total time, T^*, to reverse engineer a product, the total information, K^*, contained by a product and the total storage ability, S^*, of a product can be determined by

$$T^* = \sum_{i=1}^{N} T_i \tag{4.15}$$

$$K^* = \sum_{i=1}^{N} K_i \tag{4.16}$$

and

$$S^* = \sum_{i=1}^{N} S_i \tag{4.17}$$

where N is the quantity of information types the product has been decomposed into.

When individual information types are analyzed, the known values include F and P. With the pseudo product, however, the flow rate is calculated by

$$F^* = \frac{K^*}{T^*} \tag{4.18}$$

which enables P^* to be calculated as

$$P^* = \frac{K^* F^*}{S^*} \tag{4.19}$$

Note that Eq. 4.19 is obtained by rearranging Eq. 4.13 and solving for P.

Only now that the effective rate at which information can be extracted from the pseudo product and the power required to extract information are known, the effective barrier for the entire product can be determined by using Eq. 4.10. It is important to note that the barrier and time to reverse engineer a product are dependent upon skills and resources available (both affecting the flow rate of information). Therefore the barrier to reverse engineer a product may vary depending upon the group performing the reverse engineering activities [103]. In general, the metrics presented in this chapter will be more accurate if the individual reverse engineering is familiar with the reverse engineering process, the tools to be used while extracting information, and has a gen-

eral understanding of the product being reverse engineered since the rate of information extraction often changes rapidly for those learning new processes or tools.

4.4 Model Limitations and Sensitivity Analysis

In this section we present the limitations for the reverse engineering metrics presented in this chapter as well as a sensitivity analysis of the input parameters.

The accuracy of the time and barrier to reverse engineer a product is dependent upon accurate selection of the parameters K, F, and P. Depending upon the reverse engineering perspective taken, some parameters may be more accurate lending to a better estimation of the time and barrier to reverse engineer a product. Recall that there are at least two practical reverse engineering perspectives: that of the original designer who seeks to determine, and even maximize, the difficultly to reverse engineer their product; and that of the competitor who seeks to reverse engineer the innovative product.

When the original designer uses the relationships presented in this chapter, he/she is able to accurately determine the actual quantity of pertinent information, K, contained by the product but will only be able to estimate the rate at which the competitor can extract information, F. The competitors, on the other hand, will be able to accurately determine the rate at which they (the competitors) can extract information, F, but will be forced to estimate the initial quantity of pertinent information contained by the product. Additionally, it may not be obvious to the competitor what information is pertinent and what is superfluous – especially if the designers developed the product to be difficult to reverse engineer. It is likely that the original designers can estimate information extraction rate for the competitors more accurately than the competitors can estimate the quantity of pertinent information contained by a product. A simple approach would be for the original designer to specify a flow rate of information extraction based on their own skill and motivation, as it is likely that their competitors have similar skills and motivation. Also, as discussed in Sec. 4.5, products must be of a sufficient complexity to ensure accurate estimations of B and T.

There are also limitations regarding the input parameter P. In this chapter, we present $P_0 = 1$ for all of the presented examples. This is because the conditions defining $P_0 = 1$ can be understood in terms of product development which involves a maximum effort being put forth

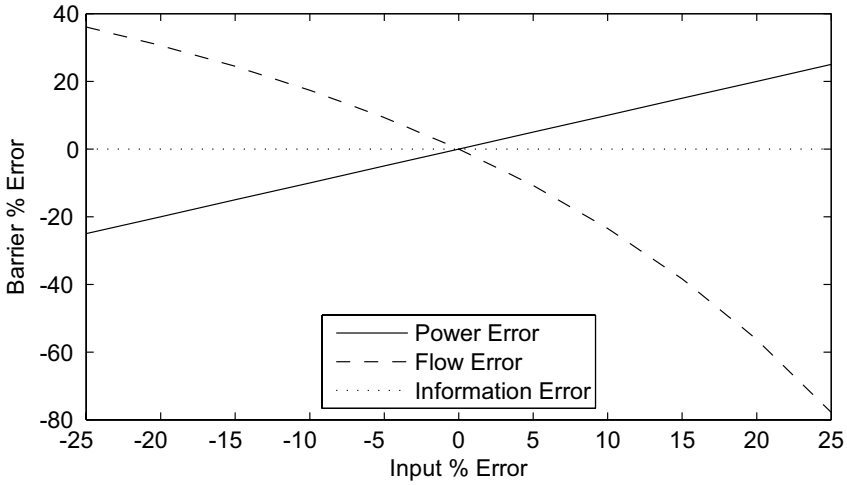

Figure 4.3: First order sensitivity analysis of the reverse engineering barrier.

with maximum work achieved. Unfortunately, the conditions defining P less than one, are not yet understood and are the focus of a separate study by the authors. Fortunately, the conditions defining $P_0 = 1$ are also the most conservative. It is additionally beneficial that the term P, does not affect the time estimation. The parameter P cancels out in the T equations therefore negating any error that may be introduced due to a poor selection of P, however, the barrier estimation is still affected.

The first order sensitivity analysis confirms this notion and shows the sensitivity of B and T to the input parameters which may be seen in Figures 4.3 and 4.4 which present the percent error of the calculated B and T, respectively, with respect to the error of the input parameters. As can be seen from the figures, the flow rate of information extraction generally has the largest impact on the accuracy of the barrier and time estimations. Therefore, it is likely most beneficial to ensure that the flow rate is accurate. In our studies we have found that a typical F error has been found to be $+/-5\%$ when F is determined by the methods outlined in this chapter.

4.5 Empirical Validation of Developed Metrics

In this section, we present an empirical study with the purpose of showing that the time and barrier to reverse engineering can be estimated by the relationships presented in this chapter

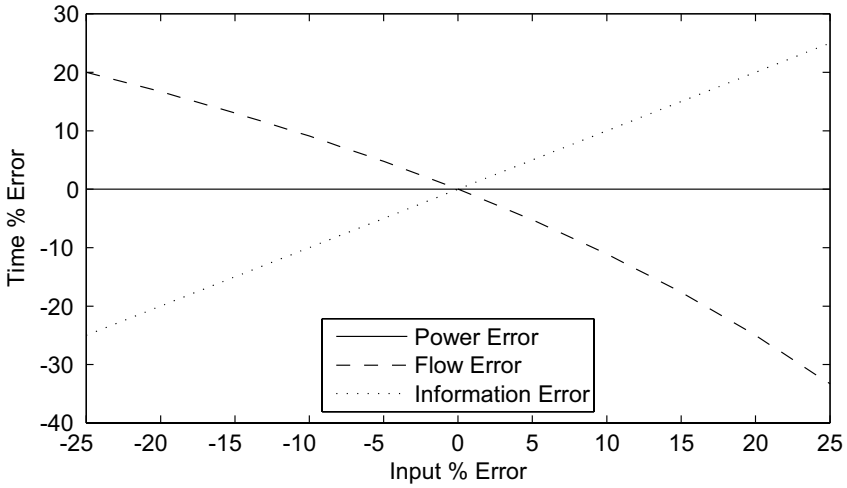

Figure 4.4: First order sensitivity analysis of the time to reverse engineering a product.

for products of sufficient complexity. For the empirical studies presented here, only geometric information is considered and K is assumed to be $0.05K_0$ (see Eq. 4.11).

For any information type, the time to extract a unit of information varies from unit of information to unit of information (within a product) and from product to product. An effective and efficient way to handle the differing times is to determine an individual's general rate of information extraction; by general we mean valid for all products of sufficient complexity. As a note, this extraction rate is the rate of information extraction $F(\tau)$ as described in Section 4.3.2. We obtain $F(\tau)$ for geometric information experimentally by issuing a uniform dimension extraction test. The test is set up to allow the individual to familiarize themselves with the dimension to be extracted then instructed to extract that dimension with a measurement tool while the time is recorded. This process is repeated multiple times for different dimensions to obtain an average dimension extraction rate of the individual using the measurement tool – a rate that is independent of time spent developing the dimension extraction sequence or checking to ensure all dimensions have been extracted. The dimension extraction rate (F) is then used in Eq. 4.10 enabling calculation of T by Eq. 4.11 to estimate the time to reverse engineer any product of sufficient complexity as discussed in this section. The accuracy of the exponential time estimations are dependent upon accurate measurement of the information extraction rate. When the actual information extraction rate is known, the estimated time is the same as the actual time to reverse engineer a product. The

Figure 4.5: Part 127 as presented in Sec. 4.5.

test we use has been found to be an adequate measure of information flow rates resulting in time estimations with an average error of 12.2%.

To illustrate, four individuals were asked to reverse engineer Part 127 and Part 128 as seen in Fig. 4.5 and Fig. 4.6, respectively. Before beginning the reverse engineering process, the information extraction rate, F, was determined for each individual by the process outlined above, K was determined by counting the dimensions required to fully describe each part, and the initial power was selected to be $P_0 = 1$ assuming that individuals put forth a maximum effort with maximum work achieved. The individuals, without knowing the values of K, F, and P, were then instructed to extract and record the dimensions with enough detail that the product could be recreated if needed.

The plots seen in Fig. 4.7 and Fig. 4.8 are the results of a single individual reverse engineering each product and compared to the linear and exponential time approximations. The linear relationship is defined as

$$T = \frac{K}{F} \tag{4.20}$$

where the information extraction rate (F) of the individual is the slope and the number of dimensions (K) to be extracted is the y-intercept on a plot of dimensions versus time. While the plots are for a single individual, they are representative of all the individuals that reverse engineered the products and are consistent with other tests we have performed. The data in the plots has been re-

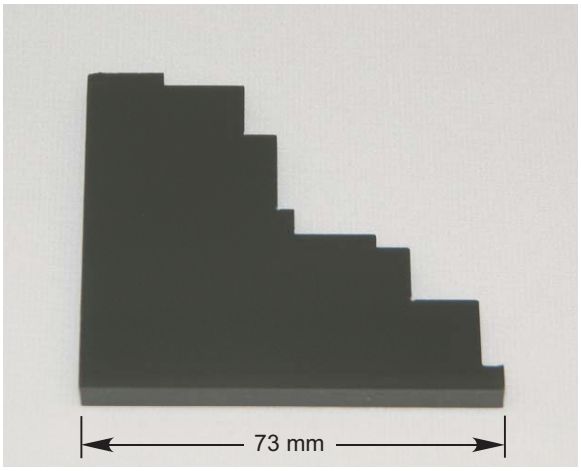

Figure 4.6: Part 128 as presented in Sec. 4.5.

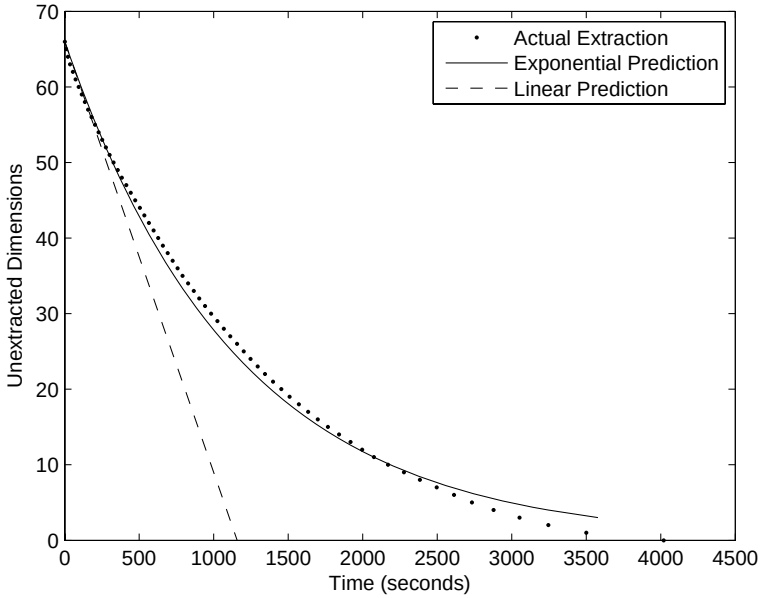

Figure 4.7: Plot of unextracted dimensions remaining in Part 127 versus time as compared to the linear and exponential time predictions for Individual 1.

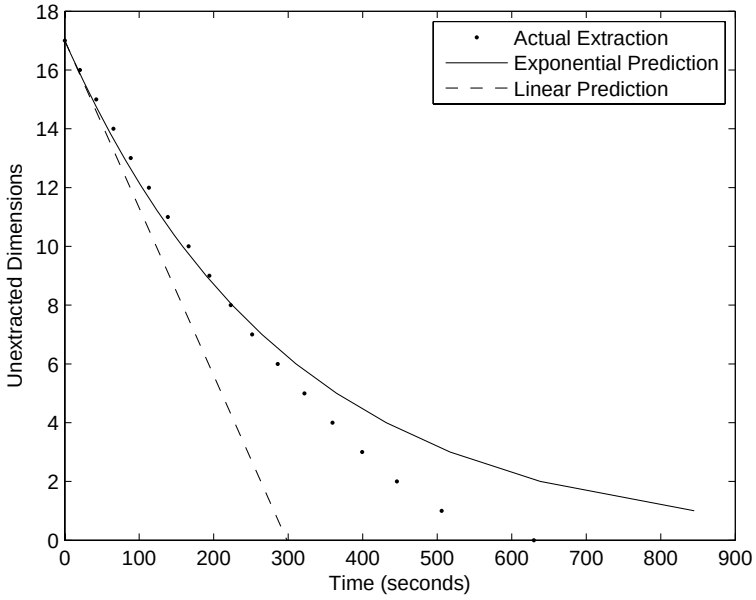

Figure 4.8: Plot of unextracted dimensions remaining in Part 128 versus time as compared to the linear and exponential time predictions for Individual 1.

Table 4.2: Table of predicted and actual times to extract geometric information from Part 127. Time is in seconds.

Individual	**Actual Time**	**Linear Prediction**	**Linear % Error**	**Exponential Prediction**	**Exponential % Error**	**Barrier**
1	4020	1158	-71.20%	3579	-10.97%	307.8
2	3473	847	-75.60%	2656	-23.51%	339.2
3	1367	517	-62.19%	1433	4.84%	260.9
4	2201	826	-62.48%	2323	5.55%	272.8

arranged according to the time to extract each dimension - with the shortest times plotted first - and are not plotted in the order of dimension extraction. Tables 4.2 and 4.3 present the predicted time to reverse engineer each product, for each individual, as well as the calculated barrier to reverse engineering. From Tables 4.2 and 4.3 we see that the barrier to reverse engineering is the same for both parts for each individual. This is due to the fact that the barrier is only dependent upon the individual and the type of information being extracted and not dependent upon the quantity of information extracted.

Table 4.3: Table of predicted and actual times to extract geometric information from Part 128. Time is in seconds.

Individual	Actual Time	Linear Prediction	Linear % Error	Exponential Prediction	Exponential % Error	Barrier
1	629	298	-52.65%	845	34.16%	307.8
2	568	298	-44.48%	887	56.20%	339.2
3	595	242	-59.28%	656	10.27%	260.9
4	522	264	-49.33%	733	40.49%	272.8

To determine the validity of the relationships presented, multiple individuals have reverse engineered multiple products resulting in over fifty sets of data for geometric information extraction. By observation and data analysis, we have verified that the time to reverse engineer the geometry of a product can be approximated by an exponential relationship. We have also observed that simple products tend to be less accurately estimated by the exponential relationship. Part 128 was specifically selected to test the exponential relationship near the limits of application and it may be seen that a linear approximation may be more accurate for the simplest of parts. However, Part 127, while still relatively simple, has been found to be sufficiently complex to be accurately estimated by the exponential relationship. As a note, the calculated error does not include the error associated with parts that are not sufficiently complex such as Part 128.

Products of higher degrees of complexity have also been analyzed and have also been found to be accurately represented by the exponential relationship. To illustrate this, we briefly discuss the reverse engineering of Apple Inc.'s recently released computer keyboard as seen in Figs. 4.9 and 4.10. As with the previous examples, we will only reverse engineer geometry and do not reverse engineer the material properties or the keyboard electronics. However, if the flow rate of information extraction is determined for extracting material properties and analysis of electronics, the same relationships used for estimating the time and barrier to extract geometric information can also be used to estimate the time and barrier to extract information about material properties and the electronics of a system.

We reverse engineered the keyboard to the degree that we could recreate keyboard parts that would be interchangeable with the current product. In order to fully extract the geometric information contained by the keyboard, some disassembly was required. While disassembly time

Figure 4.9: Figure of keyboard before disassembly.

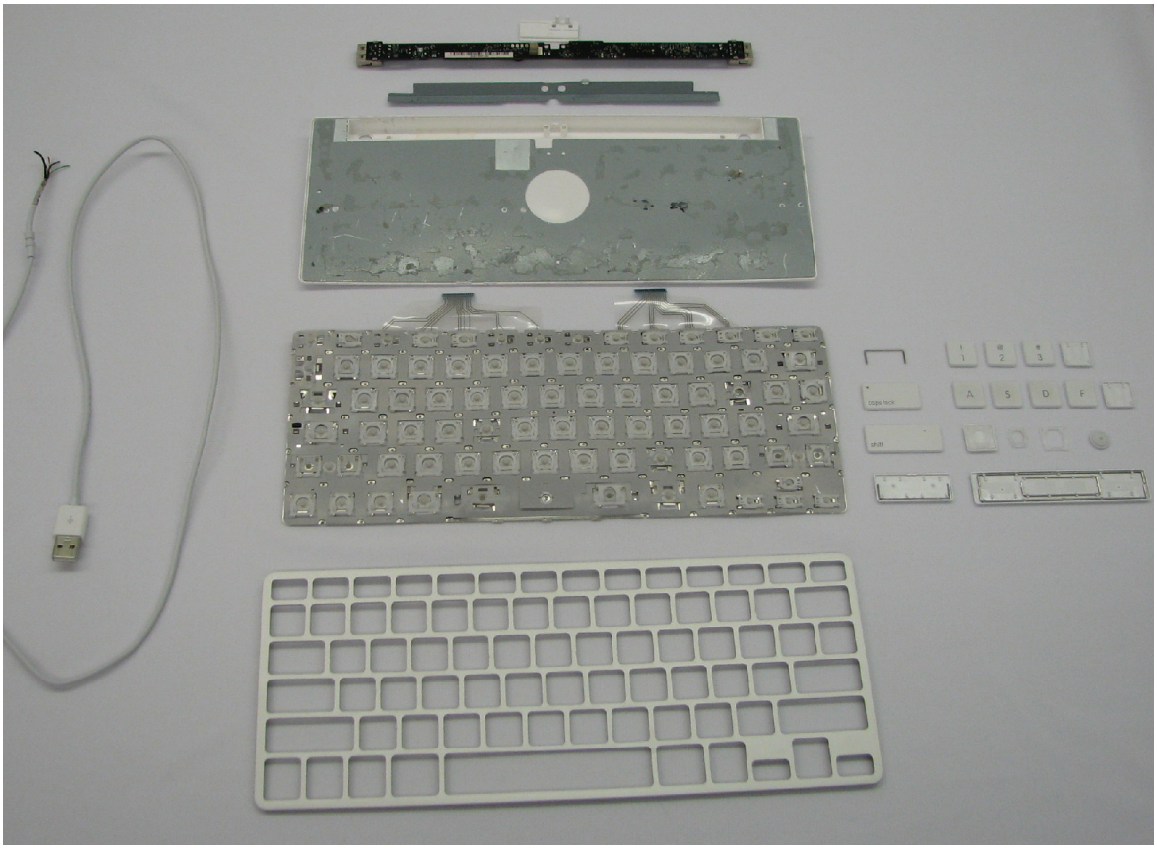

Figure 4.10: Figure of keyboard disassembled.

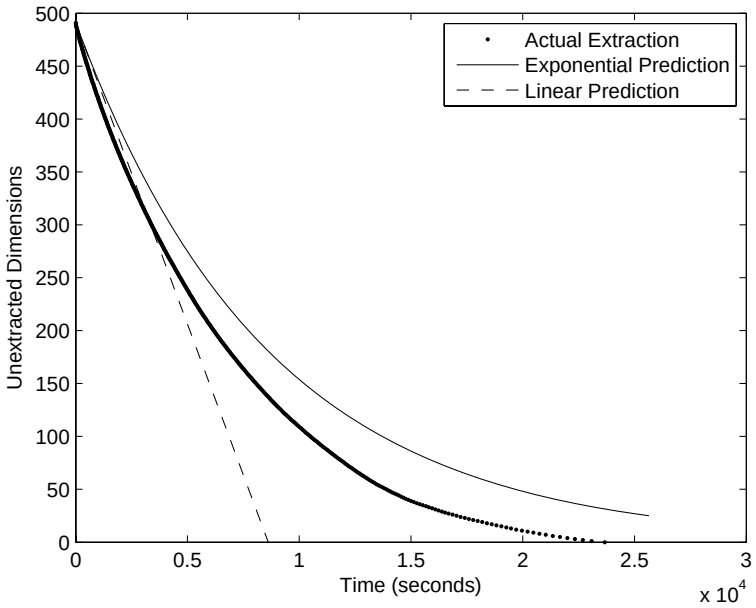

Figure 4.11: Plot of unextracted dimensions remaining in keyboard versus time as compared to the linear and exponential time predictions.

may be important to quantify, [124, 125] it was not the focus of this study or of the developed metrics. Therefore, the keyboard was considered disassembled when reverse engineering began. Utilizing the relationships presented in this chapter to estimate the time and barrier to reverse engineer the keyboard resulted in a barrier of 307.8 and an estimated time of $25,649$ seconds. In actuality, it took $23,667$ seconds to reverse engineer the keyboard - an 8.38% error when compared to the predicted time of $25,649$ seconds. The estimated and measured times were determined independently so that neither influenced the other. Figure 4.11 compares the actual time to reverse engineer the keyboard with the exponential and linear predictions.

4.6 Chapter Summary

In this chapter, we have presented general metrics for evaluating the barrier and time to reverse engineer a product. We have also defined supporting metrics and parameters for evaluating the barrier and time. The metrics and parameters presented are adapted from Ohm's Law and are based on resistor-capacitor circuits and capacitor discharge time estimates. The effectiveness of the metrics outlined in this chapter has also been demonstrated with an empirical study.

The presented relationships enable a systematic and consistent comparison of products – pre or post production. This brings the designer a distinct ability to quantify the amount of time to reverse engineer different variations of a product while in the early design stage. Such quantification can readily support trade-off studies of production costs with market strategies. The ability to quantify the barrier and time to reverse engineer a product early in the design process enables designers to strategically implement product features that will increase the difficulty of reverse engineering the product, while minimizing implementation cost. For those reverse engineering, the systematic estimation of the reverse engineering time facilitates management decisions such as reverse engineering costs, project timelines, and market strategies.

CHAPTER 5. CHARACTERIZING THE EFFECTS OF LEARNING WHEN REVERSE ENGINEERING MULTIPLE SAMPLES OF THE SAME PRODUCT

5.1 Chapter Overview

The work presented in this chapter builds upon the reverse engineering metrics that are developed and presented in Chapter 4. Specifically, this chapter addresses the issue of characterizing the reverse engineering time and barrier when multiple samples of the same product are reverse engineered. Frequently in practice, a product will be repetitively reverse engineered to increase accuracy, extract tolerances, or to gather additional information from the product. In this chapter, we introduce metrics that (i) characterize learning in the reverse engineering process as additional product samples are evaluated, and (ii) estimate the total time to reverse engineer multiple samples of the same product. Additionally, an example of reverse engineering parts from a control valve is introduced to illustrate how to use the newly developed metrics and to serve as empirical validation.

5.2 Introduction and Literature Survey

When one product is reverse engineered, the part, in most cases, is just a single member of a distributed population, where variation is undoubtedly present [45]. As a result, an appropriate statistical analysis needs to be performed in order to test hypotheses on the true nominal values of information contained by a product. This involves determining an adequate product sample size to be reverse engineered based on a predetermined confidence level and acceptable error [126]. As the number of available parts for the sample size increases, so does the accuracy of the extracted data [127].

Another purpose for reverse engineering a product multiple times is to reverse engineer geometric tolerance data. Reverse engineering with the intent of reconstructing a product for future manufacturing is incomplete until tolerances are allocated to the product. If the dimensions

of a product vary more than the allowable tolerances, then the probability of the product failing to assemble or function correctly increases. This will inevitably lead to costly repairs, poor performance, and dissatisfied customers, all of which diminish the product's effectiveness [128]. Optimally allocating tolerances is a typical, yet challenging task in engineering design. An overview of the many methods used to allocate tolerances when designing a product can be found in [129]. When reverse engineering, the process becomes more difficult [130], as it requires a significant amount of skill and experience to match the original tolerances of a product. As a consequence, various methods have been presented in the literature to help approximate dimensional and geometric tolerances when reverse engineering [131–133]. One in particular involves performing dimensional analysis on multiple samples of the same product and comparing the results to discover possible manufacturing variations as an aid to establishing tolerances [133].

If multiple samples of the same product are reverse engineered, then learning will take place – knowledge about the product's form, composition, and function will be retained from previous iterations of the process. Learning can be defined as *change in behavior that occurs as a result of experience* [134]. Learning can occur at an individual level or on an organizational level [135]. Several researchers have characterized the learning curve for various industrial settings and determined the factors that influence learning [136, 137]. However, research has not been published regarding learning during reverse engineering.

In this chapter, we introduce parameters and metrics that (i) characterize a person's learning capability in the context of reverse engineering, and (ii) predict the total barrier and time to reverse engineer multiple samples of the same product. To do this, we begin by presenting metrics that are capable of estimating the time and barrier of tolerance extraction in Sec. 5.3. Demonstrating the use of the metrics, including metric validity and limitations, is illustrated by a case study presented in Sec. 5.4. Concluding remarks are provided in Sec. 8.6.

5.3 Metrics Development

In this section, we develop the metrics for predicting the time and barrier to reverse engineer multiple samples of the same product. The presentation of the metrics is divided into three main parts. In Sec. 5.3.1 we discuss how the flow rate of information changes during the process of reverse engineering multiple samples of the same product. In Sec. 5.3.2 we develop and present

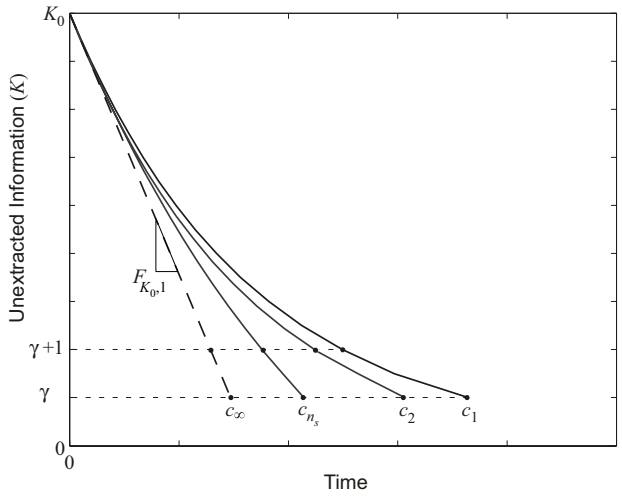

Figure 5.1: Unextracted information in a product as a function of time. The curves for multiple reverse engineering samples are compared.

the metrics. Finally, in Sec. 5.3.3, we explain how to use the metrics to estimate the time to reverse engineer multiple samples of the same product.

5.3.1 The Behavior of Information Flow Rates when Reverse Engineering

When we reverse engineer a product, we extract information from that product. Typically, these pieces of information are discrete in nature; thus, it is advantageous to look at K and F at discrete values of K, which we call *unextracted information levels*. Additionally, the values of F will vary depending on the reverse engineering sample (i.e., how many samples of the product have been reverse engineered). Therefore, we will use the subscripts $[\,]_{k,s}$ to distinguish unextracted information level, k, and reverse engineering sample, s. For example, the information flow rate when three dimensions still need to be measured on the fourth product sample would be denoted $F_{3,4}$.

The way in which the flow of information varies when reverse engineering is illustrated in Fig. 5.1, which plots the amount of unextracted information in a product as a function of time for several reverse engineering samples of the same product. The first curve, labeled c_1, represents the first product sample that is reverse engineered. This curve resembles an exponential decaying relationship and is derived in Chapter 4. When $K = K_0$, the slope of c_1 is relatively steep, which means the extraction of information per unit time, or information flow rate, is large in comparison

to when $K = \gamma$, where γ is the lowest unextracted information level of interest. This variation in information flow rate can be credited to the fact that reverse engineering encompasses more than just measuring dimensions, for example. It includes secondary procedures such as deciding which dimensions are pertinent, finding the dimensions in the product, documenting or recording the dimensions on a hand drawing or in a CAD system, and verifying that all the needed dimensions have been extracted. When all of the aforementioned steps are performed, the flow rate of information is low, in comparison to when none or few of the secondary procedures are necessary for information extraction. This implies that the fastest, or largest, flow rate occurs when information is simply extracted without utilizing any secondary procedures.

When a person reverse engineers a second sample of a product, he or she utilizes some of the knowledge gained while reverse engineering the product the first time, obviating some of the steps of the reverse engineering process. For example, if someone is reverse engineering the geometry of a piston for the second time, the pertinent dimensions of the piston have already been determined during the first reverse engineering sample, as well as an appropriate documentation procedure. This is characterized in Fig. 5.1, where the slopes along the curve for the second product sample, labeled c_2, are generally steeper than those of c_1, resulting in less total time to reverse engineer the product. Reverse engineering additional samples, denoted c_{n_s} in the plot, will yield similar results – flow rates will continue to increase and the reverse engineering time will continue to decrease. If the reverse engineering sample size is sufficiently large, then the sample curves will approach the dashed line in the plot, marked as c_∞. This line represents the reverse engineering process when it has achieved maximum efficiency.

The slope of c_∞ in Fig. 5.1 is the fastest theoretical flow rate or the *initial flow rate*, $F_{K_0,1}$, and is described in detail in [14]. We also assume that the initial flow rate is the initial slope of each sample curve, or

$$F_{K_0,s} = F_{K_0,1}, \ \forall \ s \ \in \{1,2,\ldots,n_s\} \tag{5.1}$$

where n_s is the number of reverse engineering samples. Based on this assumption, the initial flow rate remains the same for an individual, regardless of reverse engineering sample. Moreover, information requiring less extraction time is extracted from a product *first*, followed sequentially by units of information requiring more time. This may or may not happen in practice; regardless,

when empirical data gathered by the authors is rearranged according to the time to extract each unit of information – with the shortest times placed first – this relationship generally holds true (see Sec. 5.4).

The horizontal dashed lines in Fig. 5.1 help to visually track unextracted information levels along different sample curves. The lowest unextracted information level in the plot is γ, which is the closest integer value of K for which the following is approximately true

$$\gamma = 0.05 * K_0 \tag{5.2}$$

This is the value typically used for K to predict the total time to reverse engineer a product once [14]. If the information flow rates of different samples at any unextracted information level, K_0 through γ, are compared to one another, we assume the following to be true

$$|F_{k,1}| \leq |F_{k,s}| \leq |F_{k,n_s}|, \begin{cases} \forall\, k \in \{\gamma, \gamma+1, \ldots, K_0\} \\ \forall\, s \in \{1, 2, \ldots, n_s\} \end{cases} \tag{5.3}$$

In other words, the flow rate at a particular unextracted information level k is bound by the flow rate of the first reverse engineering sample, $F_{k,1}$, and the flow rate of the last reverse engineering sample, F_{k,n_s}. Additionally, as stated above, if the product sample size is sufficiently large, the curves in the plot approach a linear prediction with the slope of the initial flow rate, $F_{K_0,1}$, or

$$\lim_{s \to \infty} F_{k,s} = F_{K_0,1},\ \forall\, k \in \{\gamma, \gamma+1, \ldots, K_0\} \tag{5.4}$$

This suggests that as an individual learns while reverse engineering multiple samples of the same product, they drive the flow of information towards maximum efficiency.

The question remains as to how quickly (in terms of reverse engineering samples) information flow rates approach the initial flow rate. Some individuals are slow learners with regards to reverse engineering, while others are not. In the next section, we introduce a parameter, reflective of the rate at which a person can learn, to help characterize this behavior.

5.3.2 Metrics for Reverse Engineering Multiple Samples of the Same Product

The metrics for reverse engineering multiple samples of the same product are derived from the first order response of a simple resistor-inductor circuit [123, 138]. Thus, we are extending the electrical analogy presented in Chapter 4 to include inductance, for two reasons: (i) we have observed that when reverse engineering multiple samples of the same product, the flow of information at an unextracted information level behaves like the first order response of electrical current in a resistor-inductor circuit and (ii) the inductance in a circuit provides an applicable parameter that can be used to characterize how quickly a person learns while reverse engineering.

The flow rate of information for any sample and unextracted information level, $F_{k,s}$, is calculated as

$$F_{k,s} = F_{k,1}e^{-(s-1)*B/Z} + F_{K_0,1}\left(1 - e^{-(s-1)*B/Z}\right) \tag{5.5}$$

where B is the barrier to reverse engineering and Z is termed the *learning factor*. The flow rate from the first reverse engineering sample at any unextracted information level, k, is denoted by $F_{k,1}$. This value is determined by solving for K from the relationship for T (refer to Eq. 4.11), and substituting into $F = dK/dt$, which yields

$$F_{k,1} = \frac{-K_0}{BS}e^{-T/BS} \tag{5.6}$$

This equation can be further simplified by substituting the relationships for B, S, and T in (refer to Eq. 4.10, Eq. 4.13, and Eq. 4.11 respectively) allowing $F_{k,1}$ to be rewritten as

$$F_{k,1} = \frac{F_{K_0,1} * k}{K_0} \tag{5.7}$$

where k has been substituted for K because we are interested in the flow rate at discrete, unextracted information levels. In this form, the first flow rate for each unextracted information level can easily be calculated and used in Eq. 5.5. Notice that when $s = 1$ in Eq. 5.5, the second term on the right hand side of the equation drops out and Eq. 5.5 simplifies to $F_{k,s} = F_{k,1}$. On the other hand, as s approaches infinity, Eq. 5.5 simplifies to $F_{k,s} = F_{K_0,1}$. This is the same behavior for information flow rates that we described in Sec. 5.3.1.

The learning factor, Z, is a measure of a person's ability to learn while reverse engineering multiple samples of the same product, given a particular measurement tool. A large Z indicates a high resistance to change in information flow rates, or in other words, it is difficult for the individual/team performing the reverse engineering to utilize information gained during previous iterations of the process. A small Z may indicate that the process is nearly automated, meaning that secondary reverse engineering procedures do not need to be repeated after the first reverse engineering sample. An example would be using a coordinate measuring machine to automatically scan geometry or using a scanning electron microscope to extract the material microstructure from several samples – the set up procedure is only done once, and then the process is automated. If all other parameters are equal, a person with a smaller Z will reverse engineer multiple samples of the same product quicker than someone with a larger Z.

The learning factor is calculated as

$$Z = \frac{B\left(F_{K_0,1} - F_{k,s}\right)}{dF_{k,s}/ds} \tag{5.8}$$

where $dF_{k,s}/ds$ indicates the change in information flow rate, $F_{k,s}$, per reverse engineering sample, s, for any flow rate besides the initial flow rate, $F_{K_0,1}$. The parameters that comprise Z are experimentally determined for an individual; more information on how this is done is provided in Sec. 5.3.3. A similar equation to Eq. 5.8 exists for inductance in a simple resistor-inductor circuit. In fact, the learning factor is analogous to inductance in an electrical circuit – both measure resistance to change in flow rates (electrical current or information flow rates). We note that Z does not change as information flow rates increase, nor is it dependent on the unextracted information level or reverse engineering sample – we assume that a person's *aptitude* to learn remains constant during the reverse engineering process. Again, this is similar to an inductor in an electrical circuit, where the inductance value remains constant, regardless of the electrical current flowing through it.

With a relationship defined for how the flow rate of information during reverse engineering changes, we can now calculate the total time to reverse engineer multiple samples of the same product as

$$T = -BS\ln\left(\gamma/K_0\right) + \sum_{(s=2)}^{n_s}\sum_{(k=\gamma+1)}^{K_0}\frac{1}{F_{k,s}} \tag{5.9}$$

where the 1 in the numerator represents one unit of information, ensuring that T has units of time. The first term on the right hand side of Eq. 5.9, $-BS\ln(\gamma/K_0)$, represents the time to reverse engineer the first product sample. The second term of the equation accounts for all remaining samples; thus, the outer summation is initialized at $s=2$ and continues until n_s. For each sample, the reciprocal of $F_{k,s}$ is summed for all unextracted information levels starting with $k=\gamma+1$ up through K_0. The flow rates at the unextracted information level γ are not included because this is a forward difference approximation, and inclusion of the flow rates at the lowest unextracted information level would overestimate the total time. The parameters and metrics that make up Eq. 5.9 can easily be calculated for any individual or product. As a result, the task of accurately estimating the time to reverse engineer a product becomes simple and straightforward. More information on how this is to be done is included in Sec. 5.3.3.

The time required for each individual reverse engineering sample (beyond the first) can also be determined by modifying Eq. 5.9 to get

$$\hat{T}_s = \sum_{k=\gamma+1}^{K_0} \frac{1}{F_{k,s}} \tag{5.10}$$

where the subscript s distinguishes the reverse engineering sample in question and the 1 in the numerator signifies one unit of information. It is important to note that the metrics developed here use discrete unextracted information levels to determine F, using Eq. 5.7. Because discrete points are used to characterize the entire curve, approximation error is introduced into the model. Therefore, to maintain a higher degree of accuracy, it is more appropriate to use the relationship for T in Eq. 4.11 for the first reverse engineering sample.

Up until this point, the metrics introduced have not considered the type of information being extracted from a product. Information type is a significant factor in reverse engineering, as the barrier and time for reverse engineering depend on the type of information that is contained in a product [14]. Each information type has a distinct initial flow rate, $F_{K_0,1}$ and learning factor, Z. Therefore, every information type needs to be considered separately. This will result in a different time to reverse engineer each information type. The total time to reverse engineer all the

information types in a product, T^*, is calculated as

$$T^* = \sum_{i=1}^{n_I} T^i \tag{5.11}$$

where the superscript $[\,]^i$ is used to distinguish information type, making T^i the time to reverse engineer one type of information as calculated with Eq. 5.9, and n_I is the total number of information types contained in the product.

The barrier to reverse engineer multiple samples of the same product is the same barrier that has been defined in Eq. 4.10. Each information type has a unique barrier; however, this barrier does not change with additional reverse engineering samples, despite the fact that information flow rates do increase. This is similar to a resistor in a resistor-inductor circuit – the value of its resistance remains the same, even though the current passing through it can change. Therefore, the effective barrier to reverse engineer multiple samples of an entire product is still calculated using the relationships presented in [14].

5.3.3 How to Use the Metrics

In this section, we explain how to use the metrics that were presented in Sec. 5.3.2 to estimate the time to reverse engineer multiple samples of the same product. This could be done in industry by original designers who are trying to protect their products, or by those performing benchmarking activities. In the first case, the designer would have the advantage of knowing how much information is contained by the product; however they would be required to estimate the initial flow rate and the number of samples used by their competitors. In the second case, the person reverse engineering the product would be required to estimate how much information is in the product, while all other parameters would be known.

The process is described by the flow chart in Fig. 5.2. To start the process, one must determine the number of information types, n_I, that are needed to reverse engineer the product. The index to count the number of information types, i, is initialized at 1.

Step 1 is to experimentally determine the initial flow rate, $F^i_{K_0,1}$, for a particular information type i [139]. This is done by using a uniform dimension extraction test. The goal of the test is to measure the average rate at which a person can extract information from a product when no

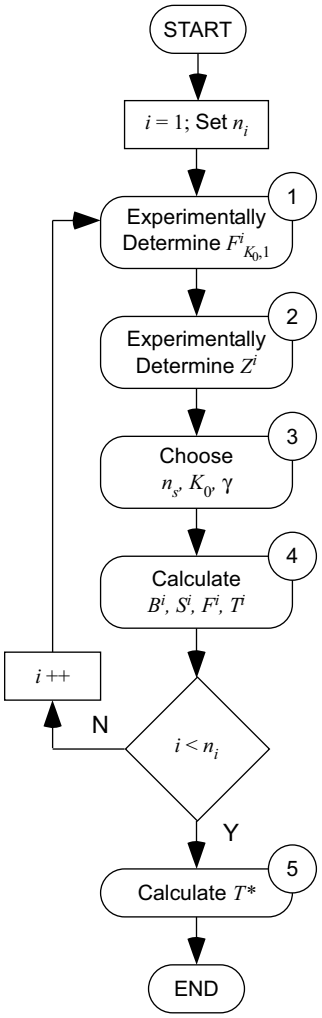

Figure 5.2: The process for predicting the time that it would take to reverse engineer several samples of the same product.

secondary reverse engineering procedures are performed. In the test, an individual is asked to familiarize themselves with a particular dimension on a product. After this is done, the individual receives a measurement tool and the time is then recorded for them to measure the dimension. The process is repeated for many different dimensions of the same information type and the extraction rates are averaged to determine $F^i_{K_0,1}$. The resulting $F^i_{K_0,1}$ determined by the test can be used to calculate the metrics in step 4 for any product that contains the appropriate information type. In practice, the test only needs to be done once and then the value for $F^i_{K_0,1}$ can be reused for information type i, or a generic database containing the initial flow rates for typical measurement tools and operator skill levels could be developed.

Step 2 is to experimentally determine and calculate the learning factor, or Z^i. It is calculated using Eq. 5.8, which requires a flow rate, $F^i_{k,s}$, other than the initial flow rate, and its associated derivative with respect to reverse engineering sample, $dF^i_{k,s}/ds$. These values are determined for an individual using a uniform dimension extraction test, similar to how $F^i_{K_0,1}$ is determined. However, in this test the person must extract dimensions from multiple product samples. During the test, the person is handed a product and asked to extract several difficult pieces of information. Then they are asked to repeat the measurements on a new sample of the same product. $F^i_{k,s}$ and $dF^i_{k,s}/ds$ are recorded, and Z^i is calculated with Eq. 5.8. It is important that the information in this test be difficult to extract, so as to emphasize differences in flow rates between samples due to actual learning that occurs in the process, and not natural human variation.

Step 3 is to choose the number of samples, n_s, and the total amount of unextracted information, K_0. With K_0 defined, γ can be calculated using Eq. 5.2. In practice, when a person reverse engineers a product, n_s will be known initially, while K_0 will not. Otherwise, for the person using these metrics to predict the reverse engineering time of their competitors, n_s must be estimated, but K_0 will be known. Accurately predicting n_s can be a challenging task, as the number of samples used for reverse engineering will vary for different products and companies; however, an estimate can be made based on a statistical analysis to determine an adequate sample size. Additionally, if the price is significantly high for one product, then n_s will likely be small.

Step 4 is to calculate the barrier, B^i, storage capability, S^i, the flow rates, F^i, and time T^i. The P, F, and K typically used to calculate B^i and S^i are $P = 1$, $F = F^i_{K_0,1}$, and $K = K_0$, respectively. Steps 1-4 are then repeated for each information type of interest in the product, after which the total time to reverse engineer the product, T^*, is then calculated in Step 5 with Eq. 5.11. Thus, the time to reverse engineer a product can be estimated, without having to actually reverse engineer the product. In the next section, we discuss the accuracy and limitations of the model with a case study.

5.4 Case Study and Validation

In this section, we present an empirical study with the purpose of showing that the time to reverse engineer multiple samples of the same product can be estimated by the relationships presented in this chapter. For this study, only geometric information was extracted and analyzed.

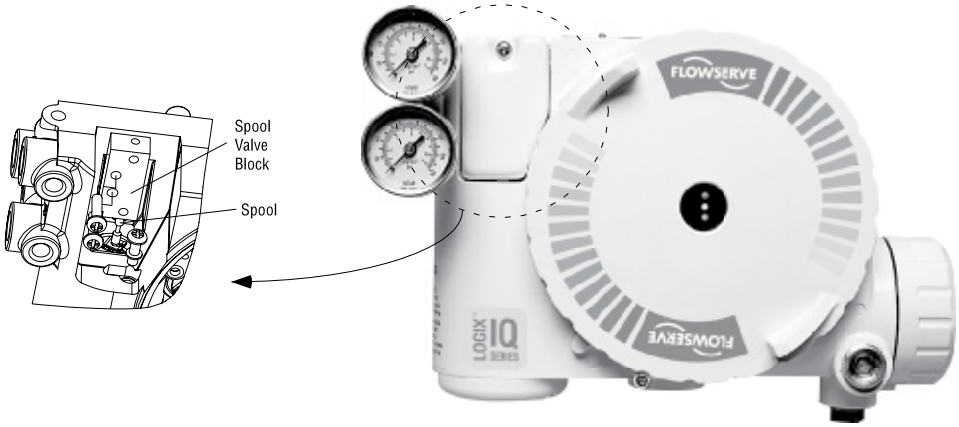

Figure 5.3: Flowserve 3400iq digital positioner with spool block valve and spool shown. Image adapted from [2].

Table 5.1: Parameters and metrics determined for geometric information of Flowserve spool and spool block valve.

Individual	Part	$F_{K_{0,1}}$ (dim/s)	Z	n_s	K_0	γ	B	S	$T^*(s)$	Actual $T^*(s)$	$\lvert\varepsilon\rvert$ (%)
#1	Spool	0.065	2127	30	24	1	236.7	1.560	13613	14611	6.8
#2	Spool	0.057	2912	10	23	1	307.8	1.311	6606	5966	10.7
#1	Block	0.065	2127	10	34	2	236.7	2.210	8179	7630	7.2
#2	Block	0.057	2912	29	35	2	307.8	1.995	21668	21791	0.6

Table 5.2: Comparison of different models to predict the time to reverse engineer multiple samples of the same product.

Individual	Part	Linear Model $\lvert\varepsilon\rvert$ (%)	Exponential Model $\lvert\varepsilon\rvert$ (%)	Combined Model $\lvert\varepsilon\rvert$ (%)	Learning Model $\lvert\varepsilon\rvert$ (%)
#1	Spool	27.3	140.9	21.7	6.8
#2	Spool	35.3	112.1	20.6	10.7
#1	Block	35.5	94.2	22.5	7.2
#2	Block	23.0	133.9	17.5	0.6
Average		30.3	120.3	20.6	6.3

Two individuals were asked to reverse engineer multiple samples of a spool valve block and its associated spool from a Flowserve Digital Positioner seen in Fig. 5.3. According to sources at Flowserve, the spool valve block and spool have been reverse engineered and imitated by competitors of Flowserve; therefore, these parts merit our attention in this study on reverse engineering.

Before beginning the reverse engineering process, the initial flow rate and learning factor of both individuals in the study were determined as described in steps 1 and 2 from Sec. 5.3.3. The individuals were then instructed to extract and record geometric dimensions using digital calipers with enough detail that the product could be recreated if needed. Multiple samples (between 10 to 30) of both parts were analyzed by the individuals while the time to reverse engineer was recorded.

Independently, the number of samples, n_s, and the total amount of unextracted information, K_0, were chosen. This enabled the calculation of the barriers to reverse engineering, storage capacities, information flow rates, and times to reverse engineer the product samples. These values, excluding the information flow rates to preserve clarity in presentation, are located in Tab. 5.1. The actual extraction times along with the errors are also listed in Tab. 5.1. As shown, the total errors ranged from -10.7% to 6.8%.

For comparison purposes, we will look at several models for predicting the time to reverse engineer multiple samples of the same product. Each model is described below and the total absolute error, $|\varepsilon|$, for each model is compared in Tab. 5.2.

Linear Model – The time for one sample predicted by this model is calculated as $\hat{T}_{lin} = (K_0 - \gamma)/F_{K_0,1}$. In other words, to calculate the total time for one sample, the quantity of information contained in a product is divided by the initial flow rate. This results in a linear relationship between K and T. The total time, T^*_{lin}, is then calculated as $T^*_{lin} = n_s * \hat{T}_{lin}$. This is the simplest model, and does not account for any variation in information flow rates. As shown in Tab. 5.2, the average absolute error when using this model was 30.3%.

Exponential Model – For this model, the total time, T^*_{exp}, is calculated as $T^*_{exp} = n_s * \hat{T}_{exp}$, where $\hat{T}_{exp}$ is determined from Eq. 4.11. This is the time that is predicted using the previous metrics [14], where learning is not accounted for. It is called the exponential model because when K is plotted against T, it resembles an exponentially decaying relationship. As stated in Sec. 5.2, this model will typically overestimate the time to reverse multiple samples of the

same product. This is especially evident for this case study, where the average $|\varepsilon|$ shown in Tab. 5.2 for the exponential model was 120.3%.

Combined Model – This model is a combination of the linear and exponential models. The total time is determined as $T^*_{com} = T^*_{exp} + (n_s - 1) * T^*_{lin}$. We note that the exact same result will occur if Z is nearly zero in the learning model. In this case study, the combined model had the second best time prediction in Tab. 5.2, with an average error of 20.6%.

Learning Model – This is the model developed in this chapter. The total time is calculated here with Eq. 5.9, because we are only dealing with one information type. Without exception, the learning model outperforms the other models for predicting the time to reverse engineer multiple samples of the same product. The learning model predicted the times with an average absolute error across all tests of 6.3% (see Tab. 5.2). The stark contrast in accuracy between the learning model and the other models suggests that learning plays an important role in reverse engineering when using manual equipment such as digital calipers to extract information from a product.

The plots in Fig. 5.4 display the actual results and model predictions for spool samples 2, 5, 10, and 30 of individual #1. While the plots are for a single individual and product, they are representative and consistent with other tests that we have performed. The combined model is not explicitly called out in the plots, because it is only a combination of the linear and exponential models, both of which are shown. As the sample number increases, the data, which is marked by the asterisks in the plot, moves away from the exponential prediction towards the linear prediction. Likewise, the learning model curve, begins at the exponential curve and moves toward the linear curve at a rate that closely matches the real data.

We note that the data in the plots have been rearranged according to the time to extract each dimension - with the shortest times plotted first - and are not plotted in the order of dimension extraction. According to our assumptions given by Eqs. 5.1, 5.3, and 5.4, the flow rates should never be larger than $F_{K_0,1}$, which is the slope of the linear prediction in Fig. 5.4; however, some of the flow rates for reverse engineering sample # 30 are clearly larger than $F_{K_0,1}$. This is explained by how we obtained $F_{K_0,1}$ – by averaging the quickest times to extract several simple dimensions from an arbitrary product (see Sec. 5.3.3 Step 1). Since the $F_{K_0,1}$ used here is an average, it is

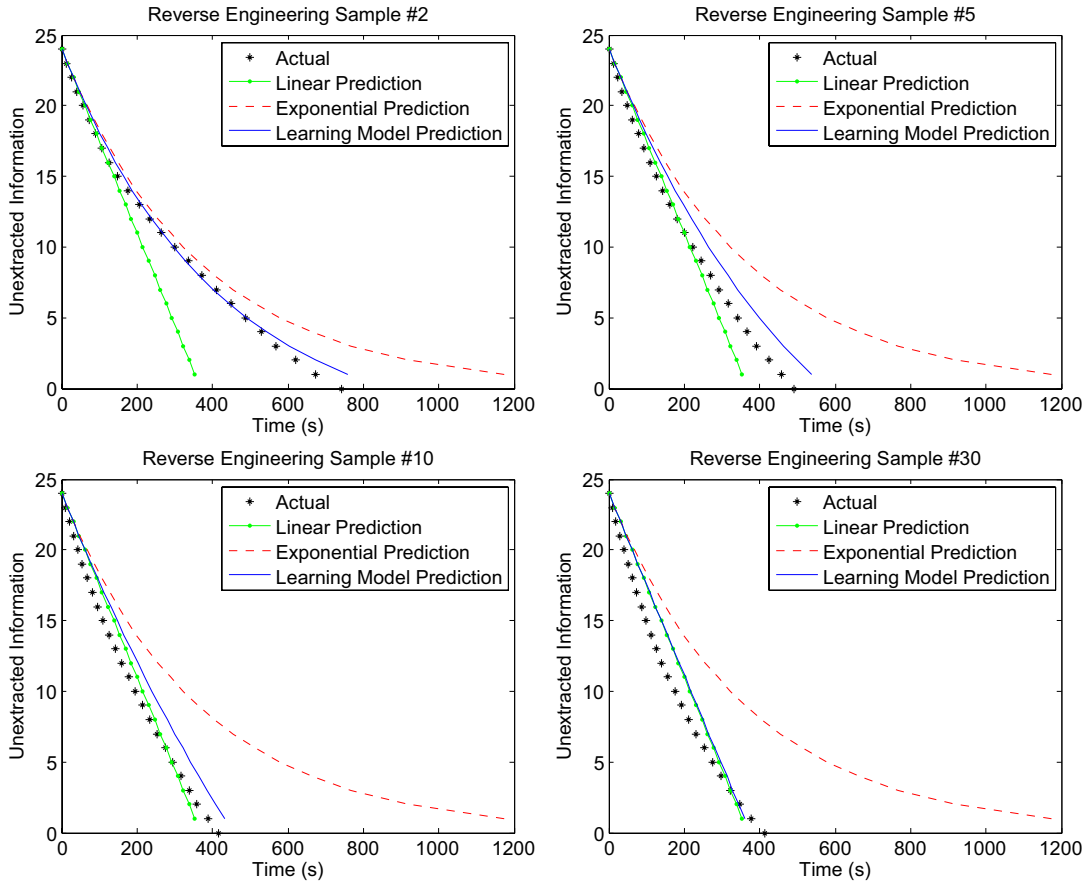

Figure 5.4: Unextracted dimensions as a function of time for spool valve block samples 2,5,10, and 30.

likely that some information will be extracted quicker due to natural variation. If the data is not rearranged according to the time to extract each dimension for sample #30, with the shortest times plotted first, the actual data appears more linear in nature and strongly correlates with the linear prediction.

5.5 Concluding Remarks

In this chapter, we have presented general metrics for evaluating the time to reverse engineer multiple samples of the same product, which is a continuation of the research presented in Chapter 4. An exponential decay function adequately describes the relationship between unextracted information remaining in a product and time for the first reverse engineering product sample. With subsequent samples, the relationship becomes more linear, due to changes in the

flow of information. We have introduced supporting metrics that characterize this change in information flow rates due to learning.

A study involving multiple product samples of a spool and a spool valve block from a Flowserve Digital Positioner has been offered to both demonstrate the use of the metrics and serve as empirical validation. The study confirms that as reverse engineering samples increase, the flow rates at all unextracted information levels increase toward the same asymptotical limit - the theoretical fastest flow rate, much like the response of electrical current in a resistor-inductor circuit. Moreover, the example suggests that if certain information is known about a product, the person reverse engineering, and the product sample size, then the metrics can be used to accurately estimate the total time needed to reverse engineer the geometry of a product, and, in this case with an average absolute error of 6.3%. Although this chapter focuses on geometric information, the metrics defined here can also apply to other information types such as electrical conductivity, elasticity, tensile strength, or even color.

CHAPTER 6. A FRAMEWORK FOR EVALUATING THE COST TO IMPLEMENT BARRIERS TO REVERSE ENGINEERING

6.1 Chapter Overview

Designing products with built-in barriers to reverse engineering can impede competitors from gathering critical information from innovative products and delay the production of product imitations. However, incorporating barriers to reverse engineering requires additional time and resources to design, develop, and manufacture. As these elements of barriers are conflicting, it is important to understand the tradeoff and the overall impact on the product return on investment. This chapter presents a framework for evaluating the cost to design and implement barriers to reverse engineering, thus, providing a valuable tool to assist the designer while designing barriers to reverse engineering. Two case studies show that using the presented framework to evaluate a barriers return on investment is an essential part of ensuring a profitable endeavor.

6.2 Introduction

Product developers can influence the effectiveness of barriers based on calculated and sometimes even uncalculated design decisions. Those design decisions can range from how to obtain parts (i.e., make versus buy) to what the composition of the material microstructure should be. The effectiveness of a barrier is measured relative to the person trying to break the barrier, and the metrics for calculating a barrier are discussed in Chapter 4. In conjunction with calculating the barrier, the time it takes to reverse engineer and imitate a product can also be calculated. Knowing these parameters is necessary to estimate the return on investment for a product. Knowing how design decisions affect a firm's bottom line is a key factor in making barrier implementation decisions. While implementing barriers to reverse engineering and imitation may be costly, Shapiro [52] and Nelson and Winter [53] emphasize that the harder a product is to imitate the less incentive there is for competitors to imitate the product. Furthermore, Crockford [20] states that

any improvement that can be economically taken to reduce the risk of the product being successfully reverse engineered is worth taking.

This chapter (i) proposes a framework for calculating the return on investment when implementing a barrier strategy, thus helping designers to manage the tradeoffs of barrier implementation, and (ii) recommends a barrier strategy as a method to protect intellectual property and maintaining competitive advantage.

6.3 Calculating Return on Investment while Considering Market Lost to Product Imitations

The business strategy behind implementing barriers to reverse engineering is two fold. The first is to protect trade secrets. The second objective is to capture as much of the market share as possible for as long as possible. Maintaining a large market share helps increase return on investment (R). There are two key components to estimating the return on investment. The first is an estimation of all the costs associated with the product's development and production. The second is an estimation of the sales and market performance of the product. In the following section we explore how, with given models, a firm can estimate the sales and costs of its product. In the past, most designers have been far removed from financial estimations. The development of concurrent engineering has drawn designers closer to the financial estimation for a project and helped them make more educated design decisions [140]. The purpose here is not to prescribe estimation models, but to show how given models can be applied to help designers make better barrier implementation decisions based on the return on investment.

Product Development Costs

There are a variety of methods for estimating project costs and how those costs will be distributed over time. The method used is usually determined by the firm developing the product. Product complexity can be a major factor in determining product development costs. At the onset of a project, it can be difficult to get an estimate of the product development costs. Ulrich and Eppinger [141] suggest that the costs associated with the product can be separated into four categories: development, ramp-up, marketing and support, and production. Development costs include

all design, testing, and refinement costs up to production. Magrab [142] outlines several models for determining the development costs. Magrab states that the product's total cost is computed as

$$C_p = N_p(M+L+R)+T_0+S+D \tag{6.1}$$

where N_P is the lifetime product volume, M is the material cost per unit, L is the manufacturing labor per unit, R is the production resource usage/unit, T_0 is the capitalization costs, S is the indirect costs, and D is the development costs.

There is no model that is assumed to be a "one-fits-all" solution. As stated above, it is left up to members of the individual firm to decide which model works best for them. Another way to measure product development costs is by product complexity. One way to measure product complexity is by the information content of a product [23]. Because more complex products are, in most cases, more expensive to develop, we use information content as a key measurement for product development costs in the example below.

Market Revenue Prediction

Predicting a product's sales can often be a very involved process. Some companies commit massive amounts of resources to predicting how a product will perform in the market and some go by gut instinct. There are methods and models that are available to alleviate some of the uncertainty and help a developer estimate the future sales of a product. The purpose of this chapter is not to prescribe a specific method for predicting how a product performs in the market, but to show how, with a given model, a developer can predict the return on investment. This is done under the assumption that a competitor will eventually release an imitation of the product of interest to market (no sooner than the reverse engineering and imitating time), thus, stealing market share and reducing the innovator's return on investment.

One model that has proven to be a good predictor of sales for consumer durables is the Bass Diffusion Model [143]. This model works well for our application because it tells us how the sales vary over time and is not just a lump sum of sales. Knowing how sales vary over time is important, because the entrance of a competitor to the market will have varying effects depending on the level of sales in the market at that time. The Bass model has proven to be a good predictor of how

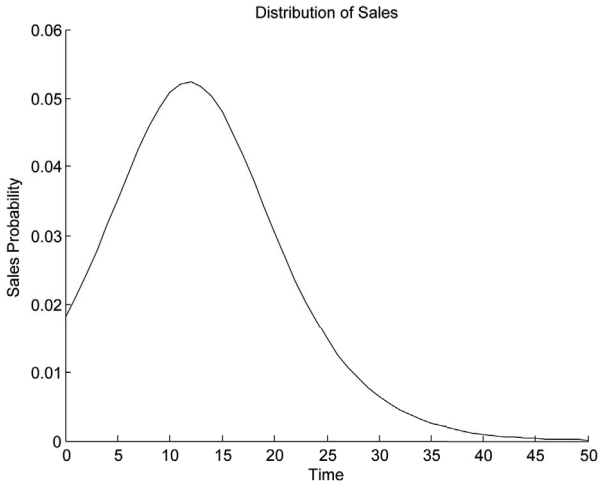

Figure 6.1: Generic representation of the Bass Diffusion Model. Note that the sales shown are not cumulative, but are time dependent.

quickly sales of new consumer durables grow and how much of the potential market a product can capture [144]. The term "consumer durables" refers to products that are replaced by the consumer at a very low rate. Examples of consumer durables are refrigerators, televisions, washing machines, and lawn mowers. For this dissertation, we assume that the products in question will have no repeat buyers; lending itself easily to the Bass Model.

The Bass model is expressed as a probability density function that spreads the total expected market sales of a product over time, τ, and is defined as

$$n(\tau) = \frac{(\alpha+\beta)^2}{\alpha} \frac{e^{-(\alpha+\beta)\tau}}{\left(\frac{\beta}{\alpha}e^{-(\alpha+\beta)\tau}+1\right)^2} \tag{6.2}$$

where α is the coefficient of early adoption and represents the probability of an initial purchase at $\tau = 0$, and β is the coefficient of late adoption and represents the influence that previous buyers have on future buyers.

Fig. 6.1 is a generic representation of the Bass Diffusion curve where the area under the curve represents the cumulative sales probability of a product.

The Bass model places buyers into two categories: early adopters and late adopters. The timing of *early adopters'* purchases is not based on how many previous buyers there have been, while the timing of the *late adopters'* purchase is based on the quantity of previous buyers. The

last component needed in order to predict the quantity of sales at time τ is the overall market size, m. With the total market size estimated, the sales, Ψ, at time τ are

$$\Psi(\tau) = m\frac{(\alpha+\beta)^2}{\alpha}\frac{e^{-(\alpha+\beta)\tau}}{\left(\frac{\beta}{\alpha}e^{-(\alpha+\beta)\tau}+1\right)^2} \tag{6.3}$$

and the time at which sales peak, τ_u, is found by differentiating Ψ and solving for τ when $d\Psi/d\tau = 0$. Therefore,

$$\tau_u = \frac{1}{\alpha+\beta}\ln\left(\frac{\beta}{\alpha}\right) \tag{6.4}$$

The cumulative sales Ψ_t at τ is

$$\Psi_t(\tau) = m\int_0^{\tau} n(\tau)d\tau \tag{6.5}$$

Obtaining a good prediction of sales is based upon good estimates of α, β, and m. Obtaining good estimates of α, β, and m can be done in various ways, but one simple way is to use data from a similar product and market. Research suggests that when time is in years an average value for α is 0.03, but is often less than 0.01, and β ranges between 0.3 and 0.5 with an average value of 0.38 [144]. The parameters should be scaled according to the time scale. It is important to emphasize that this discussion of the Bass model has been to facilitate the discussion of how a given sales model can be applied to make design decisions. Once again, we are not suggesting that the Bass model is one that should be used for all applications. Firms should use discretion when deciding what model to use to estimate the sales of its product.

6.3.1 Return on Investment Calculation

Calculating return on investment starts with estimating the costs and revenues of the product. The costs are broken down into two categories: development and manufacturing. The product development time is calculated using a baseline cost and the reverse engineering metrics with a development flow rate. In most cases, firms will be able to relate product development time to cost, because they will know their costs per time to utilize their resources. Therefore, to further facilitate

this discussion, product development cost, C_d, has a linear relationship with product information content and is defined as

$$C_d = C_\tau \tau_d \tag{6.6}$$

where C_τ is the cost per unit time and τ_d is the product development time.

The manufacturing cost correlates directly with sales and is defined as

$$C_g = C_m \Psi(\tau) \tag{6.7}$$

where C_g is the cost of goods sold, C_m is the unit cost of manufacturing. The total product cost is defined as

$$C = \int_0^{\tau_d} C_d d\tau + \int_{\tau_d}^{\tau_f} C_g d\tau \tag{6.8}$$

where τ_f is the time at which the product reaches the end of its life.

The revenues for the product are obtained using the Bass Diffusion model, but with one caveat: the sales will be diminished by the entrance of an imitation to the market, thus affecting the distribution and quantity of sales. To accomplish this the total market diffusion, $\psi(\tau)$ is first calculated assuming that no imitation enters the market. Second, the amount of market that an imitation is able to capture is then calculated. Predicting the rate and magnitude at which an imitation will sell is done using the Bass model as well. An *early adoption* and *late adoption* rate, α_I and β_I respectively, is defined for the imitation product. Additionally, the potential market size is reduced to what is currently remaining when the imitation product enters the market. Actual sales for the innovator are then defined as

$$X_t(\tau) = X(\tau) - X_I(\tau) \tag{6.9}$$

where $X_t(\tau)$ is the total sales in dollars for the innovator up to time τ, $X(\tau)$ is the total potential market sales in dollars up to time τ, and $X_I(\tau)$ is the total sales in dollars for the competitor up to time τ.

Figure 6.2: KitchenAid Artisan Stand Mixer. [3]

An alternate approach to calculating R is to choose a required R for a project. Then, designers can solve for the information flow rate needed to achieve the required R. Once the information flow rate is calculated, designers can use intuition and/or estimation methods outlined by Harston and Mattson [14] to decide if the flow rate will, in reality, allow the firm to capture the required R.

6.4 Case Study 1: KitchenAid Stand Mixer

In order to illustrate how the models described above are used together, a KitchenAid Stand Mixer will be examined. According to Euromonitor International [145], KitchenAid sold approximately 24 million units of kitchen appliances from 2005 to 2010. KitchenAid has numerous product offerings, but this example will focus on its popular stand mixer. Based on the number of different kitchen appliances offered, the data provided by Euromonitor, and the Stand Mixer being KitchenAid's number one selling product, it is estimated that the market size for the stand mixer is

10 million units. To illustrate the return on investment analysis for implementing barriers to reverse engineering, the Bass diffusion model will first be invoked where no barriers have been strategically implemented, and a competitor is introduced. Under this scenario, KitchenAid's return on investment is calculated to be 1.145. This means that the project will return 100% of the costs for the product plus 14.5% above the total cost. Second, strategic barriers to reverse engineering and imitation are introduced, and the Bass model is re-executed. Though there is added cost of designing and manufacturing the barriers, material barriers can be used to achieve a 6.4% gain in return on investment.

The parameters used in this example are listed in Tab. 6.1. The development rate, F_d, is set to 0.036, which is the rate at which the microstructure (i.e., size, orientation, and distribution of crystallographic grains) barrier used in this case study can be designed into the product in units of information per hour. The parameters $F_R(1)$, $F_I(1)$, $K_R(1)$, and $K_I(1)$ are the geometry flow rate and information content of the stand mixer as they pertain to reverse engineering and imitating. The parameters $F_R(2)$, $F_I(2)$, $K_R(2)$, and $K_I(2)$ are the material microstructure flow rate and information content of the stand mixer. Notice that $F_R(1)$ and $F_I(1)$ are noticeably larger than $F_R(2)$ and $F_I(2)$. This is simply due to the fact that geometric information (i.e., dimensions) can be extracted much faster than microstructure information. The power exerted by KitchenAid's product development team to develop the stand mixer is represented by P_d. The reverse engineering and imitating power is represented by P_R and P_I, respectively. Recall that these values are set to "1" as it is the most conservative approach.

As stated above, the Bass model is invoked to illustrate the diffusion of the stand mixer market. The parameters α and β are the coefficients of early adoption and late adoption, respectively, for the Bass model. The values for these coefficients were chosen based on research presented by Sultan et al. [146] for both KitchenAid's stand mixer and the competitor's product. The retail price is represented by ρ. The cost for KitchenAid to manufacture the stand mixer is represented by C_m. Note that the product development costs, C_d, include all pre-launch costs, including engineering costs, marketing, tooling, and production ramp-up (30 day supply of product) and are evenly distributed over the development time.

Table 6.1: Input parameters for calculating the return on investment of a KitchenAid Stand Mixer.

Param.	Value	Decription
F_d	0.036	Development rate (info/hr)
$F_R(1)$	144	Reverse engineering. geometry information flow rate (info/hr)
$F_R(2)$	0.4	Reverse engineering microstructure information flow rate (info/hr)
$F_I(1)$	50	Imitating geometry information flow rate (info/hr)
$F_I(2)$	0.1	Imitating microstructure information flow rate (info/hr)
$K_R(1)$	800	Reverse engineering geometry information
$K_R(2)$	2	Reverse engineering material information
$K_I(1)$	300	Imitating geometry information
$K_I(2)$	4	Imitating material information
P_d	1	Development power
P_R	1	Reverse engineering power
P_I	1	Imitating power
α	2.03×10^{-5}	Coefficient of early adoption
β	5.64×10^{-4}	Coefficient of late adpotion
α_I	3.00×10^{-5}	Competitor's coefficient of early adoption
β_I	6.00×10^{-4}	Competitor's coefficient of late adoption
m	10.00×10^{6}	Market size in number of units
ρ	250	Product retail price in Dollars
C_m	200	Cost to manufacture product in Dollars
C_d	14,500	Development cost in Dollars per hour

For this example, the assumption is made that the stand mixer is a new and innovative product and that the percentage of market share a competitor can capture is inversely proportional to its launch time as shown in Eqn. (6.10).

$$m_I = m\left(1 - \frac{T_M^*}{\tau_u}\right)\left(1 - \frac{e^{-(\alpha+\beta)T_M^*}}{\left(\frac{\beta}{\alpha}e^{-(\alpha+\beta)T_M^*} + 1\right)^2}\right) \tag{6.10}$$

where T_M^* is the time to competitor market entry and τ_u is the time to the market saturation point.

Figs. 6.3, 6.4, 6.5, and 6.6 (plotted on the same scale for ease of visualization) aid in visualizing how the costs and revenues are distributed over the life of the product. Fig. 6.3 illustrates the distribution of development costs. Fig. 6.4 illustrates the distribution of sales starting immediately after product launch and if an imitation product is never released. Fig. 6.5 illustrates the sales of an

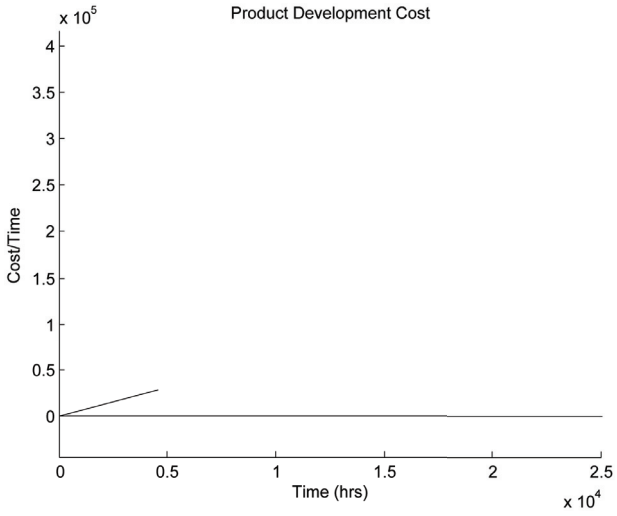

Figure 6.3: Estimated per time product development costs.

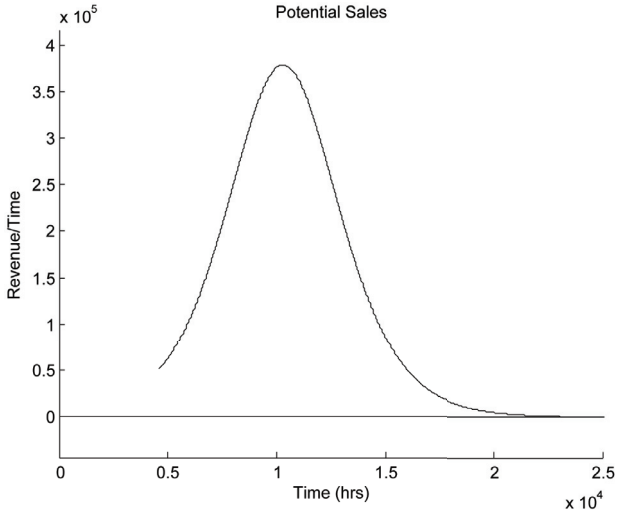

Figure 6.4: Estimated per time potential sales.

imitation released at $T_M^* = 4,771$ hours. Fig. 6.6 illustrates the cost of goods sold over the life of the product and accounts for the release of an imitation. These figures can then be superimposed to make a composite graph, as represented in Fig. 6.7. Note that in Fig. 6.7 there is very short period where KitchenAid is alone in the market, which is depicted by the "spike" in sales immediately after development. This is also the reason for the apparently vertical line in Fig. 6.6.

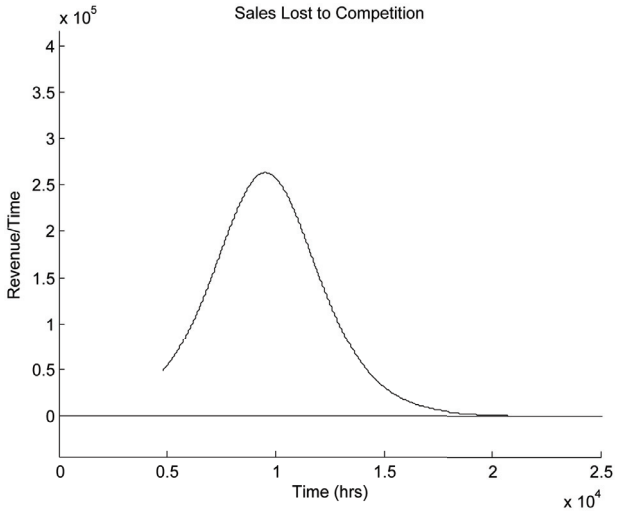

Figure 6.5: Estimated competitor's sales as a result of releasing an imitation. In other words, sales lost to the competitor.

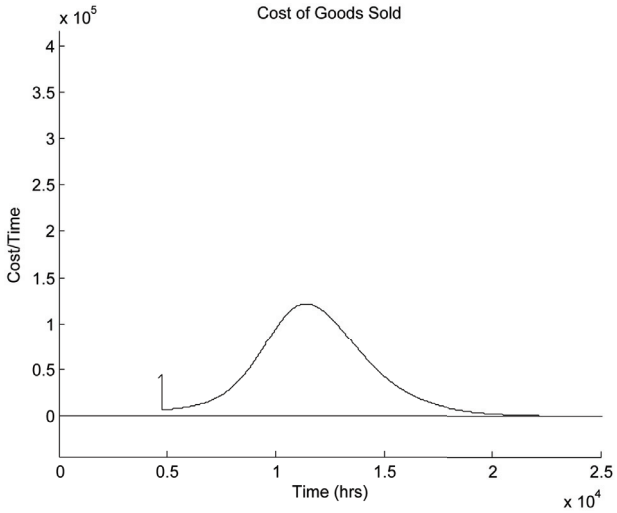

Figure 6.6: The estimated cost of goods sold over the life of KitchenAid's stand mixer.

The return on investment is calculated through integration as

$$R = \frac{\int_{\tau_d}^{\tau_f} \Psi(\tau) - \Psi_I(\tau) d\tau}{C_d \tau_d + \int_{\tau_d}^{\tau_f} C_m d\tau} \tag{6.11}$$

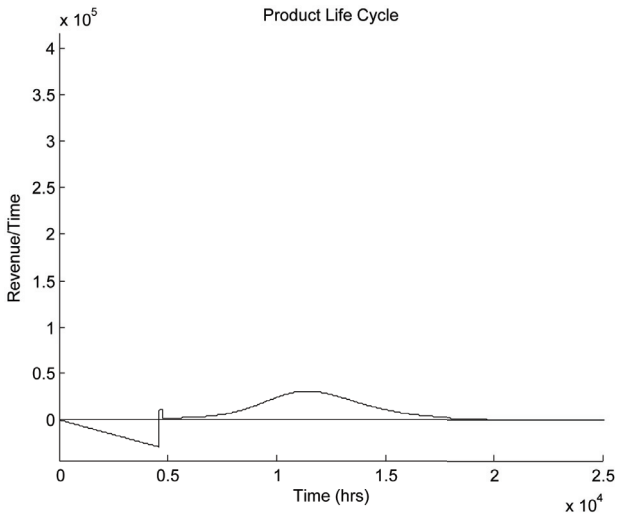

Figure 6.7: The estimated per time costs/revenues of KitchenAid's stand mixer over its entire life.

The return on investment can also be visualized as the ratio of the difference in areas under the curves of Figs. 6.4 and 6.5 to the sum of the areas under the curves of Figs. 6.6 and 6.3. From the model, R is calculated to be 1.145. Also, the calculated barrier is $1.3 \times 10^{-}3$.

KitchenAid can influence return on investment and B by incorporating different types of information and/or by varying the quantity. Doing so will likely affect the product development time, cost, and manufacturing cost, however, the added barrier will also likely delay the competitor's market entry. It is important to understand this tradeoff in order to effectively increase return on investment by implementing barriers. For the above example, assume KitchenAid strategically manipulates the material microstructure of the stand mixer in order in increase the barrier. Because the analysis of a given material's microstructure is intricate and time consuming, there will be a significant change in F for the competitor. Due to the increased difficulty of extracting microstructure information and the added information, the values of the following parameters are changed: $F_R(2) = 0.04$, $F_I(2) = 0.01$, $K_R(2) = 15$, and $K_I(2) = 30$. The additional information included in the product also increases the product development time, cost, and the manufacturing cost. The addition of more information and a slower information flow rate for the competitor results in $T_M^* = 14,797$ hrs. This change leads to $R = 1.209$, which provides the firm with an extra 6.4% return over what was previously calculated. This equates to an extra \$311 million in net sales for KitchenAid. Also, the barrier is improved to $78.0 \times 10^{-}3$. It is important to note that

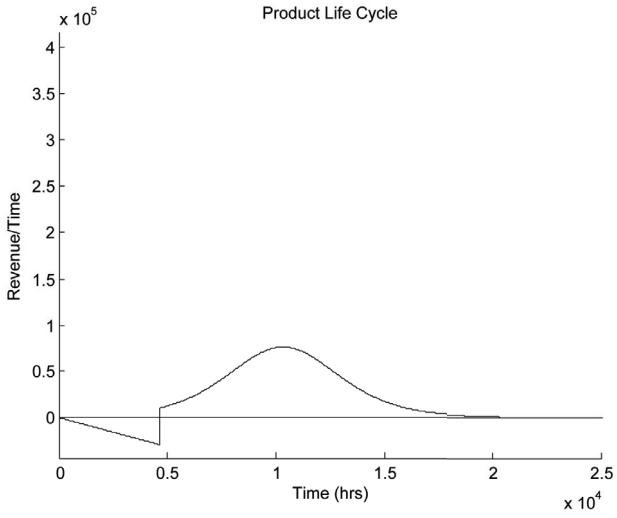

Figure 6.8: The estimated per time costs/revenues of KitchenAid's stand mixer over its entire life with a microstructure barrier.

the barrier values are intended as a comparative measure. Typically the barriers of various designs are compared to the barrier of a benchmark design. The product life-cycle plot for the improved barrier is shown in Fig. 6.8. A substantial change in the revenues of KitchenAid's stand mixer can be noticed from the plot alone.

6.5 Case Study 2: Cantilevered L-Beam

The above has illustrated how incorporating different types of information can increase the barrier and time to market entry for a competitor, thus increasing the return on investment for the innovator. The following case study illustrates the implementation of specific barriers and how those affect the return on investment for the innovator. It is borrowed from Harston et al. [4] and is extended to illustrate the point at hand. Here, an "L" shaped beam is considered, as shown in Fig. 6.9, which is fixed at one end and exposed to a prescribed deflection at the other. Note that this beam is unique in that the cross-section is composed of anisotropic layers, which have been joined using ultrasonic consolidation [4]. This particular beam is used as a contact in an electrical connector, hence the reason the dimensions are in millimeters.

Because of the geometric constraints of the application, the geometry for the L-beam is fixed. Harston et. al. first optimized the L-beam under four separate conditions to achieve a target reaction force at the free end when subjected to a prescribed displacement (δ) at the same end. The

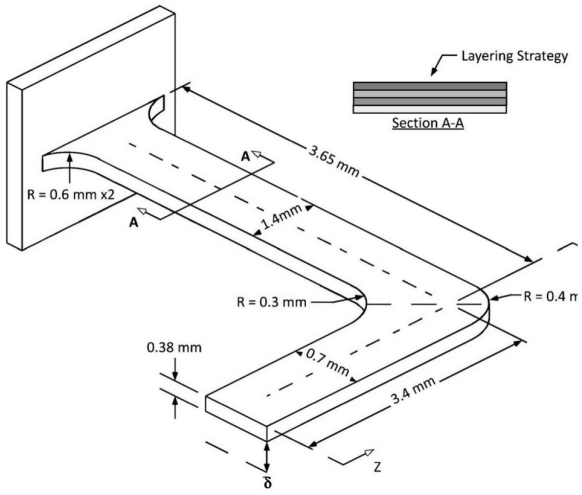

Figure 6.9: Geometry and boundary conditions for the L-beam case study.

four different conditions analyzed were (I) Single Isotropic Layer, (II) Single Anisotropic Layer, (III) Multilayer Anisotropic, and (IV) Single Layer Heterogeneously Anisotropic. Condition (I) is used as a benchmark and is manufactured using traditional manufacturing techniques. Whereas, conditions (II), (III), and (IV) are manufactured using ultrasonic consolidation and/or friction stir welding [4]. Tab. 6.2 specifies the constant input parameters that will be used to calculate R for each condition. The amount of information contained by each condition will vary, as specified in Tabs. 6.3 and 6.4.

Harston et. al. only optimized the product reaction force and yielding characteristics and did not attempt to optimize return on investment. In this case study, the L-beam is further analyzed to obtain the return on investment for each of the four conditions. Because each condition will require slightly different processes to manufacture, the manufacturing costs are adjusted accordingly. Furthermore, when a product has a superior performance the sales price will be less constrained by competitive products. Therefore, we are able to adjust the sales price to overcome the added expense of barrier implementation. Due to the added barriers, the market becomes more secure and there is less threat of having to compete on price, leaving the innovator free to dictate the price of the product. However, it is important to also consider the impact that a higher sales price will have on the overall market size. Therefore, overarching market pressures will frequently constrain the sales price of a product. For this purpose, we present return on investment under two scenarios

Table 6.2: Constant input parameters for calculating the return on investment of a cantilevered L-beam.

Param.	Value	Decription
F_d	0.036	Development rate (info/hr)
$F_R(1)$	144	Reverse engineering. geometry information flow rate (info/hr)
$F_R(2)$	0.04	Reverse engineering microstructure information flow rate (info/hr)
$F_I(1)$	50	Imitating geometry information flow rate (info/hr)
$F_I(2)$	0.01	Imitating microstructure information flow rate (info/hr)
P_d	1	Development power
P_R	1	Reverse engineering power
P_I	1	Imitating power
α	3.00×10^{-5}	Coefficient of early adoption
β	3.00×10^{-4}	Coefficient of late adpotion
α_I	6.00×10^{-5}	Competitor's coefficient of early adoption
β_I	4.00×10^{-4}	Competitor's coefficient of late adoption
m	1.00×10^{8}	Market size in number of units
C_d	1,000	Development cost in Dollars per hour

Table 6.3: The return on investment for a cantilevered L-beam with varying mechanical properties. Retail price is held constant.

Case	$K_R(1)$	$K_R(2)$	$K_I(1)$	$K_I(2)$	C_m (\$)	ρ (\$)	T_M^* (hrs)	R
(I) Benchmark	10	2	30	4	0.02	0.06	2,140	2.296
(II) Single layer	10	3	30	6	0.04	0.06	2,858	1.352
(III) Four Layers	14	15	42	30	0.06	0.06	11,726	0.935
(IV) Heterogeneous	10	18	30	36	0.05	0.06	13,642	1.113

– a fixed sales price, and a variable sales price. The results of the analysis are presented in Tabs. 6.3 and 6.4, respectively.

Let us first discuss return on investment when there is a fixed sales price as seen in Tab. 6.3. Notice that for this example, when the sales price is fixed, return on investment decreases as barriers are implemented. This is due to the increased product development and manufacturing cost that is unable to be recovered even though the product is able to capture and maintain a larger portion of the market share. This demonstrates that not all products will benefit from implementing barriers.

Table 6.4: The return on investment for a cantilevered L-beam with varying mechanical properties. Retail price varies.

Case	$K_R(1)$	$K_R(2)$	$K_I(1)$	$K_I(2)$	C_m (\$)	ρ (\$)	T_M^* (hrs)	R
(I) Benchmark	10	2	30	4	0.02	0.06	2,140	2.296
(II) Single layer	10	3	30	6	0.04	0.12	2,858	2.704
(III) Four Layers	14	15	42	30	0.06	0.12	11,726	1.869
(IV) Heterogeneous	10	18	30	36	0.05	0.15	13,642	2.782

As an alternate approach, one can consider additional barrier types and model their impact on the return on investment.

However, if the product has a superior performance, the sales price can be adjusted to help recover the increased product development and manufacturing costs. As discussed above, the L-beams were optimized for both the reaction force and yielding characteristics. We note that the heterogenous design has the best performance while the single-layer and the four-layer L-beams performed equally well. Even though the single-layer and four layer L-beams have the same performance, we assume that the four-layer L-beam is not only more difficult to reverse engineer, but is also more expensive to fabricate. All three designs out-performed the benchmark design and the sales price of each L-beam is modified to represent the increased level of performance. For the performance specifics, we refer the reader to [4]. Of the four conditions considered here, condition (IV) yields the highest return on investment due to (i) the increased product performance enabling a higher sales price and (ii) a barrier to reverse engineering that effectively delays the market entry of imitators.

6.6 Chapter Summary

This chapter has developed and presented metrics for estimating the time it takes a competitor to launch an imitation product. The launch of the imitation can have a significant impact on the return on investment of an innovator's product, because it steals away market share and reduces sales from what they could potentially be. In order to understand how implementing a barrier strategy affects return on investment we have developed a framework that considers design decisions, competitor behavior, and market performance. This framework allows designers to see how the implementation of certain design features affects the return on investment of a product.

The insight provided by the framework presented enables designers to make more educated design decisions and increase a firm's return on investment.

CHAPTER 7. HOW TO PLAN FOR, SELECT, DESIGN, AND IMPLEMENT BARRIERS TO REVERSE ENGINEERING

7.1 Chapter Overview

In Chapter 4, quantitative metrics are presented that estimate the barrier that must be overcome to reverse engineer physical hardware as well as an estimation of the time to do so. While barrier implementation can be costly, entire products can be made difficult to reverse engineer with an increased return on investment by selectively incorporating one or more barriers to reverse engineering. This chapter presents a process for barrier development by considering performance measures of interest, parameters that affect the performance measures, and generating reverse engineering barrier concepts to protect the selected performance and parameters. This process includes sensitivity analyses to determine parameter impact on product performance, considers the ease for which parameters may be modified, and analyzes the effectiveness of barrier concepts. The process is demonstrated on a solar-powered unmanned aerial vehicle.

7.2 Introduction

The purpose of barriers to reverse engineering is to (i) impede competitors from gaining valuable insight from the innovative product, and (ii) minimize loss in market share due to imitations of all or part of the innovative product [14]. Barriers to reverse engineering do not need to make a product impossible to reverse engineer. Instead, they must keep a competitor out of the market long enough to give the original developer a desirable return on investment. Some believe that a barrier is sufficient when the cost to reverse engineer is greater than the cost to develop the original product [18,19]. Military products may be an exception. In general, any improvement that can be economically taken to reduce the risk of the product being successfully reverse engineered is worth taking [20].

It may not be practical to incorporate reverse engineering barriers into all products. One must weigh the consequences of the product being reverse engineered, determine the additional cost to develop the barriers, and calculate the expected return on investment of a product that does, or does not, implement a reverse engineering prevention strategy. On one hand, designing and implementing reverse engineering barriers into a product can be costly – both in time and resources. Barrier implementation frequently requires additional design time, manufacturing costs, and assembly costs. This can result in a delayed market entry and a reduced return on investment. On the other hand, innovative products have lost a significant portion of the market share due to reverse engineering and product imitations – many companies have discontinued competing in the markets they originally created due to competitors reverse engineering and imitating their innovative product [27]. While barriers to reverse engineering may be costly to implement, entire products can be made difficult to reverse engineer by selecting and designing barriers to reverse engineering into one critical element [32]. Therefore, it is important that the critical elements of a system be identified, and that barriers are selected to make these elements more difficult to reverse engineer.

Identifying, characterizing, and understanding the critical elements of a system are not novel ideas. The basis of risk management [17, 58], security, [59] and defense-in-depth (the use of multi-layered or redundant protections) [60,61] is to identify the critical elements and improve their designs to decrease risk or increase security of the system. Software designers seek to identify the critical modules of code to facilitate early defect detection and reduce intrinsic downtime [65, 66]. In product design, designers seek to understand what features of a product are critical to user satisfaction [62], understand the impact of critical elements on a system when they are redesigned and replaced [63], and perform analyses to systematically identify possible failures and estimated risks [38]. Grand [19] suggests that before any security/barrier features are designed into a product, risk assessment in the following three areas should be performed to help identify critical elements: (i) what needs to be protected (ii) why does it need to be protected, and (iii) whom it is being protected against. Furthermore, Pooley and Graves [64] recommend locating the most valuable information in a product, and focusing resources and efforts on that element. We note that the barrier development process presented in Sec. 8.3 is built upon the work of Edwards [63], Grand [19], and Pooley and Graves [64].

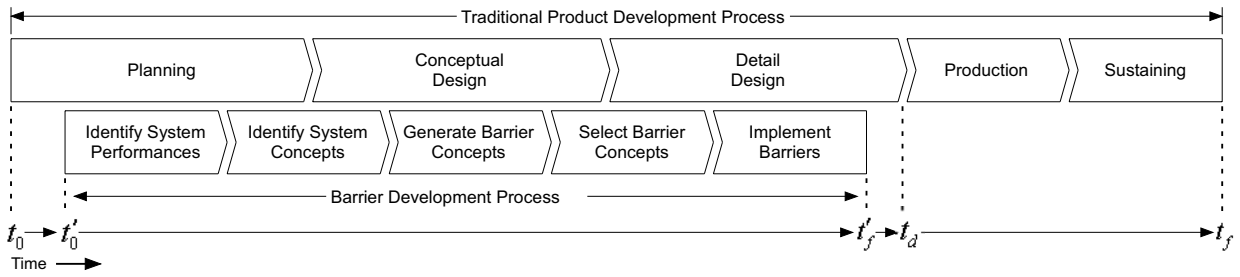

Figure 7.1: Illustration of the (i) barrier development process, (ii) a general product development process, and (iii) their interaction with each other where t_0 is the time the product development process begins, t_0' is the time the barrier implementation process begins, t_f' is the time the barrier implementation process ends, t_d is the time "Detail Design" ends, and t_f is the time the product development process ends.

Similar methods used in the software industry apply graph theory concepts to improve information security evaluations for electronic communication devices. Rae and Fidge [65] present an approach that significantly reduces analysis time by forgoing analysis on elements that do not affect information security and focus on the critical elements that are most likely to cause failures. Furthermore, Ebert [66] presents a number of classification techniques to help software designers detect source code defects early in the development process and to focus defect detection on the error-prone areas. While these approaches provide useful insight on how to select critical software elements, they have been developed specifically for code-based modules and cannot be directly adopted for discovering critical elements of physical hardware.

The purpose of this chapter is to present a barrier development process that enables designers to identify the critical elements of a physical system and to develop reverse engineering barriers to protect them. Specifically, this process considers (i) which product performances need protection, (ii) what parameters affect the product performances, and (iii) what barriers best protect the selected parameters and product performances.

7.3 Selection and Implementation of Barriers to Reverse Engineering

The purpose of this section is to provide an overview of a process that enables designers to develop barriers to reverse engineering. Following this overview, a detailed discussion of each step as applied to a solar-powered unmanned aerial vehicle is discussed in Sec. 7.4. The barrier

development process consists of five steps and can be done in parallel with the traditional product development process as shown in Fig. 7.1. The five steps are:

Step 1 Identify the set of performances, F', that are at risk of being reverse engineered. This is a subset of all system performances, F where $F = [f_1, f_2, ..., f_{n_f}]$, n_f is the total number of system performances, $F' = [f'_1, f'_2, ..., f'_{n_{f'}}]$, and $n_{f'}$ is the number of *at-risk* performances.

Step 2 Identify the parameters that influence the at-risk performances. Let P represent all such parameters and let P' represent the set of parameters (subset of P) for which barrier implementation should be considered. For notation purposes, let the ith row of P be $P_i = [p_{i,1}, p_{i,2}, ..., p_{i,n_{p_i}}]$, where n_{p_i} is the number of parameters that influence the at-risk performance i, and let the ith row of P' be $P'_i = [p'_{i,1}, p'_{i,2}, ..., p'_{i,n_{p'_i}}]$, where $n_{p'_i}$ is the number of parameters that are considered for barrier implementation to protect performance i. Often designers are interested in developing barriers for parameters that can be easily modified and have a large impact on system performance. To identify such parameters – which will ultimately populate the P' matrix – the following may be used:

$$\max_{i,j} \quad \{m(p_{i,j}), s(p_{i,j})\} \qquad i \in \{1,2,...,n_{f'}\}, j \in \{1,2,...,n_{p_i}\} \tag{7.1}$$

where $m(p_{i,j})$ is a measure of the ease of modification of parameter $p_{i,j}$, $s(p_{i,j})$ is a measure how sensitive performance i is to parameter $p_{i,j}$. Equation 8.3 seeks the values of i and j that maximize m and s. The result of this formulation is used to populate P' which may be a single parameter, or a set of parameters.

Step 3 Generate barrier concepts that protect the parameters in P'. This results in a three-dimensional matrix of barrier concepts where the barriers generated for parameter j of performance i are represented as $B_{i,j} = [b_{i,j,1}, b_{i,j,2}, ..., b_{i,j,n_{b_{i,j}}}]$ where $n_{b_{i,j}}$ is the number of barrier concepts generated for the jth parameter of the ith performance. The reader is referred to Curtis et. al. [147] for additional insights on the development of barrier concepts.

Step 4 Analyze and select barrier concepts that maximize system performance, Γ, and barrier effectiveness, β. This can be represented mathematically as

$$\max_{i,j,k} \quad \{\Gamma(B_{i,j,k}), \beta(B_{i,j,k})\} \qquad i \in \{1,2,...,n_{f'}\}, j \in \{1,2,...,n_{p_i}\}, k \in \{1,2,...,n_{b_{i,j}}\} \tag{7.2}$$

where $\Gamma(B_{i,j,k})$ is the performance of the system when barrier concept $B_{i,j,k}$ is implemented, and $\beta(B_{i,j,k})$ is the reverse engineering barrier effectiveness when barrier concept $B_{i,j,k}$ is implemented. The result of this formulation is used to populate B' which is the set of barrier concepts that may be favorably implemented. B' is a subset of B and is defined as $B'_{i,j} = [b'_{i,j,1}, b'_{i,j,2}, ..., b'_{i,j,n_{b'_{i,j}}}]$ where $n_{b'_{i,j}}$ is the number of barrier concepts that may be favorably implemented to protect parameter j of performance i. The reader is referred to Harston and Mattson [14] for a discussion and calculation of barrier effectiveness, β.

Step 5 Implement selected barrier(s).

Note that when any index is used, the first index identifies the performance at risk of being reverse engineered, the second index identifies the parameter that affects that performance, and the third index identifies the barrier concept for the respective parameter and performance. Once a set has been reduced – as denoted by $[\ ]'$ – the indices reference the reduced set. Importantly, this methodology does not constrain designers to select and implement a single barrier, or to consider performances independently. If desired, sets of performances, parameters, and barriers may be analyzed.

7.4 Practical Implementation: Solar-Powered UAV

In this section, the proposed process presented in this chapter is used to develop reverse engineering barriers to protect a solar-powered unmanned aerial vehicle (UAV). The solar-powered UAV is selected because it is a complicated dynamic system for which the critical element(s) and the barrier(s) to implement are not apparent. This is partially due to the dynamic system model and the cyclic nature of component interdependencies as seen in the system model diagram of Fig. 7.2 (e.g., the battery is constantly being drained by the motor while simultaneously being charged by the solar panel). Another reason for using the UAV to demonstrate the process is that this is one application where cutting-edge, proprietary technologies are used to minimize weight, maximize thrust, maximize battery life, etc. Not only can barriers to reverse engineering help maximize a return on investment for the highly competitive UAV market, but barriers to reverse engineering can also impede competitors (including military opponents) from obtaining crucial technology in the event of the UAV being lost or captured. The presented process to develop barriers to reverse engineering is now presented.

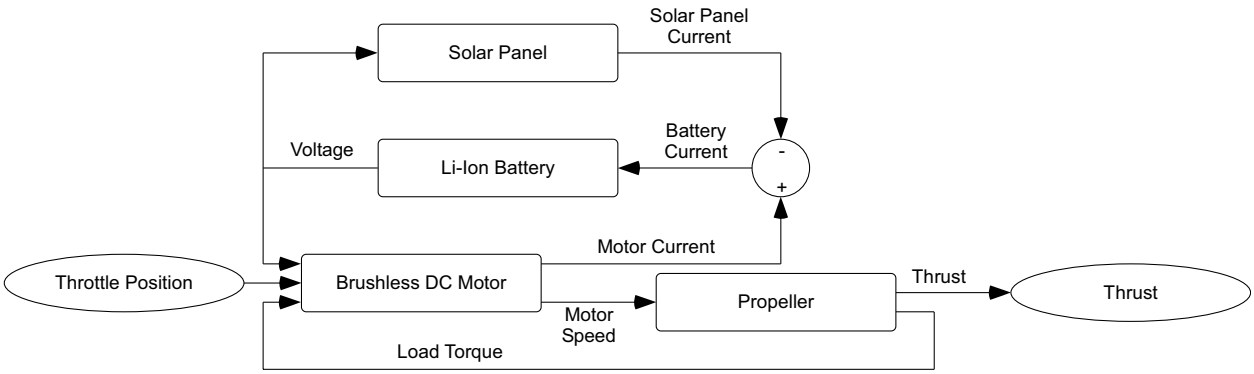

Figure 7.2: Solar-powered UAV system model.

Table 7.1: Identification of the system performances, F, and the system performances at risk of being reverse engineered, F'. ROI represents return on investment.

System Performances (F)	At-Risk Performances (F')
f_1 Weight	f'_1 Thrust
f_2 Thrust	f'_2 ROI
f_3 Battery life	f'_3 Thrust & ROI
f_4 ROI	
f_5 Thrust & ROI	
f_6 Weight & Thrust	

7.4.1 Step 1

Identify the performances that are at risk of being reverse engineered. The complexity of this system is such that it is not valuable to report the complete F. However, a portion of F, as well as the entirety of F', is presented in Table 7.1. For this example, the selection of F' is based upon the designer's intuition as to what performances most need protection. The barrier development process presented herein assists the designer in determining which performance(s) of F' are most benefited by barrier implementation. Note that F is reduced in size to lower the computation required and if desired, F' can be equivalent to F.

7.4.2 Step 2

Identify the parameters that influence the at-risk performances. A list of these parameters are shown in Table 7.2 for the UAV. With P defined, the tradeoffs between how readily a parameter

Table 7.2: Parameters that influence the at-risk performances, P. ROI denotes return on investment.

Thrust (f_1')	ROI (f_2')	Thrust & ROI (f_3')
$p_{1,1}$ Motor Current	$p_{2,1}$ Motor Current	$p_{3,1}$ Motor Current
$p_{1,2}$ Motor Frequency	$p_{2,2}$ Motor Frequency	$p_{3,2}$ Motor Frequency
$p_{1,3}$ Battery Voltage	$p_{2,3}$ Battery Voltage	$p_{3,3}$ Battery Voltage
$p_{1,4}$ Solar Panel Current	$p_{2,4}$ Solar Panel Current	$p_{3,4}$ Solar Panel Current
$p_{1,5}$ Prop Thrust	$p_{2,5}$ Prop Thrust	$p_{3,5}$ Prop Thrust
$p_{1,6}$ Motor Freq. & Prop Thrust		$p_{3,6}$ Motor Freq. & Prop Thrust
$p_{1,7}$ Motor Current & Prop Thrust		
$p_{1,8}$ Motor Freq. & Battery Voltage		

Table 7.3: The ability to modify component parameter p_{ij}. When $i = 1$ the at-risk performance is thrust, when $i = 2$ the at-risk performance is ROI, and when $i = 3$ the at-risk performance is thrust and ROI.

	f_1' Thrust	f_2' ROI	f_3' Thrust & ROI
$p_{i,1}$	3	2	1
$p_{i,2}$	3	5	4
$p_{i,3}$	1	3	3
$p_{i,4}$	5	3	2
$p_{i,5}$	5	4	5
$p_{i,6}$	4		4
$p_{i,7}$	4		
$p_{i,8}$	2		

can be modified, m, and the impact, s, the parameter has on the overall system performance are explored. This is done by characterizing m and s in Tables 7.3 and 7.4, respectively. For this example, the values of m are determined by rating each parameter on a scale from 1 (the parameter cannot be modified) to 5 (the parameter can readily be modified). If additional resolution is desired, a finer scale or alternate metrics may be used.

For this example, the impact on UAV performance is determined by varying each parameter by 10% of the nominal value and measuring the effect on the system performance. The models used for analyzing the thrust and return on investment are based upon the work of Larson and Mattson [148] and Knight et. al. [149], respectively. The reader is referred to their work for the details of these models.

Table 7.4: The impact of parameter p_{ij} on performance f_i'. When $i = 1$ the at-risk performance is thrust, when $i = 2$ the at-risk performance is ROI, and when $i = 3$ the at-risk performance is thrust and ROI.

	f_1' Thrust	f_2' ROI	f_3' Thrust & ROI
$p_{i,1}$	0.01	0.15	0.10
$p_{i,2}$	0.17	0.15	0.27
$p_{i,3}$	0.15	0.01	0.07
$p_{i,4}$	0.01	0.25	0.20
$p_{i,5}$	0.10	0.10	0.24
$p_{i,6}$	0.29		0.32
$p_{i,7}$	0.10		
$p_{i,8}$	0.35		

With an understanding of the ease for which a parameter may be modified, and the impact of the parameter on the system performance, Eqn. 8.3 can be used to populate P'. If an aggregate objective function [150] is used, a single parameter will be selected. Another approach, the approach used for this example, is to generate the data and use multiobjective decision theories to select one or more parameters to pursue [151, 152]. The tradeoffs between the two objectives – ability to modify the parameter, and impact on system performance – are shown in Fig. 7.3. From this data, the three parameters that are on the Pareto front (the non-dominated designs) are selected and considered for barrier implementation. These are (i) motor frequency and battery voltage with respect to thrust (i.e, $p'_{1,1} is defined as p_{1,8}$), (ii) prop thrust with respect to thrust and return on investment (i.e, $p'_{3,1} is defined as p_{3,5}$), and (iii) motor frequency and prop thrust with respect to thrust and return on investment (i.e, $p'_{3,2} is defined as p_{3,6}$). The undefined elements of p' are null.

7.4.3 Step 3

Generate barrier concepts that protect the parameters in P'. Designers may generate multiple concepts, one concept, or no concepts for each parameter. For this example, barrier concepts are only generated for a few parameters and may be represented in a three-dimensional barrier matrix B. Each non-zero element of B represents a barrier concept. The barrier concepts – and the only non-zero elements of B – are:

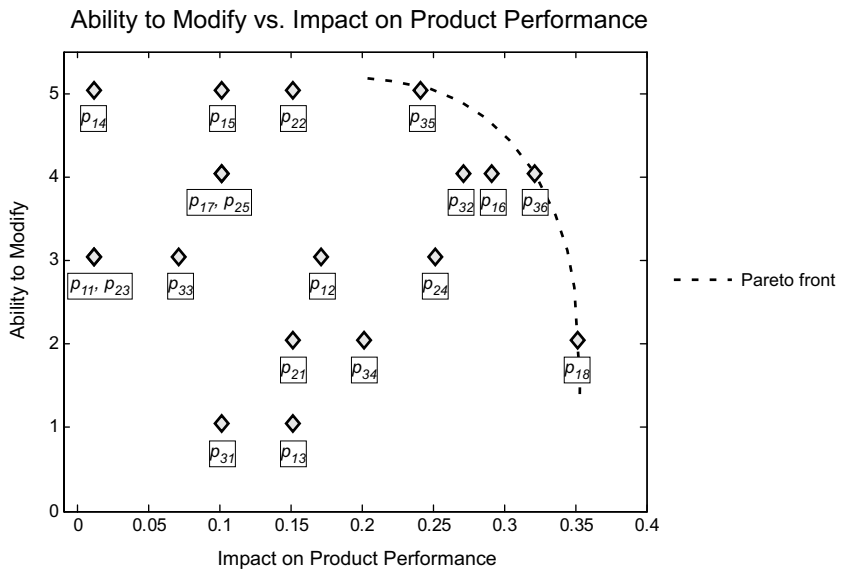

Figure 7.3: Comparing the ability to modify each parameter vs. the parameter's impact on the system performance to determine which parameters will most benefit from receiving reverse engineering barriers.

$b_{1,1,1}$: Design the motor and battery to look identical to off-the-shelf parts – but with a superior performance – and encode labels to minimize information divulged.

$b_{1,1,2}$: Design the motor and battery so that neither part can be analyzed or dissected without causing destruction.

$b_{1,1,3}$: Combine barrier concept $b_{1,1,1}$ and $b_{1,1,2}$.

$b_{3,1,1}$: Introduce voids into the aluminum propeller to (i) reduce the weight of the propeller, and (ii) increase propeller's flutter speed while meeting efficiency constraints. Flutter is a failure mode that is characterized by excessive vibrations in a propeller or wing which decreases performance and can cause catastrophic failure. Voids not only reduce weight and increase the performance of the propeller but also are difficult to detect and imitate by strategically selecting the manufacturing process (such as friction stir welding or ultrasonic consolidation) [4].

$b_{3,2,1}$: Combine barrier concept $b_{1,1,1}$ and $b_{3,1,1}$.

A summary of these barrier concepts, including the parameters and performances they influence, is shown in Table 7.5.

Table 7.5: Summary of barrier concepts.

F'	Performance	P'	Parameter	B	Barrier Concept
f'_1	Thrust	$p'_{1,1}$	Motor Freq. & Battery Voltage	$b_{1,1,1}$	Appears to be off-the-shelf
f'_1	Thrust	$p'_{1,1}$	Motor Freq. & Battery Voltage	$b_{1,1,2}$	Destructive dissection
f'_1	Thrust	$p'_{1,1}$	Motor Freq. & Battery Voltage	$b_{1,1,3}$	Couple $b_{1,1,1}$ and $b_{1,1,2}$
f'_3	Thrust & ROI	$p'_{3,1}$	Prop Thrust	$b_{3,1,1}$	Introduce voids
f'_3	Thrust & ROI	$p'_{3,1}$	Motor Freq. & Prop Thrust	$b_{3,2,1}$	Couple $b_{1,1,1}$ and $b_{3,1,1}$

7.4.4 Step 4

Analyze and select barrier concepts that maximize system performance, Γ, and barrier effectiveness, β. To understand how each barrier concept influences the system performance and barrier effectiveness, existing models are used – or developed if none exist. For this example, a total of four models are required to analyze and select barrier concepts – one model is required to determine the barrier effectiveness of the barrier concepts, and three additional models are required to determine the effect of the barrier concepts on system performance. Each of these models are now discussed.

Barrier Effectiveness Model for All Barrier Concepts

In previous work by the authors, a systematic approach for analyzing the effectiveness of barriers to reverse engineering is developed and presented [14]. This approach, based upon Ohm's Law, enables designers to estimate the difficulty of extracting critical information about the product from the product itself. Readers are referred to Harston and Mattson [14] for model details. Some barrier concepts do not impact system performance, while others may have a positive or negative impact. As such, it is important to understand the impact various barrier concepts have on the difficulty of reverse engineering the product. For this example, the barrier concepts are compared against the benchmark design – which is the UAV design that does not incorporate any barrier concepts – as shown in Table 7.6.

Table 7.6: Barrier effectiveness of barrier concepts as compared to – and normalized to – the benchmark design for the UAV. A larger value denotes a more effective barrier.

Barrier Concept	Normalized Barrier Effectiveness (β)
Benchmark	1.00
$b_{1,1,1}$	1.16
$b_{1,1,2}$	1.16
$b_{1,1,3}$	1.33
$b_{3,1,1}$	2.17
$b_{3,2,1}$	2.67

Table 7.7: Barrier concept impact – normalized to the benchmark design – on UAV system performance. A larger value denotes a superior performance.

Barrier Concept	Normalized Performance (γ)
Benchmark	1.00
$b_{1,1,1}$	1.18
$b_{1,1,2}$	1.00
$b_{1,1,3}$	1.18
$b_{3,1,1}$	1.10
$b_{3,2,1}$	1.29

Performance Model for $b_{1,1,1}$, $b_{1,1,2}$, and $b_{1,1,3}$

To analyze the barrier impact on system performance for concepts $b_{1,1,1}$, $b_{1,1,2}$, and $b_{1,1,3}$ the models developed by Larson et. al. [153], and Larson and Mattson [148] are used. These models have been shown to approximate measured data with a max error of 3.76% when properly calibrated with the physical system. The impact of the barrier concepts on UAV system performance is shown in Table 7.7.

Performance Model for $b_{3,1,1}$

In the barrier development process, barrier concepts are analyzed and selected. However, the effectiveness of a barrier concept is dependent upon how well it is designed and optimized. This may require additional numerical optimizations or multiple design iterations of the barrier concept

before it is compared against other barrier concepts. In this section, not only is the performance model presented for analyzing barrier concept $b_{3,1,1}$ (introducing voids into the propeller) but the formulation used to optimize the barrier concept is also presented.

Recall that barrier concept $b_{3,1,1}$ is being developed to improve and protect the UAV thrust and return on investment. As such, the introduction of voids into the propeller is correlated with UAV thrust and return on investment. This is accomplished by the use of existing analytical models for propeller flutter [154], propeller efficiency [155], and return on investment [149]. Note that by maximizing the propeller flutter speed and propeller efficiency, the overall UAV thrust is improved. As such, the design of the propeller seeks to maximize flutter speed and propeller efficiency.

Once the flutter speed has been reached, the propeller deforms reducing thrust output. In extreme cases, the flutter-induced vibrations may cause propellers to catastrophically fail. In general, a higher flutter speed is better as this increases the operational speed range and increases the margin of safety [156]. However, accurately modeling flutter requires understanding and interpreting highly non-linear interactions of aerodynamic, elastic, and inertial forces. In general, flutter is very difficult to accurately simulate for complex geometries [157–159]. Frequently, designers take a coupled modeling/experimental approach to characterize and design for flutter. However, there are some simplified models that enable approximation of the speed at which a wing or propeller will flutter. One approximation of the flutter speed by the National Advisory Committee for Aeronautics [154] is given by

$$V_F = \frac{Kc}{R}\sqrt{\left(\frac{t}{c}\right)^3 \frac{G}{(\rho\,(X_c - 0.25))}} \tag{7.3}$$

where V_F is the flutter speed, K is a constant dependent upon the profile, c is the mean chord length, R is the propeller radius, t is the propeller thickness, G is the shear modulus, ρ is the air density, and X_{cg} is the position of the center of gravity expressed as a fraction of the chord. It is interesting to note that when X_{cg} is at the quarter chord (i.e., $X_{cg} = 0.25$) then the flutter speed is theoretically infinite. Therefore, when voids are introduced into a propeller, it is beneficial to distribute them in a manner that moves the center of gravity close to the quarter chord mark. The numerical optimization formulation used to determine the location of the voids within the propeller is

$$\min_{S_i,\phi_i,N_{v,i},x_{i,j},y_{i,j},z_{i,j},r_{i,j}} \{-\eta - R - \sqrt{C_{T_i}^2 + C_i^2}\} \tag{7.4}$$

subject to

$$S_i \in \{1,2,3,4\} \quad \forall i = 1,2,...,N_s \tag{7.5}$$

$$-30 \leq \phi_i \leq 30 \quad \forall i = 1,2,...,N_s \tag{7.6}$$

$$0 \leq N_{h,i} \leq 10 \quad \forall i = 1,2,...,N_s \tag{7.7}$$

$$x_{L,i} \leq x_{i,j} \leq x_{U,i} \quad \forall i = 1,2,...,N_s \text{ and } \forall j = 1,2,...,N_{v,i} \tag{7.8}$$

$$y_{L,i} \leq y_{i,j} \leq y_{U,i} \quad \forall i = 1,2,...,N_s \text{ and } \forall j = 1,2,...,N_{v,i} \tag{7.9}$$

$$z_{L,i} \leq z_{i,j} \leq z_{U,i} \quad \forall i = 1,2,...,N_s \text{ and } \forall j = 1,2,...,N_{v,i} \tag{7.10}$$

and

$$0 \leq r_{i,j} \leq 1 \quad \forall i = 1,2,...,N_s \text{ and } \forall j = 1,2,...,N_{v,i} \tag{7.11}$$

where i is the cross section index, j is the hole index, η is the efficiency of the propeller [155] (defined as the ratio of available power to the engine power), R is the return on investment, $C_{T,i}$ is the target center of gravity (the quarter chord), C_i is the calculated center of gravity, S_i is the normalized cross section geometry which is then scaled by the optimization, ϕ_i is the cross section pitch, $N_{v,i}$ is the number of voids in cross section i, $x_{i,j}$, $y_{i,j}$, and $z_{i,j}$ are the cartesian coordinates of the voids, $r_{i,j}$ is the normalized radius of the voids, N_s is the number of crossections, and $x_{L,i}$,

Table 7.8: The values of η and $\overline{C}$ of an optimized propeller with voids compared against the same propeller without voids. The efficiency of both designs is the same due to the external geometry being the same for both designs. A smaller value of $\overline{C}$ denotes a higher flutter speed.

	Propeller without Voids	Propeller with Voids
η	83.23%	83.23%
$\overline{C}$	14,337	1,015

$y_{L,i}$, $z_{L,i}$ and $x_{L,i}$, $y_{L,i}$, $z_{L,i}$ are the lower and upper bounds, respectively, of the void positions within each cross section. For this example, flutter speed is determined by propeller center of mass which is represented as $\sqrt{C_{T_i}^2 + C_i^2}$ for the ith cross section. When $\sqrt{C_{T_i}^2 + C_i^2} = 0$ for all crossections the flutter speed is theoretically infinite.

The numerical optimization uses a genetic algorithm to search for the global optimum. Of the two blades comprising the propeller, only one blade was analyzed due to symmetry. The blade was divided into 100 crossections where each cross section could have a maximum of 10 voids. The number of voids was limited to reduce the computational expense. On a computer with a processer speed of 3.4GHz and 3.25 GB of RAM, the optimization took approximately 20 hours to find an optimal solution with a population size of 30 individuals. To ensure that an optimal solution has been found, the algorithm was executed multiple times and the solutions were compared. The comparison of the design without voids to the design with voids may be seen in Table 7.8 and a representation of a section of the propeller with voids is shown in Fig. 7.4. Note that the efficiency of both designs is the same. This is due to the fact that the both designs have the same external geometry – which has been improved over the initial propeller geometry. However, once the flutter speed has been exceeded, efficiency is reduced. Hence the importance of increasing the flutter speed. To characterize the flutter of the entire propeller, $\overline{C}$ is defined as the average distance between C_{T_i} and C_i over all crossections: $\overline{C} = \left(\sum_{i=1}^{N_s} \sqrt{C_{T_i}^2 + C_i^2} \right) \Big/ N_s$. A smaller value of $\overline{C}$ denotes a higher flutter speed according to Eqn. 7.3 (i.e., when $\overline{C} = 0$ then $X_{cg} = 0.25$).

The numerical model was validated for a propeller with voids and a propeller without voids by (i) analyzing and comparing the center of gravity with the numerical model, and (ii) physically measuring the center of gravity on a rapid-prototyped section of each propeller. The percent error between the physical measurements and the analytical model is less than 1% for

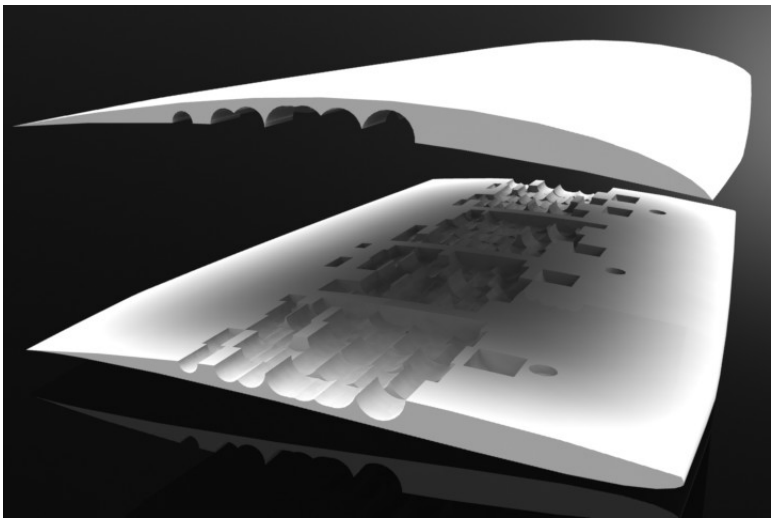

Figure 7.4: Representation of a section of the propeller with internal voids.

the wing sections tested. In addition, both the numerical model and physical measurements show that the propeller with voids has an improved mass distribution. According to the model (refer to Eqn. 7.3), the propeller with the voids will have a superior performance by being able to have a higher operational speed before flutter begins to occur. The impact of barrier concept $b_{3,1,1}$ on system performance is shown in Table 7.7 where the system performance has been normalized with respect to the benchmark performance.

Performance Model for $b_{3,2,1}$

This barrier concept is to design the motor to look identical to an off-the-shelf part, encode labels, and introduce voids into the propeller. As this is simply a combination of barrier concept $b_{3,1,1}$ and barrier concept $b_{3,1,1}$, the models required to analyze these barrier concepts are presented above. The impact of barrier concept $b_{3,2,1}$ on system performance is shown in Table 7.7 where the system performance has been normalized with respect to the benchmark performance.

Selection of Barrier Concepts

With the barrier effectiveness model and the barrier performance models defined, Eqn. 8.7 is used to select which barrier concepts to pursue (i.e., populate B'). Similar to Step 2, using an aggregate objective function results in the selection of a single barrier concept, where the use of

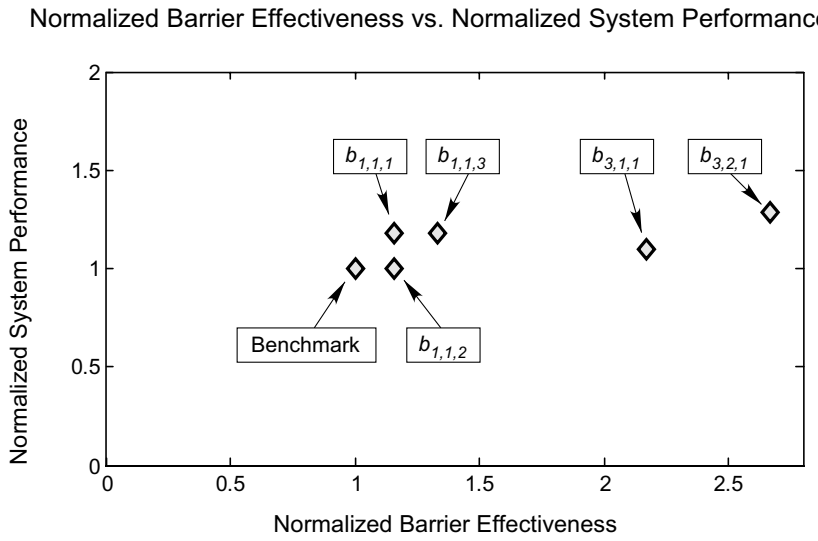

Figure 7.5: Plot of system performance (with barrier concept implemented) vs. barrier effectiveness for each of the five barrier concepts and the benchmark design. Values have been normalized to the benchmark design.

multiobjective decision theories enables the designer to select one or more barrier concepts. For this example, when barrier performance is plotted against barrier effectiveness (shown in Fig. 7.5), a single barrier concept dominates all other concepts. It is this barrier concept – barrier concept $b_{3,2,1}$ – that is selected to be implemented into the solar-powered UAV with the goal of maximizing reverse engineering difficulty, maximizing return on investment, and maximizing UAV thrust. If desired, multiple barrier concepts may be implemented simultaneously.

7.4.5 Step 5

Implement selected barrier. The selected barrier concept is to design the motor to look identical to an off-the-shelf part, encode labels, and introduce voids into the propeller. Recall that the purpose of this barrier development process presented in the current chapter is to assist the designers in identifying the critical elements of a system and to develop reverse engineering barriers to protect them. Where the first four steps of the barrier development process focused on selection of the reverse engineering barrier, the fifth step focuses on refining and implementing the barrier concept into the product. At this point, the barrier development process merges with the

traditional product development process (refer to Fig. 7.1) where additional barrier-specific design constraints are imposed to ensure the proper implementation of the selected barrier(s).

7.5 Chapter Summary

In this chapter, a process to assist designers in developing products that are difficult to reverse engineer *and* meet or exceed performance requirements is presented. The barrier development process considers (i) which product performances need protection, (ii) what parameters affect product performances, and (iii) what barriers best protect the selected parameters and product performances. To illustrate the barrier development process, a solar-powered unmanned aerial vehicle is analyzed and made difficult to reverse engineer. With multiple performances, parameters, and barriers explored for the UAV, the method assisted the designer in determining that (i) the most desirable performances to protect are thrust and return on investment, (ii) the parameters that affect the selected performances are motor frequency and propeller thrust, and (iii) a desirable barrier to implement is to design the motor to look identical to an off-the-shelf part, encode labels to minimize divulged information, and introduce voids into the propeller that decrease weight and increase flutter speed – a desirable attribute in propellers.

CHAPTER 8. CAPITALIZING ON HETEROGENEITY AND ANISOTROPY TO DESIGN DESIRABLE HARDWARE THAT IS DIFFICULT TO REVERSE ENGINEER

8.1 Chapter Overview

This chapter presents a method for treating material microstructure (crystallographic grain size, orientation, and distribution) as design variables that can be manipulated – for common or exotic materials – to identify unusual material properties and to design devices that are difficult to reverse engineer. A practical approach, carefully tied to proven manufacturing strategies, is used to tailor material microstructures by strategically orienting and laminating thin anisotropic metallic sheets. The approach, coupled with numerical optimization, manipulates material microstructures to obtain desired material properties at designer-specified locations (heterogeneously) or across the entire part (homogeneously). A comparative study is provided that examines various microstructures for a simple fixed geometry. These cases show how the proposed approach can provide hardware with enhanced mechanical performance in a way that is disguised within the microscopic features of the material microstructure.

8.2 Introduction

While others have previously coupled material properties of metals with geometry and performance optimization [82–84, 160, 161], this chapter presents a new method of tailoring the properties of metals by using thin metal laminations strategically oriented [74] and ultrasonically welded together. [162] We show how numerical optimization can be used to search through a materials design space [151, 152, 163], and that the proposed integration of optimization, manufacturing, and design methods can result in material microstructures that are (i) consistently producible from a manufacturing perspective, and (ii) difficult to reverse engineer. The proposed method can, therefore, be used to tailor new and practical materials for the design engineer's specific need.

For many product designers, material properties, such as yield strength and Young's modulus, are chosen from a set of discrete values, typically published in the form of a material properties table [164]. Under this typical approach, if one requires a part to withstand more stress before failure, the geometry is typically changed or a new material class or alloy is selected. Consider the benefit that would come to the design engineer if he or she could hold the geometry constant and, using the original material, improve the material's resistance to plastic failure or other material properties. He or she could increase product performance without resorting to more expensive materials or they could hide performance increases from competitors, since discovering the source of the increased performance would not be trivial. This chapter proposes a methodology to do this.

Recent advancements in material science enable the development of the proposed approach [73, 74]. Specifically, these advancements pertain to material microstructure, which is the composition of a material including arrangement, size, orientation and distribution density of crystallographic grains [73]. These advancements have led to predictive relationships for characterizing material properties as a function of the material microstructure. When coupled with numerical optimization and lamination technology (two other key enablers), material properties can be modified as simply as geometry, creating one more degree of freedom in the design. Additionally, the method outlined in this chapter allows one to make calculated changes to the microstructure to obtain desired results in material properties at designer specified locations (heterogeneously) or across the entire part (homogeneously).

The purpose of this chapter is to present a new design framework, in conjunction with numerical optimization, that couples microstructure manipulation and modeling with existing manufacturing processes to create products with desired performance. The microstructure sensitive design approach, as presented in this chapter, enables a product to perform (e.g., deflection, yield characteristics, shear characteristics) in a way that cannot be obtained without manipulating the material. Furthermore, the source of performance improvement is difficult to determine and recreate from a reverse engineering perspective, thus impeding competitors from successful reverse engineering.

The presented design framework is based upon the published work of two fundamental elements: microstructure characterization [73, 74, 165] and the additive manufacturing process of ultrasonic consolidation [162, 166, 167]. While microstructure characterization and ultrasonic

consolidation have been previously described in the literature, in this chapter they are coupled under an optimization framework that enables the creation of products with enhanced mechanical performance.

The framework proposed in this chapter is presented by first reviewing enabling technologies and fundamental theories supporting the work. This is presented in Section 8.3. Section 8.4 then describes the design framework used to obtain desired material properties with common materials. In Section 8.5, a comparative study is provided that examines various microstructure implementations for a simple fixed geometry. Concluding remarks are provided in Section 8.6.

8.3 Description of Enabling Technologies and Fundamental Theories

In this section we present the enabling technology of ultrasonic consolidation [162] which facilitates the joining of thin metal sheets with minimal disturbances to the microstructure in the weld areas. We also present four fundamental theories required for predicting material properties for a part, based on measurements of a material's microstructure. They are; reference frames, fundamental zone, rotations of anisotropic layers, and the lamination of those thin layers.

8.3.1 Ultrasonic Consolidation: Additive Manufacturing Process of Metals

One manufacturing technology that allows improved material properties to be obtained from common metals is the additive manufacturing process of ultrasonic consolidation (UC). UC utilizes principles of ultrasonic welding [162] to combine metal sheets, typically 150 μm thick, in a layer-by-layer process. This process is often combined with a 3-axis CNC mill to produce complicated geometry during the additive process. The UC process, as represented in Figure 8.1, begins with a heated base of the same material of the part. A rolling/rotating sonotrode applies a normal force while oscillating which results in dynamic interfacial stresses at the interface between the two mating surfaces. [162, 166, 167] The stress incurred by the high frequency oscillations, around 20 kHz, produce elastic-plastic deformation and establishes a metallurgical bond as can be seen in the polished crossection shown on the right-side of Figure 8.1. This process is repeated layer-by-layer until the part is completed with the desired number of layers.

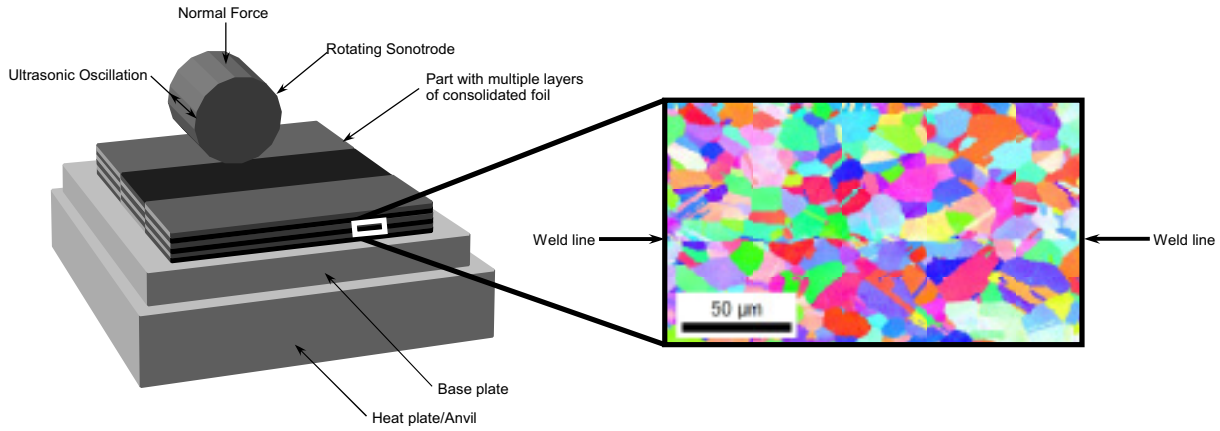

Figure 8.1: Ultrasonic consolidation process with scanning electron microscope image of grains at layer interface.

It is impressive to note that UC materials can yield a 85% to 100% linear weld density along the bonded interface. [168] A linear weld density of 100% implies that the weld has an equivalent void space, dislocations, and is as durable (both for fatigue and corrosion resistance) as the surrounding grain boundaries. Obtaining a linear weld density of 100% is feasible, however it requires proper adjustment of the UC manufacturing parameters (e.g., magnitude of the oscillations, frequency of sonotrode, normal force applied) which are typically determined through empirical studies on the material of interest [169, 170]. When the linear weld density is not 100%, products may need to be designed with a larger safety factor to take into account the weakened welds which may result in decreased fatigue life and yield strength. However, Ram et. al. [169, 170] have conducted numerous experiments with ultrasonically consolidated materials to determine optimal parameters to obtain a linear weld density of approximately 100%.

One important characteristic of UC is the low temperature at which the layers are welded together, which range from ambient to $350°F$. This results in minimal local disturbances in the weld area, thus making the layer-by-layer construction virtually undetectable, which supports the notion of hiding the source of performance increases from competitors.

Possibly the most impressive feature of UC is the number of microstructures that may be obtained thereby. It is known that extreme microstructures may be induced in metal foils by rolling and recrystallization. [171] These foils may then be combined by the UC process to create a material made with laminations. When layers with known microstructures are strategically placed,

one can effectively create a laminated material with desired properties and even consistently obtain material properties that are otherwise not used in practice.

As the additive process of ultrasonic consolidation is relatively expensive compared to traditional manufacturing processes (e.g., rolling, heat treating, machining), it is often best strategically implemented into a few critical components of a system. The quantity of components that are created with the UC process will adversely affect the product manufacturing cost, however, (i) UC enables designers to obtain microstructures (and therefore desired material properties) that are difficult, if not impossible, to obtain by other means, and (ii) when critical components of a system are made difficult to reverse engineer, by using UC to obtain unusual microstructures, it effectively impedes the reverse engineering of the entire system. Therefore the costly nature of UC can be justified in some cases by the unique benefits it brings.

8.3.2 Reference Frames and Fundamental Zone Defined

As the UC method forms a basis for microstructure manipulation by joining laminae, it is useful to define three reference frames commonly used when working with laminae: Crystal, Laminate, and Part reference frames. The main purpose of these reference frames is to have a consistent point of reference when aligning layers and defining directionally-dependent material properties. While it is important that reference frames do not vary over the design process, it does not matter how reference frames are oriented. There are however, common approaches for orientation; typically the crystal's reference frame will be aligned with the crystallographic directions, X_{cj}, Y_{cj} and Z_{cj} for the j-th crystal in a sample, [172] where the subscript c represents the crystal frame.

A convenient reference direction for a heavily rolled lamina is the rolling direction. One axis of the sample reference frame is aligned with the rolling direction and is termed "*Rolling Direction*" or D_k^R for the k-th layer. The second axis, or "*Normal Direction*" (D_k^N), is placed perpendicular to the both the rolling direction and a surface of the laminate. While it does not matter which surface is selected for the thin lamina, typically surfaces with a large surface area are used as a reference. With two axis defined, the third axis, the "*Transverse Direction*" (D_k^T), is defined with the use of the right-hand rule. [73]

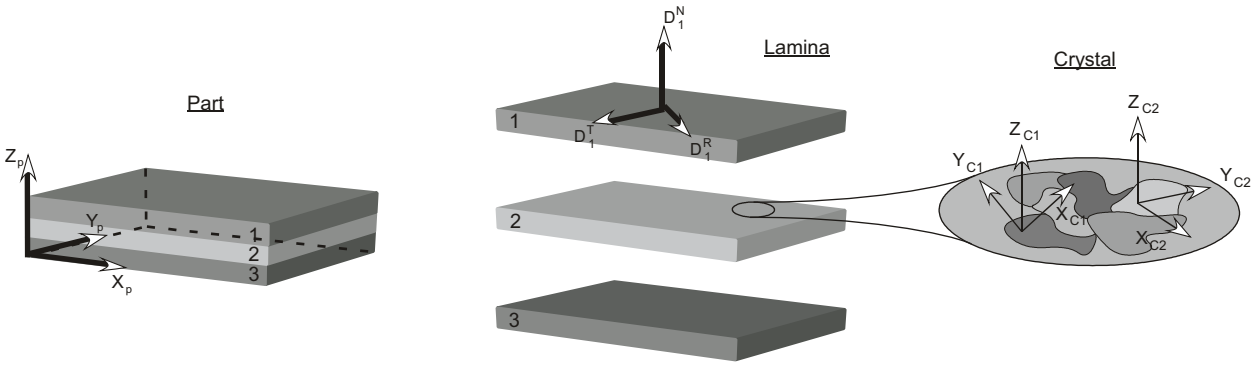

Figure 8.2: Reference frames defined for the part, lamina, and crystal.

The final reference frame to be described, the part reference frame, is defined according to the geometry and is typically aligned with a dominant geometric feature as seen in Figure 8.2 as X_p, Y_p and Z_p. The part reference frame allows one to properly align the rotated laminae in relation to the part to achieve the desired properties in the directions of interest. [172]

The orientation of one reference frame to another is represented by the standard Euler angles, ϕ_1, Φ, and ϕ_2. The Euler angles represent all possible orientations but due to symmetry, the limits on the angles may be set to $0 \leq \phi_1 < 2\pi$, $0 \leq \Phi \leq \pi$, and $0 \leq \phi_2 < 2\pi$ respectively. [172] For parts constructed with layers, it is convenient to only rotate the layers about their normal axes, which is what we do in this chapter.

Another important concept in being able to extract material properties from crystal orientation data is the Fundamental Zone (FZ). The FZ is the set of all physically-distinct orientations of the local crystal that can occur. [73] Due to the computational power required to analyze the infinite number of possible crystal orientations, the FZ is binned into groups of orientations with each bin approximated by a single orientation. The Binned Fundamental Zone (BFZ) can then be used as a simplified orientation description for all crystals in the sample. The number of bins is determined by the conflicting objectives of desired accuracy and computational time available.

8.3.3 Using Rotation and Lamination Theory to Predict Material Properties

In this section we present the microstructure-to-material-property theory, which is the process we use to predict material properties, given information about the material microstructure. In the rotation and lamination theory presented below in Section 8.3.5, it is through manipulation of

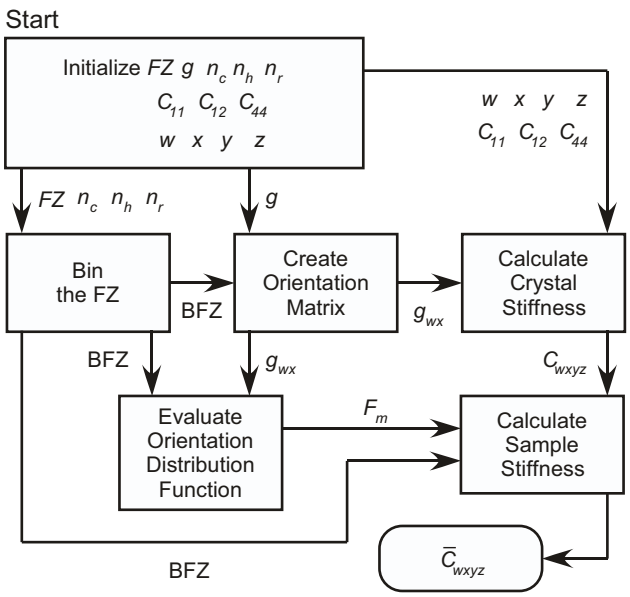

Figure 8.3: Microstructure-to-Material-Properties flowchart.

the material microstructure of each layer that one is able to obtain an overall change in material properties and product performance. Therefore, it is important to understand the microstructure-to-material-properties theory which is the crucial link in considering material properties as design variables.

The flowchart in Figure 8.3 presents the process in which material stiffness, $\overline{C}_{wxyz}$, is estimated from microstructure properties of a material. As a note, other specific material properties such as yield strength, Young's modulus, Poisson's ratio, shear modulus, and critical shear stress can also be determined from the material microstructure by a similar process if desired. The flowchart in Figure 8.3 is now described in detail.

The process to estimate material stiffness begins by initializing the variables shown in the upper left box of Figure 8.3 and by obtaining the material specific constants from the literature such as C_{11}, C_{12}, and C_{44}. [173] Next, the FZ is binned allowing multiple orientations to be approximated by a single orientation thus decreasing the number of unique orientations requiring analysis. The resolution of the binning is determined by dividing the FZ into a number of rows, columns, and layers represented by n_r, n_c, and n_h, respectively. Fewer bins equates to a faster computational time with a decrease in accuracy while increasing the number of bins improves accuracy at the expense of time. Continuing downward from the box dipicting the binning of the fundamental

zone, the Fourier coefficient, F_m, is calculated which is literally the volume fraction of crystals in the m-th bin of the BFZ. Simply stated, F_m is the percentage of crystals that are aligned in a given direction and is used for calculating the material stiffness. Before F_m can be calculated, crystal orientation data, g, obtained by Orientation Image Microscopy [73] (OIM) is converted to an orientation matrix, g_{wx}, which forms a link between the raw OIM data and the BFZ. One of the key factors in obtaining a continuous range of material properties is the understanding of the initial microstructure as determined by OIM. Without the details of the starting microstructure (characterized by g in the upper left box of Figure 8.3) for the specific material to be used, the desired material properties cannot be obtained with the rotation/lamination theory.

A simple way to determine the percentage of crystals occupying a bin is to use the Orientation Distribution Function (ODF). The ODF is a function that receives information about the BFZ and orientation matrix, g_{wx}, and enables a description of all crystal orientations in a sample. Evaluating the ODF with a single direction results in a scalar representing the percentage of crystals aligned in that direction. When the ODF is calculated for multiple directions, the results are a scaler representing the percentage of crystals aligned in the multiple directions defined – such is the case of a bin in the BFZ.

As is true with all material properties, stiffness of the sample is a function of the stiffness of each crystal. In fact, the sample stiffness, $\overline{C}_{wxyz}$, is estimated by the average stiffness of all crystals. Parameters required to determine crystal stiffness are the direction of interest as defined by the designers (w, x, y, z) and three material properties which come from literature; C_{11}, C_{12}, and C_{44}. Note that the additional parameters related to binning the fundamental zone are not required unless reducing the computation cost is required. With F_m and C_{wxyz} known, it is a simple matter to compute $\overline{C}_{wxyz}$, since $\overline{C}_{wxyz}$ is the average stiffness weighted by F_m. For the derivations of these estimations and their limitations we refer the reader to [174–176].

8.3.4 A Criteria for Plastic Failure

The failure criteria used in this chapter to determine if the material plastically deforms under the applied loading conditions is presented in this section. Two approaches can be taken to characterize plastic failure; the first involves developing a general estimate of the material's yield strength, which can be found directly from microstructure data and calibrated with a single

tensile test. Another approach uses the classic power law viscoplasticity failure model, which requires both material microstructure information and loading conditions. In this chapter we use the viscoplasticity failure model, which can be expressed as

$$\overline{D}_{ij} = D_{ij} = \dot{\gamma}_0 \sum_{s=1}^{s} \left| \frac{(\sigma'_{kl})\alpha_{kl}^{(s)}}{\tau^{*(s)}} \right|^n sign\left((\sigma'_{kl})\alpha_{kl}^{(s)}\right)\alpha_{ij}^{(s)} \tag{8.1}$$

where $\dot{\gamma}_0$ is the reference shear rate, s is the total number of slip systems in the material, σ'_{kl} is the local deviatoric stress for a given direction, [177] $\alpha_{kl}^{(s)}$ and $\alpha_{ij}^{(s)}$ are simple combinations of the slip directions and the slip plane normals, [177] and $\tau^{*(s)}$ is the estimated shear stress required before dislocations move on the slip plane. The only value on the right side of the equation that cannot be obtained from literature is the local deviatoric stress which can be determined using finite element analysis with known loading conditions. The local strain rate, D_{ij}, can then be calculated. One assumption often made when using the viscoplasticity failure model is that the average of the local strain rates is equivalent to the macroscopic strain rate, $\overline{D}_{ij}$, of the material at that point. Therefore plastic deformation of a material is directly related to the material strain rate. It follows that when

$$D^* \leq \overline{D}_{ij} \tag{8.2}$$

where D^* is the critical strain rate, we can know that the material has plastically deformed at that point. In the current chapter, we have selected the critical strain rate to be 0.001 s^{-1}. The finite element analysis returns the stress at each node which we use to determine the total number of nodes that have yielded by the relationships above. As there will always be some quantity of nodes that fail under any loading condition, we specify that a material fails when when 15% or more of the nodes have plastically deformed. For the full development and application of Equation 8.1, the reader is referred to Adams et. al., [165] Fromm et. al., [177] Taylor, [178] and Asaro and Needleman. [179]

8.3.5 Part Construction by the Rotation and Lamination Theory

We now consider approaches by which microstructures can be intentionally created to have certain characteristics. We have explored a variety of manufacturing processes that allow for mi-

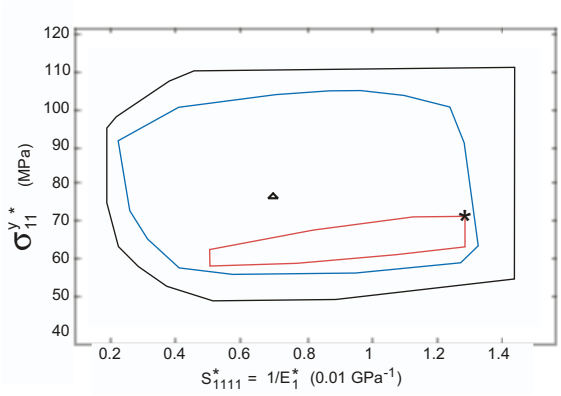

Figure 8.4: Property closure of yield strength vs. compliance for Ni 201. The outer loop is the property closure, the triangle represents an isotropic material with the same material properties in all directions and the inner loop represents all material properties that can be obtained by applying the rotation and lamination theory to a material that starts with the microstructure shown as a star. The middle loop represents material properties that can be obtained when the layer rotations are not constrained to a single plane.

crostructure manipulation such as friction-stir welding, [180] heat treatment, and introducing voids into the material. While these processes may be utilized in many different ways, strategically orienting and laminating thin sheets is a more flexible and predictable way to consistently obtain designer selected values of material microstructures. The theory of rotations and laminations allows one to take any initial microstructure and create a new microstructure by stacking and welding thin metal layers – with directionally dependent material properties – at specific rotations. This theory, coupled with UC technology, allows the designer to hold the alloy fixed, yet modify material properties by choosing layer configuration and orientation.

Recall that the material property closure is the set of all material properties that are possible if one could create all possible microstructures. Since not all microstructures are practically obtainable, the achievable space in the property closure is limited. Implementation of rotation and lamination theory, however, greatly expands the achievable space in the property closure as shown in Figure 8.4 for Ni 201 – a first-order approximation of the property closure. The axes shown in Figure 8.4 represent two different material properties; material compliance (elasticity) on the x-axis and yield strength on the y-axis. Note the subscripts, which represent desired directions for which the properties apply. The outermost loop, and the area it contains, represents every possible combination of these two properties. A single point represents a specific value for both the

compliance and the yield strength which may be mapped to one or more microstructures that will have those properties. The triangle in Figure 8.4 represents isotropic material properties for Ni 201 while the star represents the starting microstructure of the material – as defined by OIM – in the direction of interest. As a note, the starting microstructure is the material microstructure for a a thin metal sheet before reorientation or inclusion in a laminae. The inner loop that intersects the star, and the area it contains for multilayered structures, represents all properties that can be obtained by implementing the rotation and lamination theory to that starting microstructure when all rotations about the normal axis of the respective layer are considered. The remaining loop and the area it contains represents material properties that may be obtained by performing the rotation and lamination process twice (rank 2 lamination) to obtain even more complicated microstructures. It is important to note that any microstructure obtained by conventional methods, such as heavy rolling, can be enhanced to obtain new microstructures and thus enable new combinations of material properties that are typically thought to be unobtainable.

8.4 Design and Optimization Framework for Enhanced Performance Through Microstructure Manipulation

In this section we present a generic framework that enables us to obtain an enhanced, and desired, mechanical performance created by strategically manipulating the microstructure of common metal alloys using the rotation and lamination theory. Specifically, when given a target performance, the direction(s) of interest, and the desired number of layers, this optimization routine will find an optimal orientation of each layer in an effort to obtain the desired performance in the direction(s) of interest. The generic optimization framework may be seen in Figure 8.5(a) and a framework specific to structural design, and used in the case study section of this chapter, may be seen in Figure 8.5(b). There are six main parts to the optimization framework. Part 0 – initialization of system parameters. Part I – gathering microstructure data for selected alloy. Part II – definition of feasible range of material properties obtainable by rotations and laminations. Part III – material property exploration and selection using optimization techniques. Part IV – performance measurement. Part V – constraint analysis. Each part of the process is now described in detail.

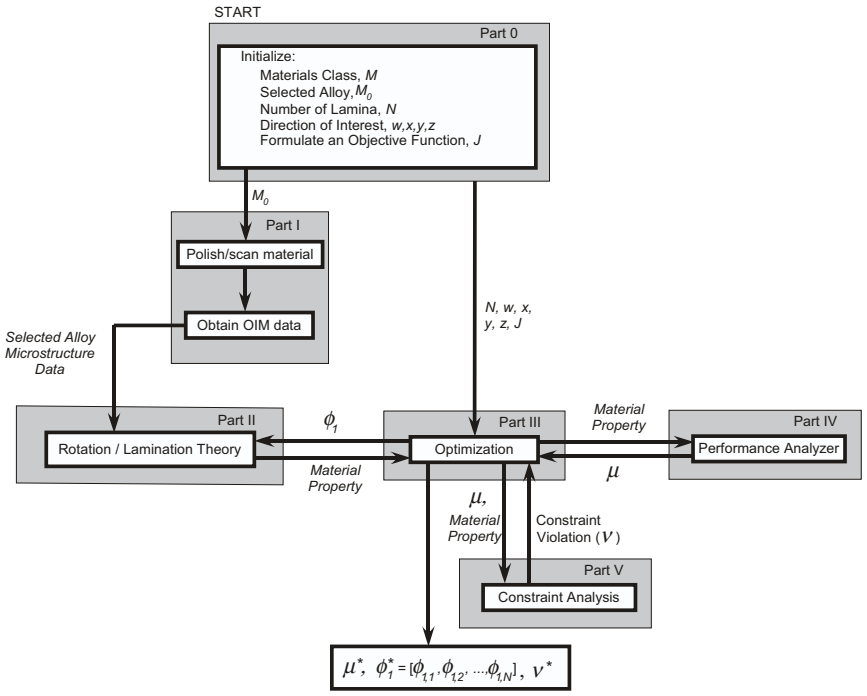

(a)

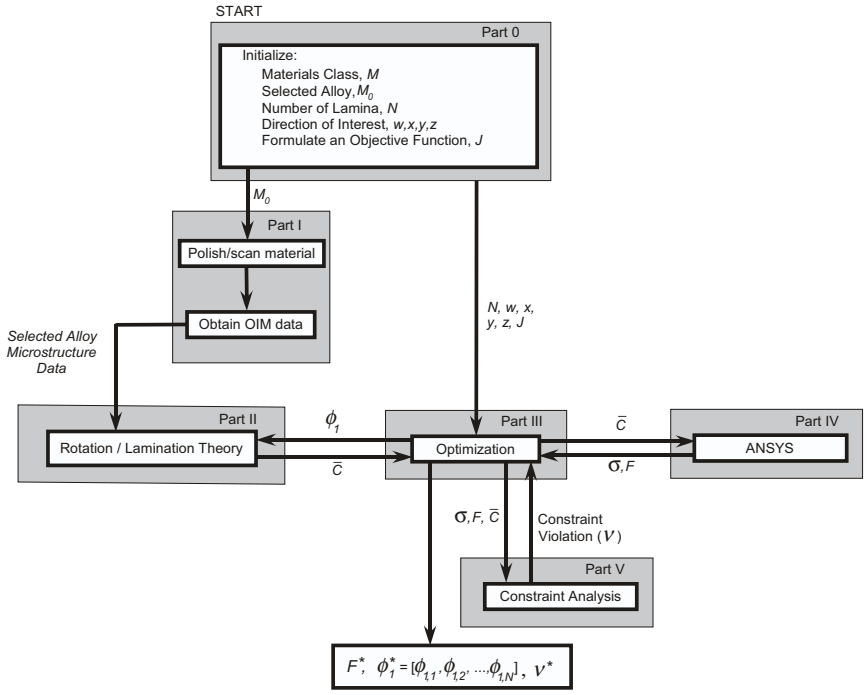

(b)

Figure 8.5: (a) Flowchart of a generic optimization framework to obtain improved performance with common materials and (b) an optimization framework specific to structural stiffness.

8.4.1 Part 0 – Initialize Input Parameters

Let us first consider Part 0. This part of the framework requires the designer to identify the optimization parameters and variables, and formulate the objective function, J. The designer also selects the material class, M, a specific alloy, M_0, from the chosen class to be used as the lamina material, the number of lamina, N, in the lamination, and at least one direction of interest, which is represented by w, x, y, and z. Assuming a uniform layer thickness, the number of layers required is dependent upon the thickness of the part being created.

8.4.2 Part I – Characterize Microstructure of Selected Alloy

Before we can obtain the desired material stiffness of a material, we first need to acquire microstructure information about that material. This is done by polishing and scanning the sample with a scanning electron microscope and analyzing the data with OIM software. [73] The data collected includes grain size, grain distribution, grain orientation and other microstructure information specific to the sample. Once microstructure data is gathered, the range of material properties may be determined as described in Part II.

8.4.3 Part II – Determine the Full Range of Material Properties Obtainable with Rotations and Laminations for the Selected Alloy

The range of properties obtainable by rotation and lamination depends upon the material microstructure. A material that is isotropic will always have the same properties independent of the material orientation. On the other hand, anisotropic materials made with a single crystal have the most directionally dependent material properties as the properties may change dramatically even with a small rotation. The OIM data found in Part I determines the microstructure of the selected alloy, thus determining the degree of anisotropy that exists in the sample. The OIM data is then used in the rotation/lamination theory to determine material properties in a given direction. Application of the rotation/lamination theory for every orientation from $0-2\pi$ reveals the range of material properties that may be obtained with the sample-specific microstructure. When symmetry exists in the microstructure, the complete range of material properties may be obtained with a reduced set of microstructure orientations. A convex hull encloses the resulting range of material

properties and is principally used to help the designer know the feasible range of material properties for the given microstructure. This is the process that was performed on Ni 201 to obtain the property closure in Figure 8.4.

8.4.4 Part III – Determine Rotation/Lamination Strategy Required to Obtain Desired Performance for Selected Alloy

In Part III, we use an optimization routine to determine the manufacturing strategy – specifically the orientation of each layer – to create a laminated material with the desired material properties in the direction of interest. The optimization requires the number of laminations, N, the direction of interest, w, x, y, z, and the objective function, which are all determined by the designer in Part 0. The optimization selects a value of ϕ_1 for each lamina, sends the lamina orientation through the rotation and lamination model and receives the material properties of interest. The optimizer then sends those material properties to the performance analyzer of Part IV, which evaluates and returns the design objective values, μ, and/or any other needed analysis such as those pertaining to constraints. Part V evaluates the constraints and determines the magnitude of constraint violation, v. The process is repeated until the optimization determines the optimal orientation of each layer. On the final iteration, the optimization outputs the optimal value of the design objectives, μ^*, the constraint violations, v^*, and the optimal orientation of each layer, ϕ_1^*. Note that by *optimal* we mean numerically optimal as characterized by the designer-made performance models (e.g., finite element analysis) and characterized by the optimization problem statement, which in its generic form is as follows:

$$\min_{\phi_1} J = \{\mu_1, \mu_2, ...\mu_{n_\mu}\} \tag{8.3}$$

subject to

$$g_q \leq 0 \qquad \forall q = 1, 2, ..., n_g \tag{8.4}$$

$$h_v = 0 \qquad \forall v = 1, 2, ..., n_h \tag{8.5}$$

$$0 \leq \phi_{1,i} \leq \pi \qquad \forall i = 1,2,...,N \tag{8.6}$$

where $\phi_1 = [\phi_{1,1}, \phi_{1,2}, ..., \phi_{1,N}]$ and represents the orientation of each layer, and μ_i denotes the i-th generic design objective. Note that due to symmetry the design variable is constrained from 0 to π. In some cases, it may be necessary to expand the variable space to avoid active constraints that point to local, as opposed to global, optima.

During the optimization process, each layer is strategically oriented to create a new microstructure in an effort to obtain the desired mechanical performance. If a target material performance is not possible for any combination of material properties obtainable with the rotation/lamination theory, the optimization routine will find feasible material properties that result in the best performance possible as measured by the objective function.

8.4.5 Part IV – Performance Analysis

The performance analyzer in Part IV receives the material properties as determined in Part II and Part III and outputs the design objective values. In the case of structural design (Figure 8.5(b)) the performance analyzer receives the material stiffness matrix, $\overline{C}$, as an input and determines the force required to achieve a prescribed deflection with a predetermined geometry. It also determines the stresses that develop throughout the part as a result of the force. The finite element analysis software, ANSYS, then returns the force, Q, and the stress, σ_i, to the optimizer where i represents the i-th node and is used to determine the deviatoric stress, σ'_{kl} in Equation 8.1

8.4.6 Part V – Constraint Analysis

The constraint analysis is a designer-defined function that simply determines if the current design selected by the optimization meets the design criteria. The constraint analysis calculates the constraint violation, v. Returning to the structural design example in Figure 8.5(b), the constraint analysis will receive the stress (calculated by ANSYS) and the material stiffness and will determine if plastic deformation has occurred by using the power law viscoplasticity failure model as described in Section 8.38.3.4.

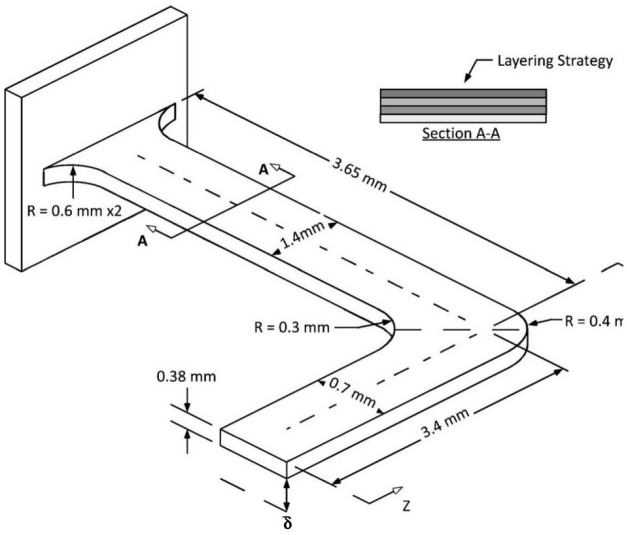

Figure 8.6: Geometry and boundary conditions for the L-beam case study.

Section 8.4 has illustrated how we use the various theories described in this chapter to explore the materials design space and search for desirable material properties that enhance mechanical performance. In the following section, we consider a simple mechanical element and show how the use of the aforementioned design and optimization framework leads to desirable mechanical performance – the source of which is hidden in the tailored material microstructure that results from the design and optimization approach.

8.5 Case Study

This section illustrates the benefits that can come from implementing the theories and methodologies presented in the previous sections of this chapter. For this case study, and all sub-studies presented herein, a simple L-beam geometry, fixed at one end, and exposed to a prescribed deflection at the other is considered. The L-beam is chosen to illustrate the process because of the its simplicity and because it is derived from an actual L-beam designed by one of the authors for a popular mobile phone. As such, the geometry, parameters, and so forth are representative of a realistic industrial application.

We pause now to describe why we fix the geometry throughout this case study and explain the effect this has on reverse engineering. The geometry is fixed for two principle reasons. First, during the design of the L-beam used in the mobile phone, the geometry was already at the up-

per bounds of a very constrained component envelope. Therefore, any permissible change in the geometry would have an undesirable affect on the performance, as shown below. Second, when a component such as this is reverse engineered by a competitor, the most likely reverse engineering strategy is to copy the geometry and the chemical composition of the material. As is shown below, this common reverse engineering approach will not lead to a functional replica. Instead it leads to a design represented by the benchmark design below. A desirable performance can only be achieved through microstructure manipulation. It is important to note that it is unlikely that the competitor will be able to determine the complex material microstructure created by the lamination of independently oriented thin metal foils. Should the competitor determine the complex microstructure, the extremely difficult task of determining how to manufacture that complex microstructure poses yet another barrier to reverse engineering.

Six sub-studies of the L-beam are provided here for comparative purposes. The illustration provided in Figure 8.6 represents the fixed geometry and boundary conditions used throughout the entire case study. The six sub-studies consider (I) an isotropic one layer lamina, (II) an anisotropic one layer lamina, (III) a multilayered anisotropic laminate, (IV) a heterogeneously distributed microstructure in single layer, and (V and VI) a special exploration into when multilayered laminates out perform single layer lamina and vice-versa. Each sub-study shows how the performance of the fixed L-beam geometry can be enhanced by material manipulation.

8.5.1 Sub-studies I through IV

For sub-studies I through IV, the design objective is to minimize the reaction force (in the normal direction) at the free end of the beam, when subject to a prescribed displacement (δ) at the free end and subject to the material being within acceptable yielding conditions. As a note, for applications such as those of the mobile phone, normal forces larger that 1.2 N can result in excessive wear on the mating surfaces of these parts, which are often used to transmit electrical current. [181]

The optimization problem statement used for sub-studies I-IV is:

$$\min_{\phi_1} J = Q \tag{8.7}$$

subject to

$$P < 0.15 \tag{8.8}$$

$$0 < Q \leq 1.2 \text{ N} \tag{8.9}$$

and

$$0 \leq \phi_1 \leq 90^o \tag{8.10}$$

where Q is the reaction force at the point of the applied deflection, and P is the fraction of nodes that have plastically deformed.

During the optimization procedure, only the material orientation, $\phi_{1,i}$, is changed where i represents the i-th homogeneous material segment, such as a single layer. For the isotropic L-beam and the single anisotropic layer L-beam, $i \in \{1\}$. For the laminated L-beam four layers are considered, so $i \in \{1,2,3,4\}$. And the heterogeneous L-beam is divided into two segments, therefore, $i \in \{1,2\}$. The material used throughout the case study is pure copper, which for sub-studies II through VI has been rolled and heat treated to create a very strong texture in the rolling direction. As a note, all material microstructures were obtained by measuring the microstructure of the sample as described in Section 8.48.4.2. In consideration of manufacturing process simplicity, we only allow material orientations belonging to the set {0 5 10 15 20 25 30 35 40 45 50 55 60 65 70 75 80 85 90} expressed in degrees.

Each of the sub-studies presented in this section used a genetic algorithm to find the material orientation that minimized the reaction force, and ensured compliance with a material yielding criteria. The genetic algorithm was selected as the optimization algorithm as it is capable of searching over a design space with multiple local minima. Since we are interested in potentially orienting multiple layers, and since the orientation of each layer influences the effective properties of the part as a whole, many local minima exist in the design space. Due to the nature of genetic algorithms, it is possible for the optimization routine to converge on different solutions – which may or may not be the global optimal solution – for different optimization runs. To increase the likelihood that the global optimal solution is found, the optimization routine was executed multiple times for each

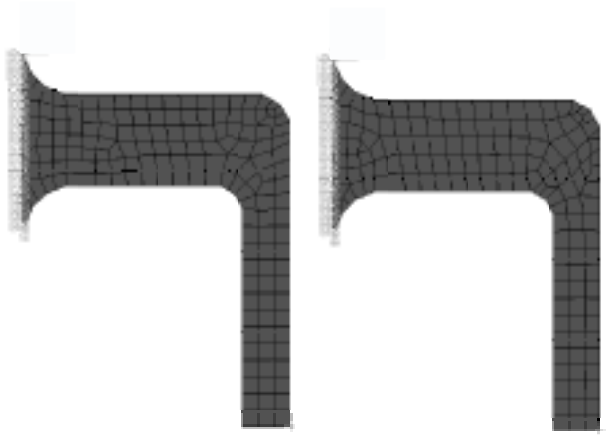

Figure 8.7: (a) Finite element mesh for the isotropic, single layer, and four layer L-beams, and (b) finite element mesh for the heterogeneous L-beam.

sub-study. For the examples presented in this chapter, each run of the optimization routine resulted in approximately the same solution for a given sub-study. The genetic algorithm parameters were the same for each of the sub-studies presented in this chapter which are: a population size of 30 individuals, a maximum number of 30 generations, a mutation rate of 0.01, and a crossover rate of 0.50. While the optimization was permitted to run up to 30 generations, an optimal solution was often found within 10 generations. As a note, these same algorithm parameters are used in sub-studies V and VI.

The genetic algorithm was coupled with the commercial finite element analysis software ANSYS to analyze the force and stresses of the structure. A material stiffness matrix – determined by the microstructure and the respective orientation – was input into ANSYS (using anisotropic element shell281) which then output the force required to achieve the prescribed deflection of the L-beam and also output a 6x1 stress vector for each node (refer to Figure 8.5(b)). As a reference, the mesh used for sub-study I-III, V, and VI may be seen in Figure 8.7(a) and the mesh used for sub-study IV may be seen in Figure 8.7(b) where a line at approximately 45^o separates the horizontal and vertical beams for the heterogeneous material. The 6x1 stress vector is then analyzed by the failure criteria presented in Section 8.38.3.4 to determine if failure has occurred. Using a Xeon 3.4 GHz processor and 3.25 GB of RAM, the analysis took roughly 25 seconds per individual. This time includes both the genetic algorithm calculations and finite element analysis.

We now briefly provide additional information regarding each sub-study and refer the reader to Tables 8.1 and 8.2 for a summary of results.

Sub-study I, Single Isotropic Layer L-Beam

The single layer isotropic L-beam is considered the benchmark design in this study as it is based on the same assumptions used in the design of the mobile phone previously mentioned. Namely those assumptions are that the material used is isotropic, homogeneous, and linear elastic. With the material being isotropic, layer orientation has no affect on the performance as shown in Table 8.1. As this is the benchmark design, all other sub-studies seek improved performance over the benchmark.

Sub-study II, Single Anisotropic Layer L-Beam

Often, significant performance improvements can be achieved solely by capitalizing on the material anisotropy. We demonstrate this by showing performance increases that can be achieved in the same L-beam when created with a single anisotropic layer. This approach is beneficial as it only requires the material to be strategically oriented during the manufacturing process and does not require additional equipment such as an ultrasonic consolidation welder. By single layer orientation alone, as shown in Table 8.1, the performance increases are notable.

Sub-study III, Multi-Layer Anisotropic L-Beam

By implementing ultrasonic consolidation (Section 8.38.3.1), the L-beam may be created with multiple thin layers, each independently oriented, to achieve a desired performance. While the multilayered material strategy may be more expensive to manufacture, it has a distinct advantage in that the design space significantly expands upon using a layered material approach. However, as shown in Table 8.1, the multilayered case can not out perform the single layered case. Sub-studies V and VI explore this in further detail and illustrate that under different design objectives the multilayered case will out perform the single layer case.

Table 8.1: Optimization results for the four material strategies presented in the L-beam case study. Angles are expressed in degrees.

Case	Q (N)	P	$\phi_{1,1}$	$\phi_{1,2}$	$\phi_{1,3}$	$\phi_{1,4}$
(I) Benchmark	1.302	0.227	Isotropic	–	–	–
(II) Single Layer	0.846	0.087	70	–	–	–
(III) 4 Layers	0.846	0.087	70	70	70	70
(IV) Heterogeneous	0.744	0.056	60	15	–	–

Sub-study IV, Single Layer Heterogeneously Anisotropic L-Beam

We now consider a single layer case where the anisotropy throughout that layer is heterogeneous. For this example, $i = 1$ represents the segment of the L-beam that is in aligned with the y-axis, and $i = 2$ represents the segment that is aligned with the z-axis as seen in Figure 8.6. Through the exploration afforded by the optimization procedure, these two segments may take on any layer orientation, independent of the other. Using this approach, the improvement over the benchmark design is even more significant as shown in Table 8.1.

In consideration of the manufacturing process that might be used to create such a heterogeneous microstructure, we propose a friction stir welding (FSW) process [180]. While various metal joining process could be used to join the separate materials, FSW is desirable because it is a low temperature metal joining process. Since the material microstructure is designed to enable a specific performance, it is important that manufacturing processes does not significantly modify the material microstructure. The high temperature of traditional welding significantly changes the material microstructure at the weld site.

Results and Comparison for Sub-studies I Through IV

Now we compare the numerical results of the four sub-studies presented in this case study, which are summarized in Table 8.1. Notice the values of the benchmark design with the isotropic material. Recalling that the maximum allowable force for this L-beam is 1.2 N, the benchmark design fails by exceeding the maximum allowable force and also by plastically deforming since P is greater than the allowable 0.15 or 15%. Simply by using a single anisotropic layer strategically oriented, we are able to meet the design objectives. Notice that the single layer and multilayered

anisotropic material provide identical solutions. The reason for this is that the design objective seeks an extreme solution (i.e., minimize reaction force). Because it is an extreme solution, and not one in the center of the design space – which is the space that can be obtained by a multilayered laminate – the single layer laminate can provide an optimal solution. A more in-depth discussion of this is provided in the next section. As a final note, we can see that further improvement on the design can be achieved when a heterogeneous material strategy is taken.

8.5.2 Sub-studies V and VI

Having observed in the previous section that the multilayered anisotropic approach did not out perform the single layer anisotropic approach, we now consider the conditions under which it would. Before describing the new conditions, it is important to note that aside from the new optimization problem statement described below, all other conditions are identical to those of sub-studies I through IV. This includes all genetic algorithm parameters and finite element parameters and meshes.

Sub-study V, Multi-Layer L-Beam with Target Q and Target P

Recall the discussion on the range of material properties that can be achieved by rotation and lamination and Figure 8.4 in Section 8.38.3.5. It is difficult, if not impossible, to obtain even a few of the material properties enclosed by the property closure without utilizing a multilayered material approach. Sub-study V illustrates this point. The following optimization problem statement searches for a design that provides a specific reaction force, Q_t, and a specific fraction of yielding, P_t, by orienting four layers:

$$\min_{\phi_1} J = (Q - Q_t)^2 + (P - P_t)^2 \tag{8.11}$$

subject to

$$P < 0.15 \tag{8.12}$$

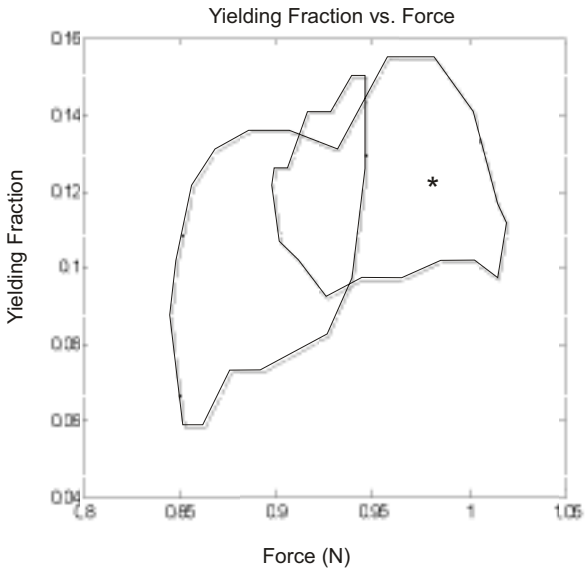

Figure 8.8: Graphical representation of the feasible design space obtainable with rotations and laminations of the copper material used for sub-study V and VI.

$$0 < Q \leq 1.2 \quad \text{N} \tag{8.13}$$

and

$$0 \leq \phi_1 \leq 90^o \tag{8.14}$$

As a reference, $i = 1$ represents the top layer of the L-beam and $i = 4$ represents the bottom layer. The target force and node yielding fraction are 0.98 N and 0.12, respectively. As shown in Table 8.2, the multilayered case is capable of reaching the target performance. This is in contrast to the single layer case which is described now.

Sub-study VI, Single Layer L-Beam with Target Q and Target P

Here we revisit sub-study V, with the modification that only one layer is possible – in contrast to the four layers considered in sub-study V. It is interesting to note that by using a single layer, only a force of 0.99 N can be achieved with a plastic yielding fraction of 0.101. Figure 8.8 provides a graphical look at the nature of sub-studies V and VI. The horizontal axes represents the

Table 8.2: Optimization results for the single and four layer L-beams with a target force and percent failure. Angles are expressed in degrees.

Case	Q (N)	P	$Q_t(N)$	P_t	$\phi_{1,1}$	$\phi_{1,2}$	$\phi_{1,3}$	$\phi_{1,4}$
(V) Single Layer	0.99	0.101	0.98	0.12	0	–	–	–
(VI) 4 Layers	0.98	0.121	0.98	0.12	10	0	5	15

reaction force, Q, and the vertical axes represents the yielding fraction, P, of the part. The solid path represents the performance combinations that are possible using only a single layer. The path and the *area enclosed by the path* can be achieved by the multilayered lamination. To illustrate more fully, we choose a point within the path and set the corresponding values of Q and P to Q_t and P_t. This point is represented by the star in Figure 8.8. The best values that can be afforded by the single layer approach is shown in Table 8.2.

We now return to the notion of making the hardware more difficult to reverse engineer. Consider for a moment using this L-beam as a mechanical fuse. One that explicitly requires a plastic yielding fraction of 0.12 at a reaction force of 0.98 N. Because this design point is *within* the area created by the solid lines in Figure 8.8, a competitor can only find this design through a multilayered approach. Any design found by a single layer would be limited to the solid path in Figure 8.8. While the single layer may be easier to manufacture, it comes at the expense of achieving the desired force and percent failure values.

Using the developments presented in Harston and Mattson, [14] it can be shown that the barrier to reverse engineering for all the sub-studies is significantly larger than the barrier to reverse engineer the benchmark design. This can be explained by the additional exploration required to determine the layer orientation, or heterogeneity associated with the non-benchmark designs.

In summary, we note that the following barriers exist for a competitor reverse engineering the hardware. (i) Discovering that a layering approach was used would be difficult and would require sophisticated microscopy. (ii) Deciphering the microstructure created by the layering approach would be difficult even for those experienced with microstructure analysis, and (iii) determining the methodology to manufacture the microstructure, if it was deciphered, would be yet another challenge – perhaps one that is prohibitive.

8.6 Chapter Summary

We have presented an approach that uses material microstructure information, numerical optimization, and state-of-the-art manufacturing techniques to create designs with a customized mechanical performance that is difficult to reverse engineer – a powerful combination for companies who wish to make innovative products and devices available to the masses without disclosing the phenomena that gives the device its customized performance. The root of the method is in manipulating the material microstructure numerically, while constrained to existing manufacturing methods (rolling, UC, and FSW). The consideration of these manufacturing approaches is embodied in the rotation/lamination theory and in the minimal negative affect that these joining processes have on the microstructures of interest. A simple study of an L-beam was presented to illustrate the basic benefits that come from the presented design and optimization approach. The case study considered one layer isotropic lamina, one layer anisotropic lamina, multilayered anisotropic laminae, heterogeneously distributed microstructures in single layer lamina, and a special exploration in to when multilayered laminae out perform single layer lamina and vice-versa. Through this case study we see that by using a microstructure sensitive design approach, coupled with numerical optimization, product performance can be customized, *and* can be made manufacturable and difficult to reverse engineer. Difficult to reverse engineer because each scenario in the case study has identical geometry and material alloy, yet notably different performance which can only be traced to difficult-to-discern microstructures.

CHAPTER 9. CONCLUDING REMARKS AND FUTURE WORK

9.1 Concluding Remarks

Reverse engineering is a common design strategy in industry. It is a term that has come to encompass a large array of engineering and design activities in both the literature and in practice. However, in its basic form, reverse engineering is simply the process of extracting information about a product from the product itself. As presented in this dissertation, it may or may not be advantageous to utilize a reverse engineering strategy. Reverse engineering, similar to any rational decision, is only favorable when the benefits from its use outweigh the investment.

This dissertation has presented numerous examples where innovative products have been reverse engineered and imitated at the expense of the original designer. Consequently, various researchers have expressed the need for general metrics, parameters, definitions, and methodologies that quantify the time and barrier to reverse engineer a product; however, none of them provide it. Specifically, the literature states the need for (i) comparative metrics for the barrier and time to reverse engineer a product or system, and (ii) a design strategy that effectively seeks to maximize barriers to reverse engineering. In this dissertation, we addressed these unmet needs by achieving the dissertation objective:

Dissertation Objective Develop an effective design framework that results in products that can be handled, used, dissected, or similarly analyzed by a competitor without disclosing the phenomena by which the product functions.

The dissertation objective was partially achieved by first gaining an understanding of the nature of barriers to reverse engineering. We demonstrated that reverse engineering barriers are affected by (i) the complexity of a product, (ii) the resources available, and (iii) the skill of the reverse engineering team. As designers can directly control the complexity of a product, they can also indirectly affect the resources available, and the skills required for successful reverse

engineering. Designing products with built-in barriers to reverse engineering impedes competitors from gaining valuable insight – such as proprietary information or trade secrets – from the product itself. This also impedes competitors from quickly imitating the product to enter the market by capitalizing on the research and development costs of the innovative company.

The anecdotal understanding of what affects barriers to reverse engineering facilitates understanding of the metrics that characterize the time and barrier to reverse engineer a product. The metrics developed in this dissertation are numerical in nature and are based on Ohm's law which is used to analyze electrical circuits. To the original designer, these numerical representations of the barrier and time can be used to strategically identify and improve product characteristics so as to increase the difficulty and time to reverse engineer them. As the metrics and parameters developed are quantitative in nature, and have been presented generically to be applied to any situation, they can be used in conjunction with numerical optimization techniques. Using optimization, we demonstrated how products can be designed with a large reverse engineering barrier and time while maximizing return on investment. This has been demonstrated with the KitchenAid stand mixer, electrical connectors used in cell phones, and a solar-powered unmanned aerial vehicle. On the other hand, these quantitative measures enable competitors who reverse engineer original designs to focus their efforts on products that will result in the greatest return on investment. The results documented herein – and demonstrated on products with various levels of complexity – indicate that the developed reverse engineering metrics are appropriate for nearly all products and are accurate to the degree of an average error of 12.2% for products that are sufficiently complex.

In some situations, it may be desirable to reverse engineer a product multiple times (i.e, increase accuracy, extract tolerances, gather additional information). If multiple samples of the same product are reverse engineered, then learning will take place – knowledge about the product's form, composition, and function will be retained from previous iterations of the process. Thus, needed additional metrics are developed and presented to characterize the time and barrier to reverse engineer multiple samples of the same product. As presented, these metrics (i) characterize learning in the reverse engineering process as additional product samples are evaluated, and (ii) estimate the total time to reverse engineer multiple samples of the same product. Use of the metrics is exemplified by the industry example of the block and spool that was repetitively reverse engineered to extract tolerance information.

An understanding of the reverse engineering time and barrier alone is not adequate for designing barriers to reverse engineering. This is principally due to the fact that barriers are costly to implement. Therefore, it is critical to have an understanding of the cost tradeoffs associated with barrier implementation. Specifically, a method is presented that enables designers to (i) estimate the return on investment for products *without* reverse engineering barriers, (ii) estimate the return on investment for products *with* reverse engineering barriers, and (iii) estimate the market captured and return on investment by product imitations as a function of the barrier incorporated into a product (or lack thereof). This is a key step, as not all products benefit from barriers to reverse engineering. In some cases, the largest return on investment may result from not incorporating any barriers at all. Importantly, a methodology is presented that enables an individual to determine the return on investment of any product as a function of the reverse engineering barrier.

While barriers to reverse engineering may be costly to implement, entire products can be made difficult to reverse engineer by strategically selecting and designing barriers to reverse engineering into one, or a few, critical components. As such, a methodology was developed to assist designers in planning for, selecting, designing, and implementing barriers to reverse engineering. This methodology systematically determines which components most benefit from reverse engineering barriers while considering (i) the difficulty of modifying components, (ii) the sensitivity of the system to the various components, (iii) the effect of barrier concepts on overall product performance, and (iv) the calculated return on investment. An overarching methodology is an essential part of this doctoral work. As such, the effectiveness of this methodology is demonstrated by making a solar-powered unmanned aerial vehicle more difficult to reverse engineer. In the example, the propeller was selected to be the critical component where a series of voids were introduced to decrease the propeller weight and increase the flutter speed (a desirable attribute in propellers).

Additionally, we have treated material microstructures (crystallographic grain size, orientation, and distribution) as design variables that can be manipulated – for common or exotic materials – to identify unusual material properties and to create effective barriers to reverse engineering. A practical approach, carefully tied to proven manufacturing strategies, was used to tailor material microstructures by strategically orienting and laminating thin anisotropic metallic sheets. The approach, coupled with numerical optimization, manipulates material microstructures to obtain desired material properties at designer-specified locations (heterogeneously) or across the entire

part (homogeneously). A comparative study was provided that examines various microstructures for a simple fixed geometry. These cases show how the proposed approach can provide hardware with enhanced mechanical performance in a way that is disguised within the microscopic features of the material microstructure.

To be clear, we now review the six sub-objectives as presented in Chapter 1 and briefly mention how each sub-objective was accomplished.

Sub-Objective 1 *Develop metrics that quantitatively approximate (i) the time to reverse engineer any product, and (ii) the barrier to reverse engineering that must be overcome to successfully reverse engineer any product.* This is accomplished with the development and validation of the reverse engineering metrics as presented in Chapter 4 and Chapter 5.

Sub-Objective 2 *Quantify the error of the reverse engineering metrics and what it means to the designer.* In addition to the presentation of the reverse engineering metrics, Chapter 4 also quantifies and discusses the error associated with the reverse engineering metrics. Specifically, the average error has been found to be 12.2%.

Sub-Objective 3 *Explore how microstructure sensitive design results in effective and efficient barriers to reverse engineering.* The entirety of Chapter 8 is focused on analyzing and understanding the effects of microstructure sensitive design on reverse engineering barriers – which have been found to be a very effective reverse engineering barrier when properly designed. In addition, the KitchenAid mixer presented in Chapter 6 uses a microstructure barrier to increase the reverse engineering barrier and return on investment.

Sub-Objective 4 *Explore the tradeoffs between reverse engineering barriers, cost, and return on investment.* Enabling the exploration of tradeoffs, a return-on-investment model is developed in Chapter 6. Furthermore, the methodology presented in Chapter 7 considers (i) the difficulty of modifying components, (ii) the sensitivity of the system to the various components, (iii) the effect of barrier concepts on overall product performance, and (iv) the calculated return on investment. This includes a discussion and presentation of techniques for exploring the associated tradeoffs.

Sub-Objective 5 *Determine what products – or product components within a system – most benefit from implementing barriers to reverse engineering.* A fundamental element of the methodology, presented in Chapter 7, is the selection of the components that most benefit from barriers to reverse engineering. The effectiveness of the component selection process is made evident in the solar-powered UAV example where the propeller was selected to be the critical component and received the barrier to reverse engineering.

Sub-Objective 6 *Use numerical optimization to search for designs that (i) meet or exceed performance requirements, (ii) maximize return on investment, and (iii) are difficult to reverse engineer.* Chapter 7 presents a multi-objective numerical optimization strategy that simultaneously considers performance requirements, return on investment, and barriers to reverse engineering. This is again demonstrated with the solar-powered UAV example. Furthermore, additional examples of using numerical optimization to simultaneously maximize product performance and barriers to reverse engineering are presented in Chapter 8.

In summary, the tools and methodologies presented herein enable designers to systematically design products that can be handled, used, dissected, or similarly analyzed by a competitor without disclosing the phenomena by which the product functions.

9.2 Future Work

While the desired goals of the dissertation have been met, a number of new areas have been identified as candidates for future research. These areas are briefly discussed below.

9.2.1 Reverse Engineering Power

In the development of the reverse engineering metrics (refer to Chapter 4), the power, P, is defined as the work per time to extract information. While P is constrained to

$$0 < P \leq 1 \tag{9.1}$$

the assumption is made that $P = 1$. This is the most conservative approach for those estimating how long it will take competitors to reverse engineer their product as $P = 1$ implies that the individual

is putting forth their best effort to reverse engineer the product. However, the reverse engineering metrics may be improved by developing a systematic approach to determine the actual value of P. This is a difficult task as it is likely that P is not only a function of the individual, but also varies as a function of the individual's perception of the accuracy required and their desire to reverse engineer the product. One possible solution may be to use an approach similar to the one developed for characterizing a person's initial flow rate, F_0 as presented in Chapter 4.

9.2.2 Exploration of Additional Information Types

The emphasis of this doctoral work focused on two information types – macroscopic geometry and material microstructures. While the reverse engineering metrics and the methodologies presented herein have been developed in a general nature, it would be beneficial to further validate the application of the metrics on additional information types. Additional information types may include: electrical conductivity, surface finish, aesthetics, color, heat transfer characteristics, thermal expansion, fatigue, stress concentrations, assembly information, etc. and the coupling of such information.

9.2.3 Topology Optimization with Anisotropic Materials

In exploring the strategic, simultaneous design of both material microstructures and macroscopic geometry, we briefly pursued the coupling of topology optimization with directionally dependent material properties. Specifically, we coupled topology optimization with finite element analysis. This combination, along with proven manufacturing techniques, enables the design and optimization of manufacturable topologies with anisotropic and heterogeneous material properties. An optimization algorithm was developed and presented in a conference paper [182] that simultaneously optimizes the topology on the macro scale and the material properties of each element at the microstructure level by selecting and strategically orienting anisotropic materials. The anisotropic materials are selected from a materials database that was created by physically testing and measuring various material microstructures. Three examples illustrated the capabilities of the algorithm to simultaneously optimize topologies and material properties.

Using this research as a foundation, advanced materials/geometry optimizations may be developed, resulting in performance improvements that cannot be achieved without consideration to both. However, there exist a number of issues that need to be addressed in this area of research. These issues include (i) computational cost, (ii) convergence criteria, and (iii) developing additive topology optimization algorithms – typical topology optimization algorithms are subtractive in nature. While this exploratory study identified fertile areas for future work, we did not pursue this topic in an effort to maintain focus on the principle objective and sub-objectives of the dissertation.

9.2.4 Methods to Automatically Determine Information Quantity

The reverse engineering metrics have been developed in a way that easily lends to numerical optimization. However, one of the limitations of using the metrics in numerical optimizations is estimating the quantity of information contained within a product, K, due to the fact that this estimation currently requires the analysis and input of a human. This is particularly problematic when the optimization is allowed to change the geometry of the product during each optimization iteration (e.g., topology optimization). Therefore, techniques for automating the quantification of K can enable numerical optimizations to continuously run without human input.

There are numerous papers from the literature that discuss how to reverse engineer geometric features utilizing CAD systems [183–185]. As such, it may be possible to extend existing techniques to the context of automatically calculating K. Toledo et al. [186] present an efficient method by which geometric information may be determined, even from complicated systems, in an effort to determine original geometric data. Vrady et al. [187] present an automated approach to create CAD representations of structures that are accurate, capture design intent, and require little or no user assistance. While additional research is needed in this area, it is possible that some of these methods may be used directly to estimate the quantity of information contained by a product.

REFERENCES

[1] Weingart, S. H., White, S. R., Arnold, W. C., and Double, G. P., 1990. "An evaluation system for the physical security of computing systems." In *The Sixth Annual Computer Security Applications Conference*, pp. 232–243.

[2] FLOWSERVE CORPORATION, 2006. *3400IQ Digital Positioner FCD LGENIM3401-00 – 06/06 User Instructions*.

[3] *KitchenAid KSM150PSER Use and Care Manual*.

[4] Harston, S. P., and Mattson, C. A., 2010. "Capitalizing on heterogeneity and anisotropy to design desirable hardware that is difficult to reverse engineer." *Journal of Mechanical Design,* **132**, p. 081001 (11 pages).

[5] Ingle, K. A., 1994. *Reverse Engineering*. McGraw-Hill, New York, NY.

[6] Otto, K., and Wood, K., 2001. *Product Design*. Prentice Hall, Upper Saddle River, NJ.

[7] Schnaars, S. P., 1994. *Managing Imitation Strategies: How Later Entrants Seize Markets From Pioneers*. The Free Press.

[8] Zhou, K. Z., 2006. "Innovation, imitation, and new product performance: The case of china." *Industrial Marketing Management,* **35**, pp. 394–402.

[9] Urban, G. L., Carter, T., Gaskin, S., and Mucha, Z., 1986. "Market share rewards to pioneering brands: An emperical analysis and strategic implications." *Management Science,* **32**, p. 6.

[10] Greenstein, S., 2004. Imitation happens Tech. rep., IEEE Computer Society.

[11] Kim, L., 1997. *Imitation to Innovation: the dynamics of Korea's technological learning*. Harvard Business School Press.

[12] Macmillan, I., McCaffery, M. L., and van Wijk, G., 1985. "Competitors' responses to easily imitated new products-exploring commercial banking product introductions." *Strategic Management Journal,* **Vol. 6, No. 1**, pp. 75–86

[13] Mansfield, E., Schwartz, M., and Wagner, S., 1981. "Imitation costs and patents: An empirical study." *The Economic Journal,* **Vol. 91, No. 364**, pp. 907–918.

[14] Harston, S. P., and Mattson, C. A., 2010. "Metrics for evaluating the barrier and time to reverse engineer a product." *Journal of Mechanical Design,* **132**, p. 041009 (9 pages).

[15] Roberts, D., 2005. "Did spark spark a copycat." *BusinessWeek,* **3919**, http://www.businessweek.com/magazine/content/05_06/b3919010_mz001.htm

[16] CNN, 2001. How soviets copied america's best bomber during wwii Tech. rep., CNN, January

[17] Branscomb, L. M., and Auerswald, P. E., 2001. *Taking Technical Risks*. MIT Press.

[18] Dam, K. W., and Lin, H. S., 1996. *Cryptography's Role in Securing the Information Society*. National Acadamy Press.

[19] Grand, J., 2004. "Practical secure hardware design for embedded systems." In *Proceedings of the 2004 Embedded Systems Conference*.

[20] Crockford, C., 1980. *An Introduction to Risk Management*. Woodhead-Faulkner.

[21] Reed, R., and DeFillippi, R. J., 1990. "Casual ambiguity, barriers to imitation, and sustainable competitive advantage." *The Academy of Management Review,* **15**, p. 88.

[22] Hill, C. W. L., 1992. "Strategies for exploring technological innovations: When and when not to license." *Organization Science,* **3**, pp. 428–441.

[23] McEvily, S. K., and Chakaravarthy, B., 2002. "The persistance of knowledge-based advantage: An emperical test for product performance and technological knowledge." *Strategic Management Journal,* **23**, pp. 285–305.

[24] Challoner, J., 2009. *1001 Inventions that Changed the World*. Quintessence.

[25] Dyson, J., 2001. *History of Great Inventions*. Constable & Robinson.

[26] de Gonzlez, A. B., Mahesh, M., Kim, K.-P., Bhargavan, M., Lewis, R., Mettler, F., and Land, C., 2009. "Projected cancer risks from computed tomographic scans performed in the united states in 2007." *Archives of Internal Medicine,* **169(22)**, pp. 2071–2077.

[27] Shenkar, O., 2010. *Copycats: Combining Imitation and Innovation to Outsmart Your Competitors*. Harvard Business Press.

[28] Gallini, N. T., 1992. "Patent policy and costly imitation." *RAND Journal of Economics,* **23**, pp. 52–63.

[29] Koeppel, D., 2007. "Clone home." *Popular Science,* **271**, http://www.popsci.com/iclone.

[30] Boyne, W. J., 2009. "Carbon copy bomber." *Air Force Magazine,* **92**(6), June, pp. 52–56.

[31] Suvorov, V., 1981. *The Liberators: Inside the Soviet Army*. New English Library.

[32] McEvily, A. J., 2005. "Reverse engineering gone wrong: A case study." *Engineering Failure Analysis,* **12**, pp. 834–838.

[33] Chikofsky, E. J., and Cross, J. H., 1990. "Reverse engineering and design recovery: a taxonomy." *Software, IEEE,* **7**, pp. 13–17.

[34] Waters, R., and Chikofsky, E., 1994. "Reverse engineering: progress along many dimensions." *Communications of the ACM,* **37**, pp. 22–25.

[35] Buss, E., De, R., Gentleman, M. M., Henshaw, J., Johnson, H., Kontogiannis, K., Merlo, E., Muller, H., Mylopoulos, J., Paul, S., Prakash, A., Stanley, M., Tilley, S., Troster, J., and Wong, K., 1994. "Investigating reverse engineering technologies for the CAS program understanding project." *IBM Systems Journal,* **33**, pp. 477–500.

[36] Nelson, M. L., 1996. "A survey of reverse engineering and program comprehension." In *In ODU CS 551 Software Engineering Survey*

[37] Muller, H. A., Jahnke, J. H., Smith, D. B., Storey, M.-A. D., Tilley, S. R., and Wong, K., 2000. "Reverse engineering: A roadmap." In *Proceedings of the International Conference on Software Engineering (ICSE).*

[38] Pahl, G., Beitz, W., Feldhusen, J., and Grote, K.-H., 2007. *Engineering Design: A Systematic Approach*. Springer, Verlag, London.

[39] Csete, M., and Doyle, J., 2002. "Reverse engineering of biological complexity." *Science,* **295**, pp. 1664–1669.

[40] Moles, C., Mendes, P., and Banga, J., 2003. "Parameter estimation in biochemical pathways: a comparison of global optimization methods." *Genome Research,* **13**, pp. 2467–2474.

[41] Kremling, A., Fischer, S., Gadkar, K., Doyle, F. J., Sauter, T., Bullinger, E., Allgwer, F., and Gilles, E. D., 2004. "A benchmark for methods in reverse engineering and model discrimination: Problem formulation and solutions." *Genome Research,* **14**, pp. 1773–1785.

[42] Benyus, J. M., 2002. *Biomimicry: Innovation Inspired by Nature*. HarperCollins Publishers Inc., New York, NY.

[43] Naumovich, G., and Memon, N., 2003. "Preventing piracy, reverse engineering, and tampering." *IEEE Computers Society,* **36**, pp. 64–71

[44] Besl, P. J., and Mckay, N. D., 1992. "A method for registration of 3-d shapes." *IEEE Transactions on Pattern Analysis and Machine Intelligence,* **14**(2), February, pp. 239–256.

[45] Vrady, T., Martin, R. R., and Cox, J., 1997. "Reverse engineering of geometric models: An introduction." *ComputerAided Design,* **29**, pp. 255–268.

[46] Myers, R. H., Montgomery, D. C., and Anderson-Cook, C. M., 2009. *Response Surface Methodology: Process and Product Optimization Using Designed Experiments (Wiley Series in Probability and Statistics)*., 3 ed. Wiley, New York, NY, January.

[47] Simpson, T., Poplinski, J., Koch, P., and Allen, J., 2001. "Metamodels for computer-based engineering design: Survey and recommendations." *Engineering with Computers,* **17**, pp. 129–150.

[48] Scherer, F. M., 1967. "Research and development resource allocation under rivalry." *Quarterly Journal of Economics,* **81**, pp. 359–94.

[49] Mansfield, E., Rapoport, J., Romeo, A., Villani, E., Wagner, S., and Husic, F., 1977. *The Production and Application of New Industrial Technology*. W. W. Norton.

[50] Christiansen, B. D., 2006. "Active FPGA security through decoy circuits." Master's thesis, Air Force Institute of Technology.

[51] Abraham, D. G., Dolan, G. M., Double, G. P., and Stevens, J. V., 1991. "Transaction security system." *IBM Systems Journal,* **30**(2), pp. 206–229.

[52] Shapiro, C., 1985. "Patent licensing and r & d rivalry." *American Economic Review,* **75**, pp. 25–30.

[53] Nelson, R., and Winter, S., 1982. *An evolutionary theory of economic change*. Belknap Press, Cambridge, Massachusetts.

[54] Glazer, A., 1985. "The advantages of being first." *The American Economic Review,* **75**, pp. 473–480.

[55] Samuelson, P., and Scotchmer, S., 2002. "The law and economics of reverse engineering." *The Yale Law Journal,* **111**(7), pp. 1575–1663.

[56] Gruca, T. S., and Sudharshan, D., 1995. "A framework for entry deterrence strategy: The competitive environment, choices, and consequences." *Journal of Marketing,* **59**, pp. 44–55.

[57] Porter, M. E., 1985. *Competitive Advantage: Creating And Sustaining Superior Performance*. New York: Free Press.

[58] Wilson, R., and Crouch, E. A. C., 2001. *Risk-Benefit Anslysis*. Harvard University Press.

[59] Salter, C., Saydjari, O. S., Schneier, B., and Wallner, J., 1998. "Toward a secure system engineering methodology." In *Proceedings of the 1998 Workshop on New Security Paradigms*.

[60] Luallen, M., and Hamburg, S., 2009. "Applying security defense-in-depth." *Control Engineering,* **56**(12), December, pp. 49–51.

[61] Bass, T., and Robichaux, R., 2001. "Defense-in-depth revisited: Qualitative risk analysis methodology for complex network-centric operations." In *IEEE MILCOM*.

[62] Han, S. H., Kim, K. J., Yun, M. H., Hong, S. W., and Kim, J., 2004. "Identifying mobile phone design features critical to user satisfaction." *Human Factors and Ergonomics in Manufacturing,* **14(1)**, pp. 15–29.

[63] Edwards, K. L., 2004. "Systematic retrofit design for manufacture - critical component substitution in machine design." *Journal of Engineering Manufacture,* **218**, pp. 129–133.

[64] Pooley, J., and Graves, C. T., 2008. *Trade Secrets*. Law Journal Press.

[65] Rae, A., and Fidge, C., 2005. "Identifying critical components during information security evaluations." *Journal of Research and Practice in Information Technology,* **37-4**, pp. 311–322.

[66] Ebert, C., 2001. "Metrics for identifying critical components in software projects." In *Handbook of Software Engineering and Knowledge Engineering*.

[67] Afshar, M. H., 2008. "Layout and size optimization of tree-like pipe networks by incremental solution building ants." *Canadian Journal of Civil Engineering,* **35**, pp. 129–139.

[68] Lassila, T., 2009. "Optimal damping of a membrane and topological shape optimization." *Structural and multidisciplinary optimization,* **38**, pp. 43–52.

[69] Kumar, A. V., and Gossard, D. C., 1996. "Synthesis of optimal shape and topology of structures." *Journal of Mechanical Design,* **118**, p. 68 (7 pages).

[70] Tavakoli, R., and Davami, P., 2009. "Optimal riser design in sand casting process with evolutionary topology optimization." *Structural and multidisciplinary optimization,* **38**, pp. 205–214.

[71] Nelson, S. A., Parkinson, M. B., and Papalambros, P. Y., 2001. "Multicriteria optimization in product platform design." *Journal of mechanical design,* **123**, pp. 199–204.

[72] Hariharan, K., and Balaji, C., 2009. "Material optimization: A case study using sheet metal-forming analysis." *Journal of Materials Processing Technology,* **209 Issue 1**, pp. 324–331.

[73] Adams, B. L., Kalidindi, S. R., and Fullwood, D. T., 2005. *Microstructure Sensitive Design for Performance Optimization*. BYU Academic Publishing, Provo, UT.

[74] Adams, B. L., Nylander, C., Aydelotte, B., Ahmadi, S., Landon, C., Stucker, B. E., and Janaki-Ram, G. D., 2008. "Accessing the elastic-plastic properties closure by rotation and lamination." *Acta materialia,* **56**, pp. 128 –139.

[75] Hyer, M. W., 1998. *Stress Analysis of Fiber-Reinforced Composite Materials*. McGraw-Hill, New York, NY.

[76] Mejia-Rodriguez, G., Renaud, J. E., and Tomar, V., 2008. "A variable fidelity model management framework for designing multiphase materials." *Journal of Mechanical Design,* **130**, p. 091702 (13 pages).

[77] Kolpakov, A. G., and Kolpakova, I. G., 1995. "Desgin of laminated composites possessing specified homogenized characteristics." *Computers and Structures,* **57**, pp. 599–604.

[78] McMahon, M. T., Watson, L. T., Soremekun, G. A., Gtirdal, Z., and Haftka, R. T., 1998. "A fortran 90 genetic algorithm module for composite laminate structure design." *Engineering with Computers,* **14**, pp. 260–273.

[79] Sinke, J., 2006. "Development of fibre metal laminates: concurrent multi-scale modeling and testing." *J Mater Sci,* **41**, pp. 6777–6788.

[80] McDowell, D. L., 2000. "Modeling and experiments in plasticity." *International Journal of Solids and Structures,* **37**, pp. 293–309.

[81] McDowell, D. L., 2001. "Materials design: a useful research focus for inelastic behavior of structural metals." *Theoretical and Applied Fracture Mechanics,* **37**, pp. 245–259.

[82] McDowell, D. L., Choi, H.-J., Panchal, J., Austin, R., Allen, J., and Mistree, F., 2007. "Plasticity-related microstructure-property relations for materials design." *Key Engineering Materials,* **340-341**, pp. 21–30.

[83] Olson, G. B., 1997. "Computational design of hierarchically structured materials." *Science,* **277**, pp. 1237–1242.

[84] Kuehmann, C. J., and Olson, G. B., 2009. "Computational materials design and engineering." *Materials Science and Technology,* **25**, pp. 472–478.

[85] Grimm, T., 2004. Reverse engineering is criminal Tech. rep., Time Compression Technologies, November/December.

[86] Ulrich, K. T., and Eppinger, S. D., 2004. *Product Design and Development*., third ed. McGraw-Hill/Irwin.

[87] McLoughlin, I., 2008. "Secure embedded systems: the threat of reverse engineering." In *ICPADS '08: Proceedings of the 2008 14th IEEE International Conference on Parallel and Distributed Systems*, IEEE Computer Society, pp. 729–736.

[88] Knight, D. C., Mattson, C. A., and Adams, B. L., 2009. "Maximizing return on investment by constructing optimal barriers against competitors' market entry." In *50th AIAA/ASME/ASCE/AHS/ASC Structures, Structural Dynamics, and Materials Conference, Palm Springs, California, AIAA 2009-2224*.

[89] Harrington, H. J., 1991. *Business process improvement: the breakthrough strategy for total quality, productivity, and competitiveness*. McGraw-Hill Professional.

[90] Raja, V., 2008. *Reverse Engineering: An Industrial Perspective*. Springer London, ch. 1, pp. 1–9.

[91] Musker, D. C., 1998. "Reverse engineering." In *Protecting and exploiting intellectual property in electronics, IBC Conferences, 10 June 1998*

[92] Pal, D. K., Ravi, B., Bhargava, L. S., and Chandrasekhar, U., 2006. "Computer-aided reverse engineering for replacement parts: A case study." *Defense Science Journal,* **56**(2), pp. 225–238.

[93] Creehan, K. D., and Bidanda, B., 2006. *Rapid Prototyping: Theory and Practice*. Springer US, ch. Reverse Engineering: A Review & Evaluation of Non-Contact Based Systems, pp. 87–106.

[94] Urbanic, R. J., and ElMaraghy, W. H., 2009. "Using a modified failure modes and effects analysis within the structured design recovery framework." *Journal of Mechanical Design,* **131**, p. 111005 (13 pages).

[95] Thompson, W. B., Owen, J. C., de St. Germain, H. J., Stark, S. R., and Henderson, T. C., 1999. "Feature-based reverse engineering of mechanical parts." *IEEE Transactions on Robotics and Automation,* **15**(1), February, pp. 57–66.

[96] Hsiao, S.-W., and Chuang, J.-C., 2003. "A reverse engineering based approach for product form design." *Design Studies,* **24**(2), March, p. 155171.

[97] Ohly, A., 2009. *Patents and Technological Progress in a Globalized Worlda*., 6 ed. Springer-Verlag, ch. Reverse Engineering: Unfair Competition or Catalyst for Innovation?, pp. 535–552.

[98] Mowery, K. A., Blanchard, D. E., Smith, S., and Betts, T. A., 2004. "Investigation of imposter perfumes using GC-MS." *Journal of Chemical Education,* **81**, pp. 87–89.

[99] Vrady, T., 2001. "Reverse engineering shapes." *ERCIM News,* **44**, January, pp. 19–20.

[100] Sarkar, B., and Menq, C. H., 1991. "Smooth-surface approximation and reverse engineering." *Computer-Aided Design,* **23**(9), pp. 623–628.

[101] Summers, J. D., and Shah, J. J., 2010. "Mechanical engineering design complexity metrics: size, coupling, and solvability." *Journal of Mechanical Design,* **132**, p. 021004 (11 pages).

[102] Maskus, K. E., Dougherty, S. M., and Mertha, A., 1998. "Intellectual property rights and economic development in china." In *Conference on Intellectual Property Rights and Economic Development*.

[103] von Hippel, E., 1998. "Economics of product development by users: The impact of "sticky" local information." *Management Science,* **44**, pp. 629–644.

[104] Campbell, R. J., and Flynn, P. J., 2001. "A survey of free-form object representation and recognition techniques." *Computer Vision and Image Understanding,* **81**, pp. 166–210.

[105] Soo, S. M. K., Yuen, E. M. W., and Yu, K. M., 2005. "Reverse engineering of a bamboo-net handicraft." In *IEEE Ninth International Conference on Computer Aided Design and Computer Graphics*.

[106] James, D., 2006. Reverse engineering delivers product knowledge, aids technology spread Tech. Rep. ED Online ID #11966, Electronic Design, January 19.

[107] Bradley, C., and Currie, B., 2005. "Advances in the field of reverse engineering." *Computer-Aided Design & Applications,* **2**(5), pp. 697–706.

[108] Ali, F., Chowdary, B., and Imbert, C., 2008. "Part design and evaluation through reverse engineering approach." In *The 2008 IAJC-IJME International Conference*.

[109] Grimm, T., 2006. Reverse engineering - 3D scanning selection guide Tech. rep., Time Compression Technologies.

[110] Grimm, T., 2006. A guide to reverse engineering Tech. rep., Time Compression Technologies, March/April.

[111] Mohaghegh, K., Sadeghi, M. H., and Abdullah, A., 2007. "Reverse engineering of turbine blades based on design intent." *International Journal of Advanced Manufacturing Technology,* **32**, pp. 1009–1020.

[112] Barbero, B. R., 2009. "The recovery of design intent in reverse engineering problems." *Computers & Industrial Engineering,* **56(4)**, May, pp. 1265–1275.

[113] USAF, 1944. Boeing b-29, November www.nationalmuseum.af.mil/factsheets/factsheet.asp?id=2527.

[114] Norby, M. O., 1978. *Soviet Aerospace Handbook*. Department of the US Air Force, May.

[115] Danelek, J. A., 2008. *UFOs: The Great Debate*. Llewellyn Publications.

[116] Livingston, H., 2007. "Avoiding counterfeit electronic components." *IEEE transactions on components and packaging technologies,* **30**, pp. 187 – 189.

[117] Dube, T. E., Birrer, B. D., Raines, R. A., Baldwin, R. O., Mullins, B. E., Bennington, R. W., and Reuter, C. E., 2008. "Hindering reverse engineering: thinking outside the box." *IEEE Security and Privacy,* **6**, pp. 58–64.

[118] Ohm, G. S., 1827. *Die galvanische Kette, mathematisch bearbeitet*. T. H. Riemann, Berlin, Germany.

[119] Akers, A., 2006. *Hydraulic Power System Analysis*. Taylor & Francis, Boca Raton, FL

[120] Chernov, I. N., Eyink, L., Lebowitz, J. L., and Sinai, Y. G., 1993. "Derivation of ohm's law in a deterministic mechanical model." *Physical review letters,* **70**, pp. 2209–2212

[121] Jiles, D., 2001. *Introduction to the Electronic Properties of Materials*. CRC Press, Boca Raton, FL

[122] Dorf, R. C., 1993. *The Electrical Engineering Handbook*. CRC Press, Boca Raton, FL.

[123] Rizzoni, G., 2004. *Principles and Applications of Electrical Engineering*. McGraw-Hill, New York, NY.

[124] Collado-Ruiz, D., and Capuz-Rizo, S., 2010. "Modularity and ease of disassembly: Study of electrical and electronic equipment." *Journal of Mechanical Design,* **132**(1), p. 014502.

[125] Thevenot, H., and Simpson, T. W., 2009. "A product dissection-based methodology to benchmark product family design alternatives." *Journal of Mechanical Design,* **131**(4), p. 041002.

[126] Montgomery, D. C., Runger, G. C., and Hubele, N. F., 2006. *Engineering Statistics*., third ed. John Wiley & Sons.

[127] Kaisarlis, G. J., Diplaris, S. C., and Sfantsikopoulos, M. M., 2007. "Position tolerancing in reverse engineering: the fixed fastener case." In *Proceedings of the Institution of Mechanical Engineers. Part B. Journal of Engineering Manufacture*, Vol. 221 221, pp. 457–465.

[128] Chase, K. W., and Parkinson, A. R., 1991. "A survey of research in the application of tolerance analysis to the design of mechanical assemblies." *Research in Engineering Design,* **3**, pp. 23–37.

[129] Chase, K. W., 1999. Tolerance allocation methods for designers Tech. rep., ADCATS Report No 996.

[130] Kaisarlis, G. J., Diplaris, S. C., and Sfantsikopoulos, M. M., 2007. "Geometrical position tolerance assignment in reverse engineering." *International Journal of Computer Integrated Manufacturing,* **21**(1), pp. 89–96.

[131] Jamshidi, J., Mileham, A. R., and Owen, G. W., 2006. "Dimensional tolerance approximations for reverse engineering applications." In *Proceedings of the 9th International Design Conference (Design 2006)*, The Design Society, pp. 855–862.

[132] Kaisarlis, G. J., Diplaris, S. C., and Sfantsikopoulos, M. M., 2000. "A knowledge-based system for tolerance allocation in reverse engineering." In *Proceedings of the 33rd International Matador Conference*.

[133] Anonymous, 2006. *US Army Reverse Engineering Handbook (Guidlines and Procedures)*. Department of Defense.

[134] Prerau, M. J., Smith, A. C., Eden, U. T., Kubota, Y., Yanike, M., Suzuki, W., Graybiel, A. M., and Brown, E. N., 2009. "Characterizing learning by simultaneous analysis of continuous and binary measures of performance." *Journal of Neurophysiology,* **102**, November, pp. 3060–3072.

[135] Argote, L., and Epple, D., 1990. "Learning curves in manufacturing." *Science,* **247**, February, pp. 920–924.

[136] Adler, P. S., and Clark, K. B., 1991. "Behind the learning curve: A sketch of the learning process." *Management Science,* **37**(3), March, pp. 267–181.

[137] Argote, L., 1999. *Organizational learning: creating, retaining, and transfering knowledge*. Kluwer Academic, Boston.

[138] Fogiel, M., 2002. *Basic Electricity*. Research and Education Association.

[139] Anderson, N., 2011. "Characterization of the initial flow rate of information during reverse engineering." Master's thesis, Brigham Young University, June.

[140] Asiedu, Y., and Gu, P., 1998. "Product life cycle cost analysis: State of the art review." *International Journal of Production Research,* **36.4**, pp. 883–908.

[141] Ulrich, K. T., and Eppinger, S. D., 2008. *Product Design and Development Fourth Edition*.

[142] Magrab, E. B., 1997. *Integrated Product and Process Design and Development*. CRC Press.

[143] Bass, F. M., 1969. "A new product growth model for consumer durables." *Management Science,* **15**, p. 5.

[144] Vijay Mahajan, Eitan Muller, F. M. B., 1995. "Diffusion of new products: Emperical generalizations and managerial uses." *Marketing Science,* **14**, pp. G79–G88.

[145] Euromonitor, 2011. Online Database, February http://www.portal.euromonitor.com.

[146] Sultan, F., Farley, J. U., and Lehman, D. R., 1990. "A meta-analysis of applications of diffusion models." *Journal of Marketing Research,* **27**, pp. 70–77.

[147] Curtis, S. K., Harston, S. P., and Mattson, C. A., 2011. "The fundamentals of barriers to reverse engineering and their implementation into mechanical components." *Research in Engineering Design,* **22**, pp. 245–261.

[148] Larson, B., and Mattson, C. A., 2010. "Developing system behavioral models by integrating discipline specific models." In *AIAA Structures, Structural Dynamics, and Materials Conference Proceedings*.

[149] Knight, D. C., and Mattson, C. A., 2011. "Return on investment for implementing barriers to reverse engineering." In *ASME IDETC/CIE 2011, Washington, DC, USA, DETC2011-47094*.

[150] Messac, A., Puemi-Sukam, C., and Melachrinoudis, E., 2000. "Aggregate objective functions and pareto frontiers: Required relationships and practical implications." *Optimization and Engineering,* **1**, pp. 171–188

[151] Mattson, C. A., Mullur, A. A., and Messac, A., 2004. "Smart pareto filter: Obtaining a minimal representation of multiobjective design space, engineering optimization." *Engineering Optimization,* **36**(4), pp. 721–740.

[152] Messac, A., and Mattson, C. A., 2005. "Pareto frontier based concept selection under uncertainty, with visualization, optimization and engineering." *Kluwer Publishers - Special Issue on Multidisciplinary Design Optimization, Invited Paper,* **6**(1), pp. 85–115.

[153] Larson, B. J., Anderson, T. V., and Mattson, C. A., 2010. "Developing system behavioral models by integrating discipline specific models." In *13th AIAA/ISSMO Multidisciplinary Analysis Optimization Conference Proceedsings, Fort Worth, Texas, AIAA-2010-9104-262*.

[154] Regier, A. A., and Hubbard, H. H., 1947. Factors affecting the design of quiet propellers Tech. rep., National Advisory Committee for Aeronautics (NACA) Research Memorandum RM No. L7H05.

[155] Hepperle, M., 2006. Design and analysis of propellers http://www.mh-aerotools.de/airfoils/javaprop.htm.

[156] Tangler, J. L., 2000. "The evolution of rotor and blade design." In *National Renewable Energy Laboratory*.

[157] Balakrishnan, A. V., Shubov, M. A., and Peterson, C. A., 2004. "Spectral analysis of coupled euler-bernoulli and timoshenko beam model." *ZAMM - Journal of Applied Mathematics and Mechanics / Zeitschrift fr Angewandte Mathematik und Mechanik,* **84**(5), pp. 291–313.

[158] Lind, R., and Brenner, M., 2000. "Flutterometer: An on-line tool to predict robust flutter margins." *JOURNAL OF AIRCRAFT,* **37**(6), November - December, pp. 1105–1112.

[159] Maute, K., 2010. *Computational Optimization*. John Wiley & Sons, Ltd.

[160] Xia, Q., and Wang, M. Y., 2008. "Simultaneous optimization of the material properties and the topology of functionally graded structures." *Computer-Aided Design,* **40**, pp. 660–675.

[161] Chen, B. S., and Tong, L. Y., 2005. "Thermomechanically coupled sensitivity analysis and design optimization of functionally graded materials.." *Computer Methods in Applied Mechanics and Engineering,* **194**, pp. 1891–1911.

[162] White, D., 2003. "Ultrasonic consolidation of aluminum tooling." *Advanced Materials and Processes,* **161**, pp. 64–65.

[163] Messac, A., and Mattson, C. A., 2004. "Normal constraint method with guarantee of even representation of complete pareto frontier." *AIAA Journal,* **42**(10), pp. 2101–2111.

[164] Norton, R. L., 2006. *Machine Design*. Pearson Prentice Hall, Upper Saddle River, NJ.

[165] Adams, B. L., Gao, X. C., and Kalidindi, S. R., 2005. "Finite approximations to the second-order properties closure in single phase polycrystals." *Acta Materialia,* **53**, pp. 3563–3577.

[166] Daniels, H., 1965. "Ultrasonic welding." *Ultrasonics,* **3**, pp. 190–196.

[167] O'Brien, R., 1991. *Welding Handbook*. American Welding Society, Miami, FL.

[168] Ram, G., Yang, Y., George, J., Robinson, C., and Stucker, B., 2006. "Improving linear weld density in ultrasonically consolidated parts." In *Proceedings of the 17th Solid Freeform Fabrication Symposium*, 17th Solid Freeform Fabrication Symposium.

[169] Ram, G. D. J., Yang, Y., and Stucker, B. E., 2006. "Effect of process parameters on bond formation during ultrasonic consolidation of aluminum alloy 3003." *Journal of Manufacturing Systems,* **25**, pp. 221–239.

[170] Ram, G. J., Robinson, C., Yang, Y., and Stucker, B., 2007. "Use of ultrasonic consolidation for fabrication of multi-material structures." *Rapid Prototyping Journal,* **13**, pp. 226–235.

[171] Bhattacharjee, P., Ray, R., and Upadhyaya, A., 2005. "Development of cube texture in pure ni, ni-w and ni-mo alloys prepared by the powder metallurgy route." *Scripta Materialia,* **53**, pp. 1477–1481.

[172] Bunge, H., 1993. *Texture Analysis in Materials Science*. Cuvillier Verlag Gottingen, Gottingen, Germany.

[173] Hertzberg, R. W., 1989. *Deformation and Fracture Mechanics of Engineering Materials*. John Wiley & Sons, Inc., New York, NY.

[174] Hill, R., 1963. "Elastic properties of reinforced solids: some theoretical principles.." *J Mech Phys Solids,* **11**.

[175] Paul, B., 1960. "Prediction of elastic constants of multiphase materials.." *Trans Metall Soc AIME,* **218**, p. 36.

[176] Fullwood, D. T., Niezgoda, S. R., Adams, B. L., and Kalidindi, S. R., 2010. "Microstructure sensitive design for performance optimization." *Progress in Materials Science,* **55**, pp. 477–562.

[177] Fromm, B., Adams, B., Ahmadi, S., and Knezevic, M., 2008. "Grain size and orientation distribution function of high purity alpha-titanium." In *ICOTOM15: The 15th International Conference on the Textures of Materials*.

[178] Taylor, G. I., 1938. "Plastic strain in metals." *Journal of the Institute of Metals,* **62**, pp. 307–324.

[179] Asaro, R., and Needleman, A., 1985. "Texture development and strain hardening in rate independent polycrystals." *Acta Metall Mater,* **33**, pp. 923–955.

[180] Owen, C. B., 2006. "Two dimensional friction stir welding model with experimental validation." Master's thesis, Brigham Young University.

[181] Weight, B. L., Mattson, C. A., Magleby, S. P., and Howell, L. L., 2007. "Configuration selection, modeling, and preliminary testing in support of constant force electrical connectors." *Journal of Electronic Packaging,* **129**, pp. 236–246.

[182] Harston, S. P., Mattson, C. A., and Koecher, M. C., 2010. "A topology optimization method with anisotropic materials." In *10th AIAA ATIO Conference September 2010 AIAA02010-9176*.

[183] Vrady, T., and Facello, M. A., 2005. "New trends in digital shape reconstruction." *Mathematics of Surfaces XI,* **3604**, pp. 395–412.

[184] Stamati, V., and Fudos, I., 2007. "A feature based approach to re-engineering objects of freeform design by exploiting point cloud morphology." In *Proceedings of the 2007 ACM symposium on Solid and physical modeling*, Vol. 2, pp. 1–9.

[185] Li, M., Langbein, F. C., and Martin, R. R., 2010. "Detecting design intent in approximate cad models using symmetry." *Computer-Aided Design,* **42**, pp. 183–201.

[186] de Toledo, R., Levy, B., and Paul, J.-C., 2008. "Reverse engineering for industrial-plant cad models." In *Tools and Methods for Competitive Engineering*, pp. 1021–1034.

[187] Vrady, T., Facello, M. A., and Terk, Z., 2007. "Automatic extraction of surface structures in digital shape reconstruction." *Computer-Aided Design,* **39**, pp. 379–388.